

Modelling in-plane behaviour of masonry shear walls through a predefined crack pattern at macro level

Marnix Verbrugge
4181425



Modelling in-plane behaviour of masonry shear walls through a predefined crack pattern at macro level

Master of Science Thesis

For the degree of Master of Science in Civil Engineering,
Track – Structural Engineering at Delft University of Technology

Marnix Verbrugge

October, 2017

Committee:
Prof.dr.ir. J.G. Rots
Dr.ir. M.A.N. Hendriks
Dr.ir. F. Messali
Ir. G.J.P. Ravenshorst
Ir. M. Pari

Faculty of Civil Engineering and Geosciences · Delft University of Technology

Table of Content

Table of Content.....	4
Summary	6
Chapter 1. Introduction.....	9
1.1 Background.....	9
1.2 Objectives.....	9
1.3 Scope	10
1.4 Thesis approach and outline	10
Chapter 2. Literature study	13
2.1 Masonry.....	13
2.1.1 Material properties	13
2.1.2 Structural behaviour of in-plane loaded shear walls	14
2.1.3 Numerical modelling	16
2.1.3.1 Micro modelling	16
2.1.3.2 Macro modelling	17
2.2 The Semi-Lumped Model (SLM).....	19
2.2.1 SLM theory	19
2.2.2 Modelling with the SLM approach	20
2.2.2.1 Interface elements	20
2.2.2.2 Continuum elements.....	21
2.2.2.3 Predefined crack pattern.....	22
2.3 The Sequentially Linear Analysis (SLA).....	23
2.3.1 General procedure	23
2.3.2 Saw-tooth curves.....	24
2.3.3 Continuum elements.....	25
2.3.4 Interface elements	25
2.3.5 Current state of development.....	26
2.4 Conclusion of chapter 2.....	26
Chapter 3. Interpretation of the SLM theory	27
3.1 Element clarification.....	27
3.2 Possible failure behaviour	28
3.3 Free-end and fixed-end boundary conditions.....	30
3.3.1 ETH Zurich wall 1 – Free-end shear wall validation.....	32
3.4 Conclusion chapter 3.....	35

Chapter 4. Numerical validation of the SLM approach	37
4.1 TU Eindhoven wall without opening (JDwall).....	38
4.2 Theoretical intermezzo – Shear deformation	41
4.3 Zero shear traction after cracking	42
4.4 Conclusion chapter 4.....	45
Chapter 5. Splitting behaviour.....	47
5.1 Theory of splitting behaviour by interface elements	47
5.2 Mesh dependence study	48
5.3 Conclusion of chapter 5.....	52
Chapter 6. Combining the SLM approach with the SLA procedure.....	53
6.1 SLM-SLA procedure – TU Eindhoven shear wall.....	53
6.2 Mesh refinement to 120 mm	58
6.3 Conclusion of chapter 6.....	58
Chapter 7. Conclusion master thesis.....	59
7.1 Recommendations.....	60
7.2 Proposed alternative of the SLM approach.....	61
Literature.....	62
Appendices	65
Appendix A – Diana10.1 error regarding constant shear retention.....	66
Appendix B – SLA interface element validation	70
Appendix C – Error observation in the SLA zero shear traction setting	75

Summary

The present work focusses on numerical modelling of masonry shear walls. The numerical simulations are performed with the Semi-Lumped Method, a simplification method which lumps the tensile and compression non-linearities into separate elements. The tensile non-linearities are analysed via tension cut-off interface elements through which a predefined crack pattern at macro level is formed. The compressive non-linearities are evaluated by smeared continuum elements which correspond to masonry crushing. The SLM approach reduces computational effort and allows for implementation of specific crack characteristics.

The goal of this thesis is to expand the SLM theory and improve the value of the approach. The research is based on the following three objectives.

1. Determine the consequences of the SLM assumptions

The SLM approach contains four element types. Horizontal interface elements to represent cracking of the mortar bed joints. Diagonal interface elements to analyse diagonal shear failure. And vertical interface elements to connect piers and spandrels to ensure a correct failure behaviour [2]. The scope of the thesis excludes openings, therefore the vertical elements are redundant and will not be further analysed. The fourth element type is a continuum element. As mentioned earlier, the continuum elements model the wall deformation as a result of compression.

By analysing the SLM softening curves it is shown all SLM-elements contribute to wall deformation but only the continuum elements can cause collapse. This means a SLM analysis will always result in collapse by crushing failure.

To evaluate the approach on a structural level it is determined which of the following failure mechanisms are correctly represented: Rocking behaviour, horizontal sliding and diagonal shear failure.

Rocking behaviour is analysed correctly by the SLM approach. The original SLM-report [1] confirms this via numerous numerical validations. Horizontal sliding is excluded as a SLM failure behaviour because the current interface elements contain a tension cut-off criteria.

It is unclear if diagonal shear failure is correctly simulated by the SLM approach. The SLM theory states opening of the diagonal interface elements is based on a compressive diagonal strut which causes deformation in perpendicular direction. This way of opening is considered a splitting type behaviour. The aim of this thesis is to determine how the SLM approach analyses diagonal shear failure and to clarify the consequences of the splitting analogy.

2. Form a description on how the SLM approach functions

The research scope is set to describe how the SLM approach represents diagonal shear failure. To study the functioning of the diagonal strut a numerical simulation is performed on the double clamped TU Eindhoven shear wall without openings [31]. This benchmark deforms by a combination of rocking behaviour and diagonal shear failure. By performing a variation study towards shear deformation the numerical analysis shows that next to the splitting behaviour also sliding along the diagonal is a critical part of the SLM approach. The shear deformation along the diagonal strut is obtained through the zero shear traction setting.

3. Determine the influence of SLM mesh choice

The SLM response, obtained during the previous objective, indicates at least half of the corner diagonal interface elements must remain closed in order to preserve a compressive zone. This suggests the interface element length may influence the obtained response. By performing a mesh variation study it is shown that the length does indeed influence the general behaviour and thereby a mesh dependency is identified. For a coarser mesh an overshoot of wall resistance is observed, where a finer mesh influences the failure behaviour. It is therefore strongly advised to further investigate the mesh influence on the SLM approach.

Next to the SLM research this thesis also contains a pilot study where the SLM approach is combined with the sequentially linear analysis (SLA). The combined approach is validated with the TU Eindhoven shear wall. The obtained results show that the SLM-SLA combination is possible, but the SLA does influence the response. After reaching the peak load a change in failure behaviour is observed where the diagonal opening is significantly reduced and merely sliding behaviour remains. To enhance the SLM-SLA procedure it is proposed to first develop the SLM approach and the SLA discrete modelling individually before combining them again.

In conclusion, the SLM approach does represent diagonal shear failure as a combination of splitting and sliding behaviour but, unfortunately, the current SLM assumptions result in a mesh dependency influenced by the length of the diagonal corner interface elements. During the final part of the thesis a solution is proposed to solve this dependency by separating the compressive zones from the diagonal strut. By enhanced investigations and improvements on how the SLM approach represents diagonal shear failure the method can still become an universal modelling tool for in-plane loaded masonry.

Chapter 1. Introduction

1.1 Background

Masonry is a building material applied worldwide for decorative and constructive purposes. The recent earthquakes in Groningen inflict damage to both the decorative and constructive masonry parts. Damage to the constructive parts influences the load-bearing resistance of the structure. To ensure safety it must be determined if the load-bearing capacity is still sufficient. Therefore, being able to perform reliable predictions regarding the structural resistance is demanded to determine whether maintenance is required.

Predicting the load-bearing capacity of a masonry structure can be achieved by laboratory experiments or via numerical simulations. This master thesis will focus on numerical simulations. Modelling masonry elements with traditional numerical procedures comes with high computational effort. A trend of simplified procedures has grown and one of these approaches is the Semi-Lumped Method. The SLM approach uses interface elements to create a pre-defined cracking pattern, including individual crack characteristics, to simplify the numerical procedure. The required number of elements is reduced and the interpretation of failure behaviour is simplified. Via numerical validations the potential of the SLM approach is proven by the original report, but the theoretical background needs to be expanded and clarified.

The goal of this master thesis is to expand the SLM theory by including literature and performing numerical validations. The research will start by showing the consequences of the SLM assumptions on an element- and structural level. By introducing masonry literature it will be determined to what extent the SLM potential reaches. Via numerical validations it will be clear which interface element input provides the most realistic failure behaviour. The final part of the SLM research contains a variation study with different element sizes to check for any possible mesh dependency.

The master thesis ends with a pilot where the SLM method and the SLA procedure are combined. In contrast to traditional numerical solutions the SLA procedure is not based on an incremental-iterative procedure, like the Newton-Raphson procedure, but is based on a damage analogy. The procedure is still under development and combining the SLM with the SLA is considered the start of solving a lumping method with the SLA procedure.

1.2 Objectives

The aim of this thesis is to expand the SLM theory so the value of the approach will increase. To do so the following objectives are set:

- Determine the consequences of the SLM assumptions
- Form a description on how the SLM approach functions
- Determine the influence of SLM mesh choice

As mentioned during the background section, part of the thesis consist of a pilot regarding the SLM-SLA combination. This is a numerical trial and setting concrete objectives for this subject is considered not meaningful.

1.3 Scope

All theory and validations of this master thesis are in the context of quasi-static, two dimensional analyses. The numerical validations are performed with the Newton Raphson procedure, except for the validations during chapter 6 where the SLA procedure is applied. With respect to benchmark selection only shear walls without openings are qualified because of their simplicity towards failure behaviour. Other benchmark specifications will be provided during chapter 3.

1.4 Thesis approach and outline

The thesis consist of seven chapters in which the described objectives are attempted to be accomplished. As a start, a literary survey is presented in chapter 2. This survey contains the necessary information to understand the SLM procedure and to start the research. Chapters 3 to 5 form the centre of the thesis where several expansions to the SLM theory are being shaped. Chapter 6 addresses the SLM-SLA pilot. This pilot consists out of numerical validations only. The final conclusions are summarized during chapter 7.

An overview of all chapters is presented below.

Chapter 2 – Literature study

This chapter summarises the necessary literature to start the research. It contains subjects regarding masonry, the SLM approach and the SLA procedure. The material characteristics of masonry are described on an element- and structural level. By presenting several numerical approaches regarding masonry modelling an overview of modern techniques is given. This overview will help selecting the background which supports the SLM assumptions. The SLM theory, based on the information from the original SLM report, is presented in paragraph 2.2. This paragraph clearly states the assumptions of the approach and why the approach is beneficial. The last part of this literary survey is a description of the SLA procedure.

Chapter 3 – The SLM potential based on literature

The obtained information from chapter 2 will be combined with the existing SLM approach. First the consequences of all SLM assumptions are reviewed. A distinction is made between elements which account for structural collapse and elements that only allow for deformation. Secondly, it is determent which failure mechanism can or cannot be represented correctly by the SLM approach. Thirdly, the failure mechanisms for which it is not clear if the SLM approach can analyse them are discussed. Clarification of this last section is the main topic of this master thesis. The last part of chapter 3 distinguishes which benchmarks are most suitable within the scope of research.

Chapter 4 – Numerical validation of the SLM approach

During the previous chapter it is discovered which parts of the SLM method need clarification. Chapter 4 will start with a numerical validation to explore how these parts really function. By comparing the obtained results with the original SLM report the required SLM-input is documented. The SLM theory is expended by including the deformation required to obtain realistic results. In combination with the obtained theory of chapters 2 and 3 it is addressed which failure mechanisms the SLM approach represents in a realistic fashion.

Chapter 5 – Splitting behaviour

The previous chapters describe how the SLM method functions. During chapter 5 a controversial assumption within the SLM approach is validated by a mesh dependency study. It is shown that element length might influence a certain response of the method. By means of three different mesh sizes this influence is discussed.

Chapter 6 – Combining the SLM approach with the SLA procedure

Via numerical validations the potential of the SLM-SLA procedure is established. The validation is performed on the benchmark used during all previous chapters.

Chapter 7 – Conclusion master thesis

Chapter 7 summarizes the conclusions gained during the previous chapters. These conclusions will confirm that the thesis objectives are accomplished. Proposed enhancements will close this final chapter of the master thesis.

Appendices

During the SLM validation a number of studies are performed. Some findings are not within the scope of research. However, in general these findings are important with respect to numerical modelling and are therefore presented in appendices A to C.

Appendix A describes a modelling error in the Diana10.1 version regarding interface elements.

Appendix B is an input validation for the SLA interface elements.

Appendix C describes a modelling error regarding interface elements of the SLA Diana9.3 version.

Chapter 2. Literature study

This chapter addresses three issues in preparation of the SLM research. To start, a summary of the masonry characteristics is presented in paragraph 2.1. This section also includes a brief review on numerical modelling strategies applicable for masonry analyses. The semi-lumped method is introduced during this review but is presented in more detail during paragraph 2.2. The SLM description contains the assumptions and element clarification of the approach. Paragraph 2.3 is a brief survey on the SLA procedure with the aim on practical application.

2.1 Masonry

Masonry is a globally used building material for it has a simple construction technique and useful characteristics. Where durability, fire safety and acoustics are pleasant characteristics the complexity of the material is a downfall. The combination of mortar, bricks and brick-mortar interfaces, each with their own characteristics, make constructive masonry a challenging material to analyse by numerical simulations. This paragraph provides an overview of the required knowledge to numerically analyse in-plane loaded masonry shear walls.

The term masonry is used to indicate any form of stone-mortar combination. During this master thesis masonry always indicates unreinforced brick masonry. Stacking the bricks can be executed in different patterns. Unless indicates otherwise, the running bond pattern is assumed for walls and corner connections.

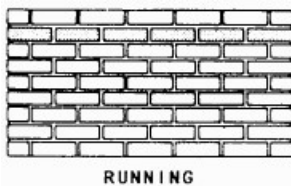


figure 1: Running bond masonry [13]

2.1.1 Material properties

The material properties are characterized by failure behaviour. Local failure is the result of crushing or cracking. Crushing behaviour occurs when the compression capacity is lower than the applied pressure. Cracking of masonry indicates surpassing the tensile capacity or the shear capacity. Three types of cracking modes are distinguished. Fracture mode I represents opening as a result of tensile failure. Mode II is the sliding mode caused by in-plane shear. Mode III is the tearing mode as a result of out-of-plane shear. All mode are presented in figure 2.

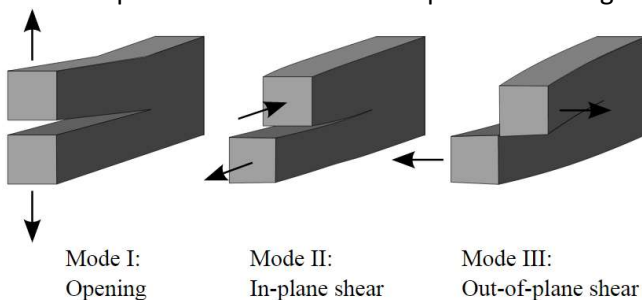


figure 2: Fracture modes [32]

Masonry is a quasi-brittle material which means cracking (or crushing) does not reduce the load-bearing resistance instantly to zero but gradually reduces resistance via a softening pattern. Softening is a decrease of strength/resistance under a continuous increasing deformation.

The type of softening behaviour is material dependent, therefore multiple softening curves are available. For masonry the most commonly applied softening curves available in Diana are presented in figure 3. These softening curves are described by the tensile strength (f_t), crack bandwidth (h) and the fracture energy (G_f).

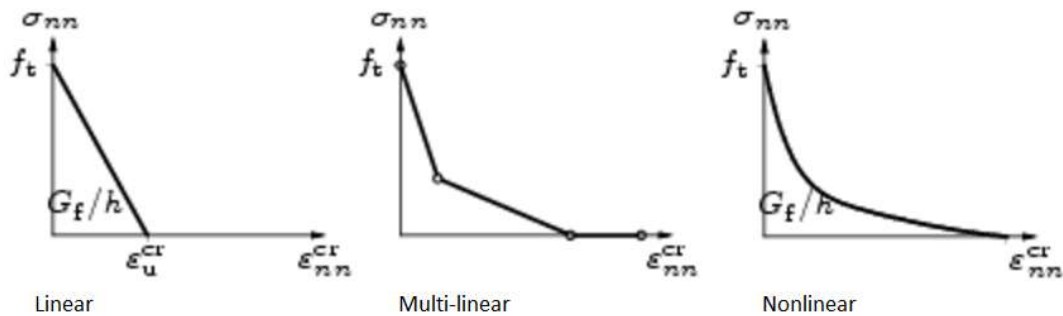


figure 3: Softening curves tension [30]

As mentioned earlier, crushing of masonry also leads to a gradual reduction of resistance. When very limited material characteristics are present ideal softening has proven to be suitable (figure 4). The parabolic softening is preferred because it allows for strength reduction which is a more realistic assumption. The parameters describing compressive softening are the compression strength (f_c), crushing bandwidth (h_c) and fracture energy (G_c).

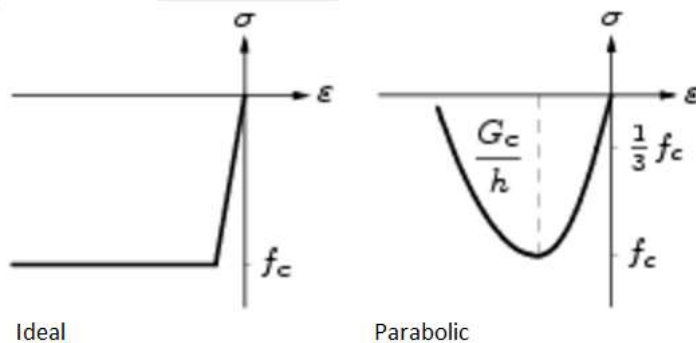


figure 4: Softening curves compression [30]

2.1.2 Structural behaviour of in-plane loaded shear walls

A shear wall is a structural part which resist lateral forces. During this section a shear wall is characterised by being non-proportional loaded in vertical direction and proportional loaded in horizontal direction. The non-proportional vertical load forms an initial compressive stress in the entire wall, representing the compressive stress caused by -for example- the above floor. The proportional horizontal load will activate a certain failure mode that eventually causes the wall to collapse.

In general three types of failure behaviour at structural level are distinguished when considering a simple free-end shear wall without openings (a masonry pier). These failure modes are rocking, sliding and diagonal shear cracking, all visualised in figure 5. Rocking behaviour consists of two stages, first horizontal cracks at the bottom corner allow the wall to rotate creating a compressive zone on the other bottom corner. If rotated far enough the pressure is higher than the compressive capacity and toe crushing is set in motion leading to collapse of the wall. In case of high vertical loading crushing may already start before cracks in the bed joints are visible. Sliding failure indicates cracked bed joints and divide the wall element in two. Diagonal shear failure is the collective term for stepwise diagonal sliding and diagonal cracking [4]. The cracking can stepwise follow the joints or may go through the brick, depending on the strength of the mortar, brick and mortar-brick interface.

Other than a free-end boundary condition, a masonry pier can also be clamped-in, for instance between two floors, which results in a more complicated failure behaviour. For slender piers rocking behaviour in combination with diagonal shear failure becomes the most likely clamped-in failure mode [12]. As presented in figure 7 the amount of vertical loading is decisive whether toe crushing or diagonal shear failure will cause the pier to collapse. Under low vertical force the pier may overturn before toe crushing occurs. Overturning is considered a loss of balance and not a collapse mechanism.

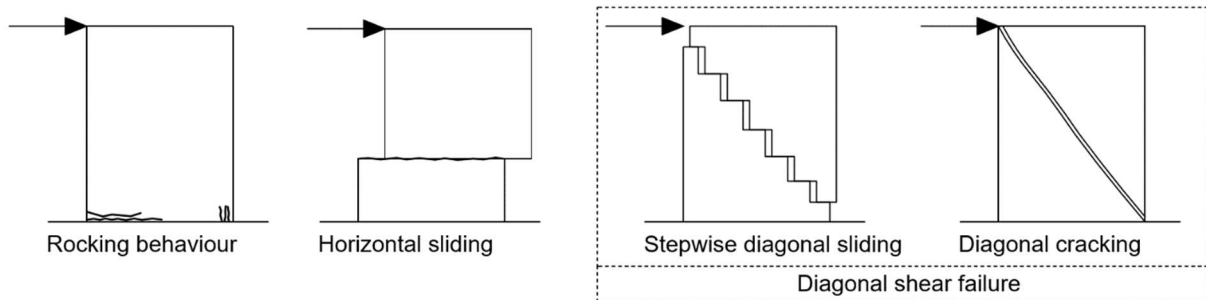


figure 5: Pier failure modes

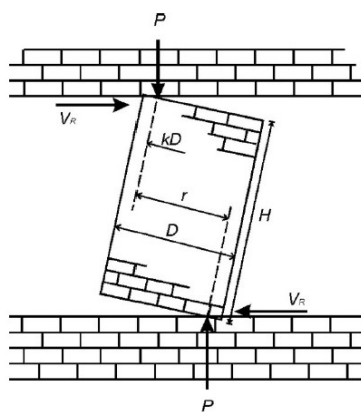


figure 6: Rocking behaviour [12]

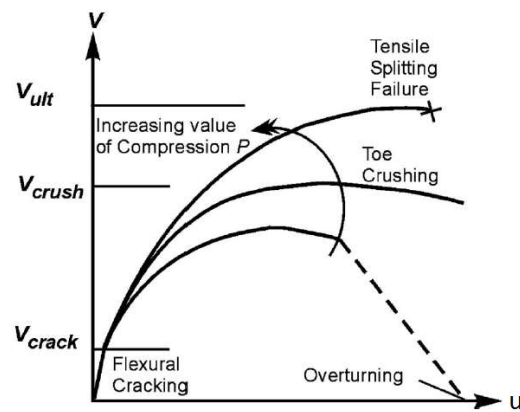


figure 7: Failure modes with respect to vertical force P [12]

A shear wall might also contain openings. An opening subdivides the wall into vertical and horizontal elements respectively piers and spandrels. The possible failure modes of a pier are already described in the text above. Failure behaviour of a spandrel depends mainly on the boundary conditions. A free-end spandrel, a top-storey boundary condition, will collapse by toe crushing. A mid-storey boundary condition, a clamped-in spandrel, will cause failure by diagonal shear failure.

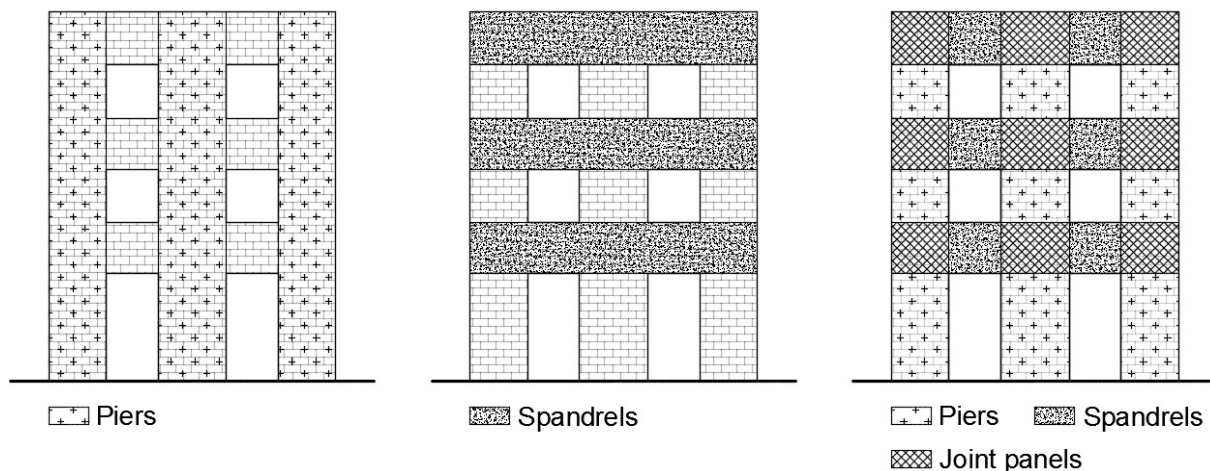


figure 8: Positions of piers and spandrels

2.1.3 Numerical modelling

This section summarizes the numerical modelling fundamentals of analysing masonry structures. A brief introduction of micro and macro modelling forms a bridge to the SLM approach (paragraph 2.2).

2.1.3.1 Micro modelling

Modelling masonry is performed on either a micro or macro scale. Micro modelling is suitable for precise modelling of a small masonry part. The mortar and the bricks are modelled via continuum elements with a Young's modulus, poisson ratio and the possibility to include inelastic properties. Discontinued interface elements represent a potential crack, crush or slip plane between the mortar and bricks (figure 9 (b)). Although accurate, this method has the disadvantage that large computer memory and long calculation time are required. To reduce required memory and calculation time the number of interfaces is reduced by expanding the continuum elements to represent both brick and mortar. Interface elements are still applied but now at the middle of the joint (figure 9 (c)). Accuracy is lost due to an average interface and the poisson ratio of the mortar is no longer implemented.

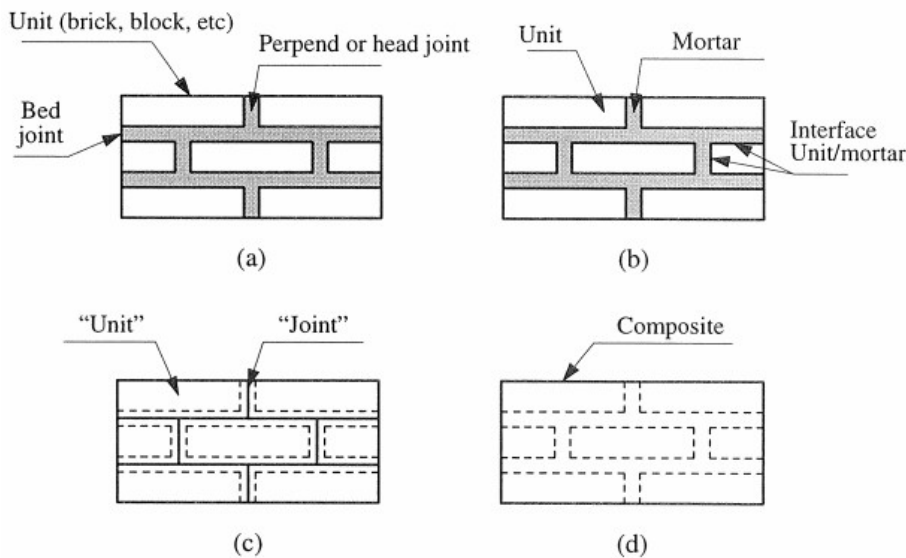


figure 9: Micro and macro modelling. (a) masonry sample, (b) detailed micro-modelling, (c) simple micro-modelling, (d) macro-modelling. [11]

Micro modelling benefits from the ability to include all five different failure modes, represented by figure 10. Joint related failures are cracking of the joint (a) and sliding along the bed or head joint (b). Brick failure is cracking of the brick in direct tension (c). Combined failures are diagonal tension cracking of the brick (d) and crushing of masonry (e).

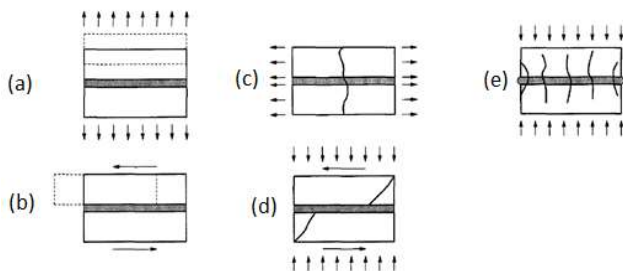


figure 10: Failure modes of masonry [11]

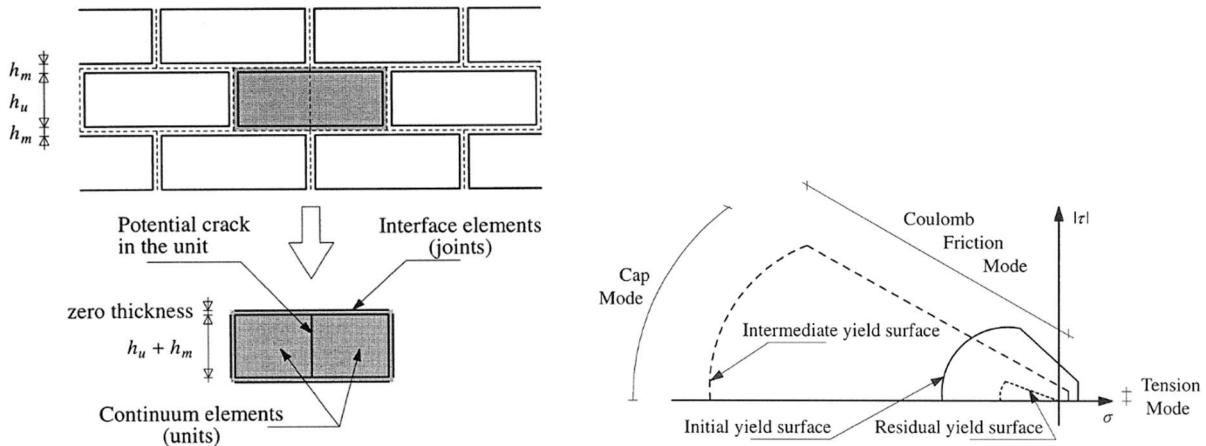


figure 11: Interface cap model [11]

An example of a micro modelling tool is the multi-surface interface model, presented in figure 11. The interface cap model allows the interface elements to represent possible crack, crush and slip planes which result in an accurate representation of reality. The interface cap model contains the tension cut-off (Mode I), the Coulomb friction envelope (Mode II) and a cap mode for compressive failure and therefore includes all failure types of figure 10.

2.1.3.2 Macro modelling

Using micro modelling techniques on a macro scaled structure requires a high computational effort. To be able to model on a macro scale simplified approaches, like smeared or lumped modelling, are developed to reduce the computational effort.

Smeared approach

The periodic pattern of masonry allows analysing a masonry surface as if it is a homogenous material (figure 9 (d)). Via homogenization techniques the structural masonry characteristics are smeared out over continuum elements with isotropic, anisotropic or orthotropic properties. Cracking (or crushing) is now represented by a part of the continuum element (figure 12) and the material properties are modified to account for the effect of cracking.

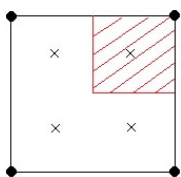


figure 12: Damaged part of a quadrilateral element indicated in red

Masonry is an anisotropic material where two orthogonal direction are distinguished. Lourenco proposed the anisotropy continuum model by creating a yield surface out of the Rankine type (tension) and the Hill type yield surface (compression)(figure 13). This approach of smeared analysis accounts for both material and geometrical properties of masonry.

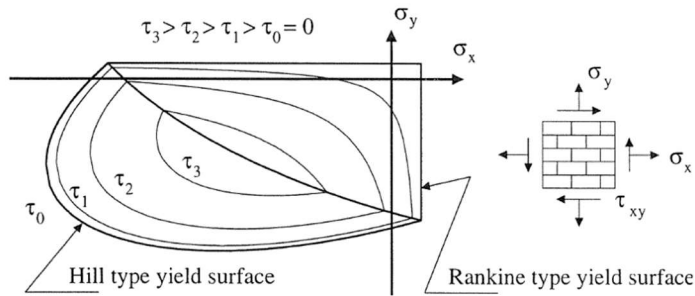


figure 13: Rankine-Hill yield surface [11]

A disadvantage of a smeared continuum model is the number of parameters required to model the correct behaviour of an anisotropic material.

Lumped approach

Reducing computational effort of macro modelling is possible by lumping structural characteristics into specific structural elements or element parts. A well-known lumped method is the equivalent frame method where, by a distinction of piers and spandrels, larger structural elements are represented by a 1-dimensional beam element. Global failure mechanisms are predicted sufficiently by this approach, but the simplifications do not allow for local failure mechanisms to be decisive.

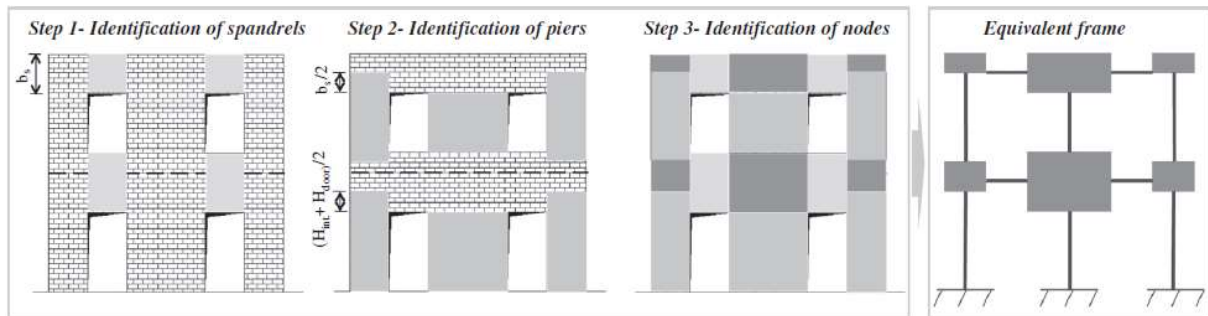


figure 14: Process of the equivalent frame model [3]

This master thesis will focus on the semi-lumped method (SLM) where tension characteristics are lumped into interface elements and continuum elements represent compressive behaviour via a smeared approach. It is considered a lumping type technique which also allows for local failure mechanisms. The next paragraph contains an overview of the available SLM literature.

2.2 The Semi-Lumped Model (SLM)

Modelling masonry façades is a challenge for many traditional finite element methods. In order to quickly analyse the in-plane action behaviour of masonry facades, Messali proposed a method of lumping the tension non-linearities and compression non-linearities into separated elements. A predefined crack pattern is modelled with interface elements where crushing behaviour is modelled via smeared continuum elements. This way of modelling does no longer provide an advanced structural behaviour analysis, but works on material level. The advantages are that less elements are necessary, very few material parameters are required, crack characteristics can be modelled more realistically and the computational effort is being reduced.

2.2.1 SLM theory

Experiments and earthquake research show that crack patterns in masonry façades usually occur in defined positions [1]. Knowing the possible crack patterns in advance is essential to the SLM approach since these possible cracks can now be represented by an interface element. An example of modelling a predefined crack pattern with interface elements is presented in figure 15.

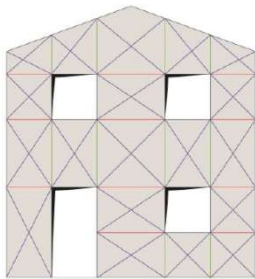


figure 15: Potential crack pattern [1]

The SLM approach distinguishes three types of possible cracks; horizontal, diagonal and vertical cracks (figure 16). Each of these crack types is linked to an interface element with specific characteristics, which are addressed in the following section. To connect the interface elements and to include crushing, the SLM approach has a fourth element type namely continuum elements. The compression non-linearities are represented by these elements.

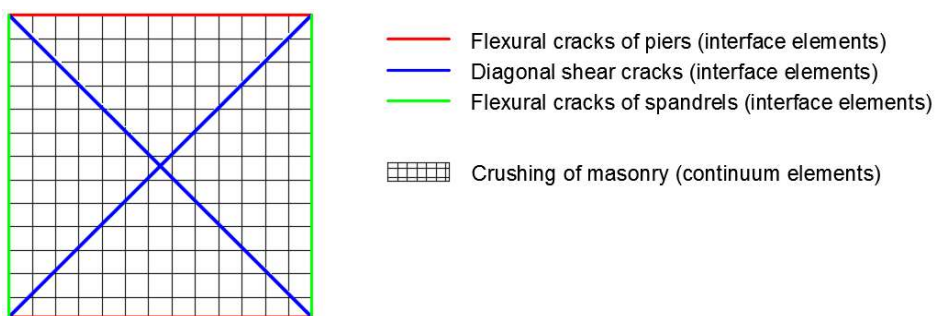


figure 16: SLM element

The back-ground of each interface element is as follows:

Flexural cracks of piers represent cracking along the mortar bed-joints. These cracks depend on the tensile resistance f_t , similar to when a smeared approach is applied. Linear softening with a low fracture energy simulate the ductile response (figure 17, red).

Diagonal shear cracks develop step-wise along the bricks and therefore create a friction area along the brick surfaces. The cracks are represented by an interface element with tensile strength f_t in

combination with a high fracture energy modelling the frictional behaviour of the bricks (figure 17, blue).

Flexural cracks of spandrels model the interlocking phenomena of piers and spandrels [2] (figure 17, green). A tensile resistance f_{ts} is based on either the tensile strength of the brick or on the bed joints' shear capacity [4]. Usually sliding along the bricks occurs and, similar to the diagonal shear cracks, infinite softening is assumed. The spandrel tensile stress is: $f_{ts} = \min \{ f_{bt}/2 ; c + \varphi \tan \phi \sigma_y \}$ where f_{bt} is the brick tensile strength, φ is an interlocking parameter, c is the mortar-unit cohesion and σ_y is the vertical compressive stress.

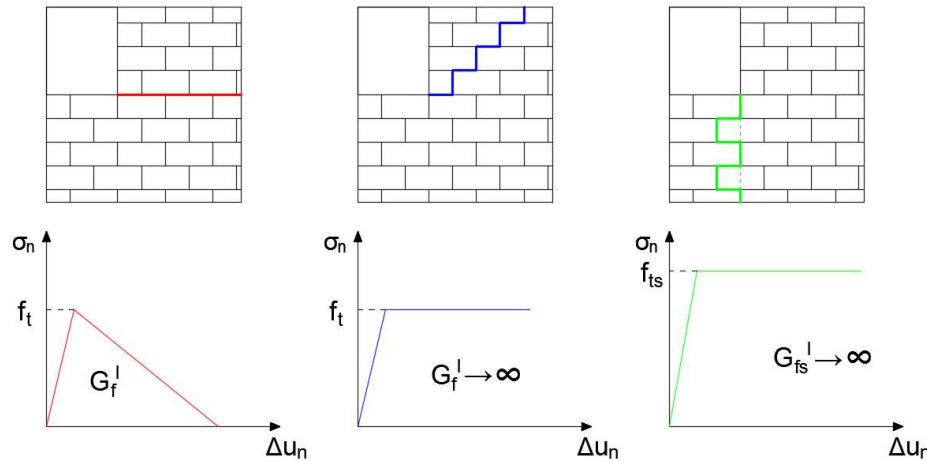


figure 17: Softening branches of the interface elements. Horizontal interface (red), diagonal interface (blue), vertical interface (green)

2.2.2 Modelling with the SLM approach

Modelling with the SLM approach is characterized by three aspects; interface elements, continuum elements and a predefined crack pattern. This section contains an element description of the interface elements and the continuum elements, followed by the assumptions regarding a predefined crack pattern.

2.2.2.1 Interface elements

To model the predefined crack pattern CL12I interface elements with quadratic interpolation will be applied.

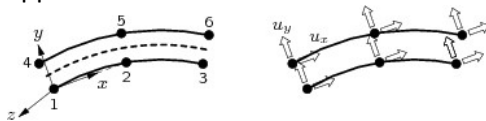


figure 18: CL12I interface element [30]

The interface elements are conform a tension cut-off criteria (figure 19). This means cracking is only possible in normal direction.

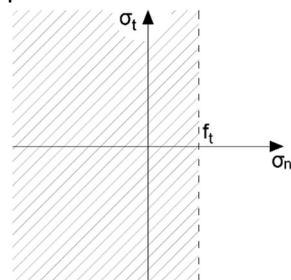


figure 19: Tension cut-off criteria of the SLM interface elements

After opening the interface elements contain different nonlinear characteristics for the crack slip and the crack opening. Stress in normal direction is calculated via a load-displacement relation between the f_n and Δu_n visualised by figure 20, where Δu_n is the crack width. After opening of the interface element the stiffness in shear direction changes from κ_t to $\beta\kappa_t$ reducing the shear stiffness by a constant shear retention factor β (assumed value is 0.01). With a low $\beta\kappa_t$ -value shear deformation is possible. Unloading and reloading are conform a secant approach. For unloading a linear relation between stress and displacement leads up to the origin, after which the initial stiffness is recovered. In other words, a re-closed interface element resets its stiffness to the initial κ_n and κ_t values.

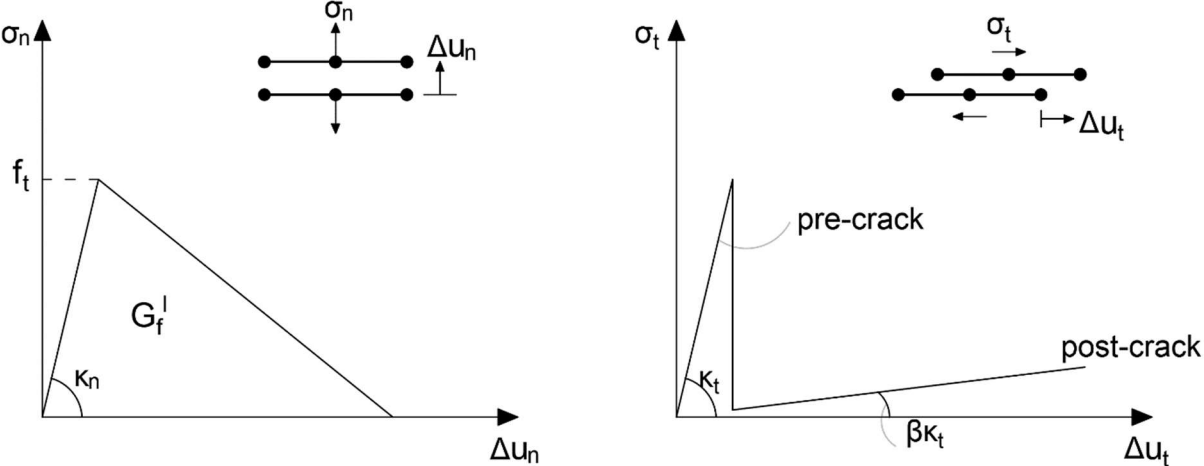


figure 20: Linear softening in normal direction (left), shear traction curve (right)

2.2.2.2 Continuum elements

Crushing of masonry is modelled by the isoparametric plane stress continuum elements CT12M and CQ16M (figure 21) based on quadratic interpolation. The fixed crack setting is applied.

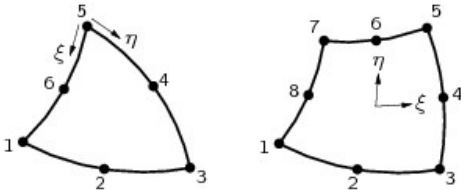


figure 21: CT12M and CQ16M element [30]

A parabolic softening curve forms the second principle stress-strain relation and represents the compressive non-linearity (figure 22). During the SLM analyses the compressive fracture energy (G_c) is assumed to be 250 to 500 times the tensile fracture energy.

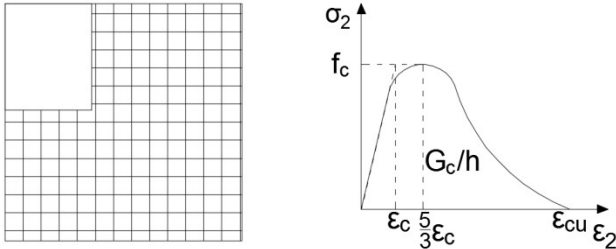


figure 22: Softening branch continuum element

2.2.2.3 Predefined crack pattern

As mention during the introduction, a predefine crack pattern is key to the SLM analogy. The location of the predefined diagonal cracks is based on top end boundary condition (figure 23). In case of a free-end section diagonal cracks go from the toe to the centre top. The SLM interface pattern is therefore triangular shaped (figure 23a). For clamped in sections the diagonal cracks go from the toe to the corner top, represented by a crossed pattern (figure 23b). These assumptions are supported by previous research on in-plane loaded masonry facades.

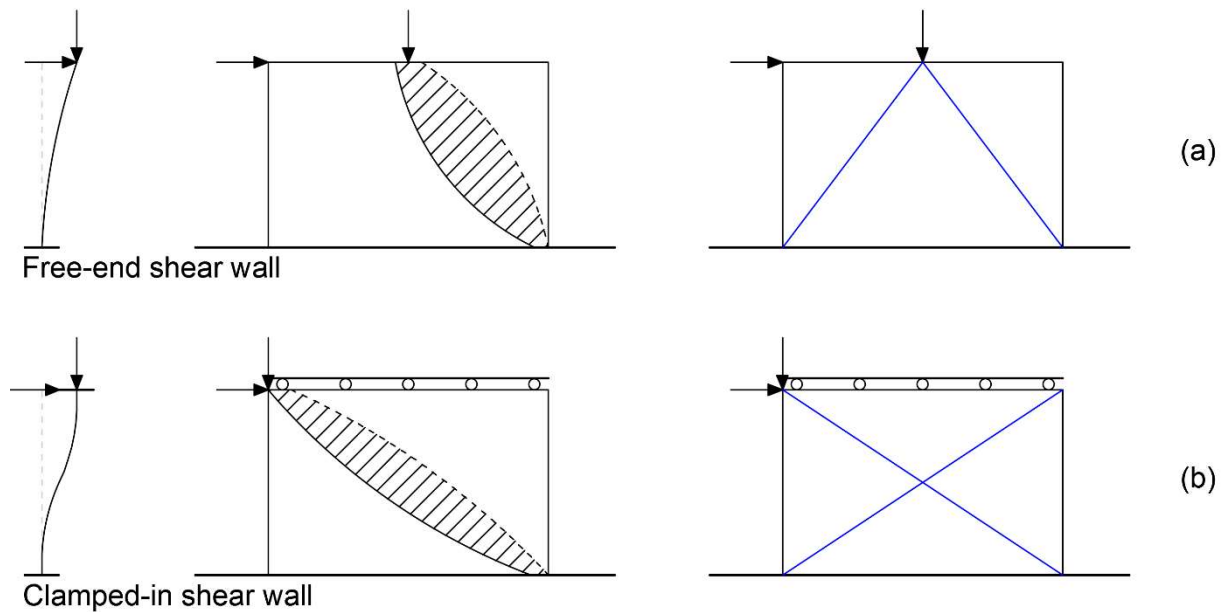


figure 23: Diagonal patterns for free-end shear wall (a) and clamped-in shear wall (b)

The predefined crack patterns enable the possibility of a principle tensile stress being larger than the masonry's tensile strength. This can happen when the principle direction is not parallel to the interface normal direction (figure 24). However, this is considered not to be a problem because when the predefined crack pattern is applied correctly the principle direction is almost in line with the normal direction of the interface element.

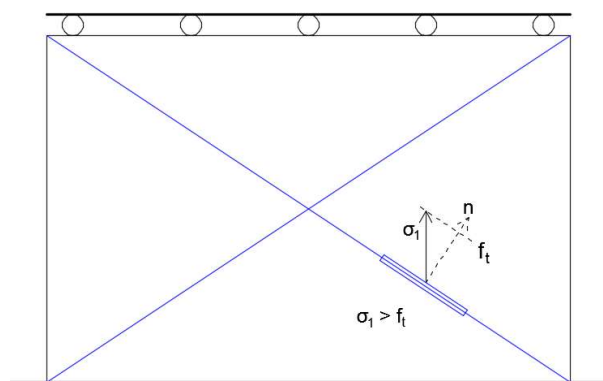


figure 24: Principle stress exceeding the tensile strength

2.3 The Sequentially Linear Analysis (SLA)

Modelling brittle material with traditional nonlinear finite element methods has proven to be difficult. Issues like bifurcations, snap-backs and non-convergence cause these difficulties. The SLA procedure has the advantage to overcome these issues. Via a series of linear analyses damage is assigned to the “critical element”. This damaged based event-by-event procedure is no longer part of an incremental-iterative procedure and therefore bifurcations, snap-backs and non-convergence are avoided. Section 2.3.1 is a summary of the general SLA procedure. The definition and selecting procedure of the critical element is part of this overview. Section 2.3.2 describes how an integration point is damaged according to the saw-tooth softening curve analogy. The current state of development is presented in section 2.3.3.

2.3.1 General procedure

SLA is a damaged based solution procedure which repeatedly performs scaled linear analyses. In between each analysis a single integration point is damaged by a reduction of stiffness and strength. This critical integration point is selected by establishing the lowest ratio of the current local tensile stress divided by the current local tensile strength considering all integration points of the entire structure. A stepwise reduction of stiffness and strength, realised by a saw-tooth based non-linear softening curve, is the fundamental concept of this event-by-event procedure.

In case of proportional loading the SLA is summarized by the following steps [15]:

- Add an external load as a unit load
- Perform a linear-elastic analysis to calculate the principle strains and stresses in all integration points.
- Extract the critical integration point. This is the point with the highest ratio of principle stress divided by its current strength (σ_1/f_t). The overall highest ratio is called the critical load multiplier λ_{crit} .
- Scale the unit load proportionally with λ_{crit} , perform a linear analysis to obtain the strains and stresses of all integration point for post-processing purposes.
- Increase the damage of the critical integration point by reducing its stiffness and strength. The Young’s modulus and tensile strength will be reduced according to the saw-tooth constitutive law (section 2.3.2).
- Repeat the previous steps for the new configuration.

The SLA procedure for proportional loading is relatively simple and robust. For non-proportional loading the selection procedure for the critical load multiplier becomes more complex. During this master thesis the SLA analyses are performed with the Diana9.3 software where the scaling procedure of DeJong [18] will determine λ_{crit} for non-proportional loading models. This solution procedure is not flawless [20], but for this master thesis it will suffice. The idea is to separate the non-proportional and proportional loading into respective loads set A and B. By splitting all loads into parts with global directions x, y and xy the following formulas become valid:

$$\sigma_{xx} = \sigma_{xx,A} + \lambda\sigma_{xx,B}$$

$$\sigma_{yy} = \sigma_{yy,A} + \lambda\sigma_{yy,B}$$

$$\sigma_{xy} = \sigma_{xy,A} + \lambda\sigma_{xy,B}$$

And the principle stresses can be easily computed by:

$$\sigma_{1,2} = \frac{1}{2}[(\sigma_{xx,A} + \lambda_{1,2}\sigma_{xx,B}) + (\sigma_{yy,A} + \lambda_{1,2}\sigma_{yy,B})] \pm \sqrt{\frac{1}{4}[(\sigma_{xx,A} + \lambda_{1,2}\sigma_{xx,B}) - (\sigma_{yy,A} + \lambda_{1,2}\sigma_{yy,B})]^2 + (\sigma_{xy,A} + \lambda_{1,2}\sigma_{xy,B})^2}$$

Applying the quadratic formula grants the $\sigma_{1,2}$ solutions. Problems arise when $\sigma_1 \neq \sigma_2$ and the correct solution has to be picked, or if $\sigma_1 = \sigma_2 = 0$ and no solution is obtained. The scope of this master thesis is set to the practical purpose of SLA and therefore the credibility of this solution method will not be

discussed any further. For proposed solutions of these issues the reader is referred to the following literature [18,20].

2.3.2 Saw-tooth curves

The SLA method is characterised by its way of applying damages to an integration point. The event-by-event strategy is realised by dividing the softening curve into linear pieces. Presented in figure 25 is the original softening curve created with a Young's modulus, tensile strength, fracture energy and the crack width h . The four options represent the most common saw-tooth approaches of the linear softening tensile regime. Option 1 shows a saw-tooth model created via strength reduction. By dividing the tensile strength into parts the number of teeth can be determined and vice versa. Option 2 uses constant reduction of the Young's modulus to create the saw-tooth curve. The options 1 and 2 turned out to be mesh dependent because the area $(G_f/h)_{\text{sawtoothcurve}}$ underestimates the fracture energy G_f/h of the original softening curve. By upscaling f_t and ϵ_u the $(G_f/h)_{\text{sawtoothcurve}}$ area of option 3 becomes equal to G_f/h and mesh dependence is being reduced. Option 4 is a more elegant formulation of the saw-tooth curve and is called the ripple-curve. The ripple-curve is bounded by two lines parallel to the softening curve each with a offset of p times f_t .

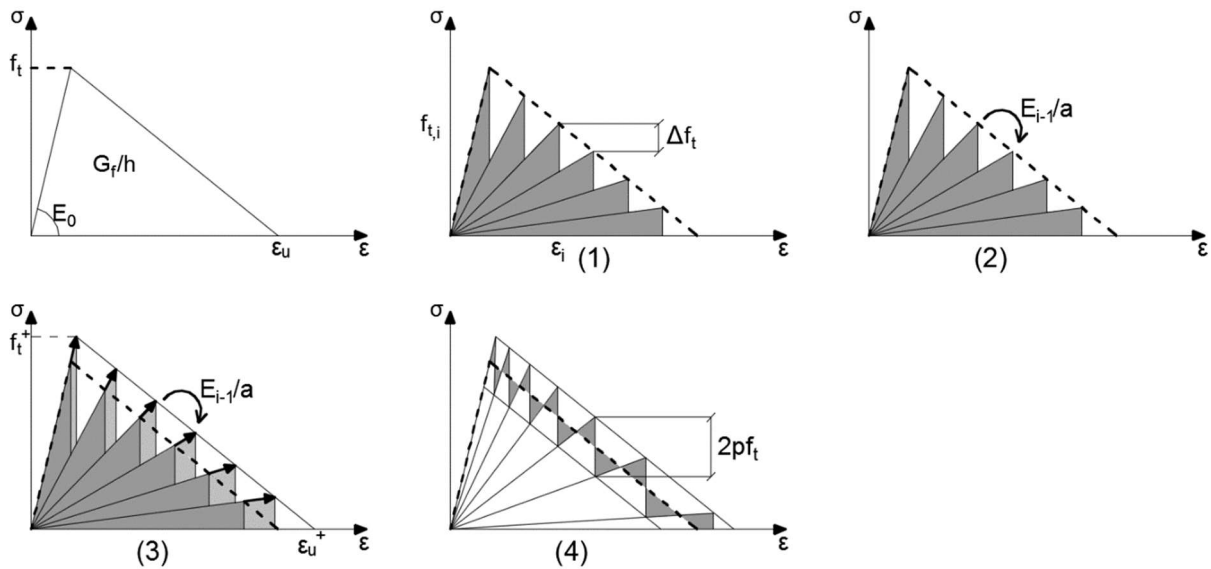


figure 25: Different saw-tooth modelling techniques

The ripple-curve is constructed with the following formulas [17]:

$$f_{ti}^- = f_{ti}^+ - 2pf_t$$

$$E_{i+1} = \frac{E_i}{a_{i+1}}$$

$$a_{i+1} = \frac{f_{ti}^+}{f_{ti}^+ - 2pf_t}$$

For this linear softening curve the f_{ti}^+ value is:

$$f_{ti}^+ = \frac{\epsilon_u^+ E_i D}{E_i + D}$$

where

$$\epsilon_u^+ = \epsilon_u + \frac{pf_t}{D} \quad \text{with,} \quad D = \frac{f_t}{\epsilon_u - \frac{f_t}{E}}$$

The ripple-curve is also available for ideal plastic softening curves [17]. Very little is published regarding a potential compressive ripple-curve, yet this master thesis will apply a compressive saw-tooth based on the ripple-curve analogy.

2.3.3 Continuum elements

Throughout the present thesis the SLA procedures are always in combination with the SLM approach, thereby excluding cracking of continuum elements. In-plane behaviour of the isotropic continuum elements before crushing is in accordance with a fixed crack model where the constitutive relation equals:

$$\begin{bmatrix} \sigma_{xx} \\ \sigma_{yy} \\ \sigma_{xy} \end{bmatrix} = \frac{E_0}{1 - \nu_0^2} * \begin{bmatrix} 1 & \nu_0 & 0 \\ \nu_0 & 1 & 0 \\ 0 & 0 & 1 - \frac{\nu_0}{2} \end{bmatrix} * \begin{bmatrix} \epsilon_{xx} \\ \epsilon_{yy} \\ \gamma_{xy} \end{bmatrix}$$

E_0 and ν_0 represent the initial Young's modulus and poisson ratio. After damage is assigned to the iteration point the follow relation holds:

$$\begin{bmatrix} \sigma_{xx} \\ \sigma_{yy} \\ \sigma_{xy} \end{bmatrix} = \begin{bmatrix} \frac{E_n}{1 - \nu_{nt}\nu_{tn}} & \frac{\nu_{nt}E_n}{1 - \nu_{nt}\nu_{tn}} & 0 \\ \frac{\nu_{tn}E_t}{1 - \nu_{nt}\nu_{tn}} & \frac{E_t}{1 - \nu_{nt}\nu_{tn}} & 0 \\ 0 & 0 & G_{red} \end{bmatrix} * \begin{bmatrix} \epsilon_{xx} \\ \epsilon_{yy} \\ \gamma_{xy} \end{bmatrix}$$

where,

$$G_{red} = E_{min}/2 * (1 + \nu_0 \frac{E_{min}}{E_0})$$

$$\nu_{nt} = \nu_0 \left(\frac{E_n}{E_0} \right)$$

$$\nu_{nt}E_n = \nu_{tn}E_t$$

Index n represents the direction of crushing.

2.3.4 Interface elements

No publications on SLA interface elements are available. However, interface elements are implemented in previous studies [22] and proven to work successfully. Still, appendix B contains a validation of the SLA interface elements on a four point bending test (without shear influence). It is assumed the following constitutive relation is valid:

$$\begin{bmatrix} \sigma_n \\ \sigma_t \end{bmatrix} = \begin{bmatrix} \kappa_n & 0 \\ 0 & \kappa_t \end{bmatrix} * \begin{bmatrix} u_n \\ u_t \end{bmatrix}$$

The Diana program offers two options with respect to shear reduction after cracking:

- Zero shear traction
- Constant shear retention; a shear retention factor β has to be specified

2.3.5 Current state of development

The current state of development is identified by four ongoing research topics.

- Determine how to improve the procedure on finding the λ_{crit} for non-proportional loading.
- Coupling of the tensile and compression saw-tooth curves with respect to crack closure [22].
- Incorporate a biaxial failure envelope in the current Diana. A biaxial failure envelope is developed by DeJong but not yet validated or implemented in the current Diana version.
- Out-of-plane modelling is still in an early development stage.

This thesis contributes to the SLA development by validating the interface element with regards to shear deformation and by combining the SLA procedure with a lumping technique.

2.4 Conclusion of chapter 2

This chapter presented an overview of all relevant information within the scope of research. The summary on masonry characteristics will clarify the potential of the SLM approach during the upcoming chapter. Including the SLA procedure during chapter 6 contributes to the knowledge regarding lumping techniques, the SLA procedure, the SLM approach and the behaviour of SLA interface elements.

Chapter 3. Interpretation of the SLM theory

The current SLM theory is numerically validated and presented in the original SLM report [1]. It is concluded that the approach has the potential to be a universal tool for modelling in-plane masonry structures. This chapter will determine the potential of the approach by including literature from chapter 2. The analysis starts on an element level during paragraph 3.1. It will be determined what elements can account for collapse mechanisms and what elements can only cause deformation. The analysis during paragraph 3.2 will focus on structural behaviour. It is determined for which failure behaviour the SLM response is as expected and when this remains unclear. The thesis scope is thereafter set to analyse whether or not the SLM approach is able to represent this unclear failure behaviour. To ensure the research quality paragraph 3.3 describes how the boundary condition influence the SLM approach and thereby setting a standard for potential benchmarks. This chapters findings are summarized in paragraph 3.4.

3.1 Element clarification

The key of the SLM approach is lumping the tensile non-linearities into tension cut-off interface elements and compressive non-linearities into continuum elements. By distinguishing three types of interface elements a predefined crack pattern, applicable for masonry façade with openings, is formed. As mentioned in chapter 1 this thesis focusses on shear walls without openings and therefore the vertical interface elements serve no purpose in this clarification.

Graphically summarizes in figure 26 are the three remaining SLM element types necessary to analyse shear walls without openings. All elements contribute to the shear wall deformation capacity. However, the softening curves indicate only the continuum elements and the horizontal interface elements are able to reduce their resistance to zero, thereby representing failure. The infinite fracture energy assigned to the diagonal interface prevents it from failure. This means the SLM approach is unable to represent cases where diagonal shear failure causes collapse.

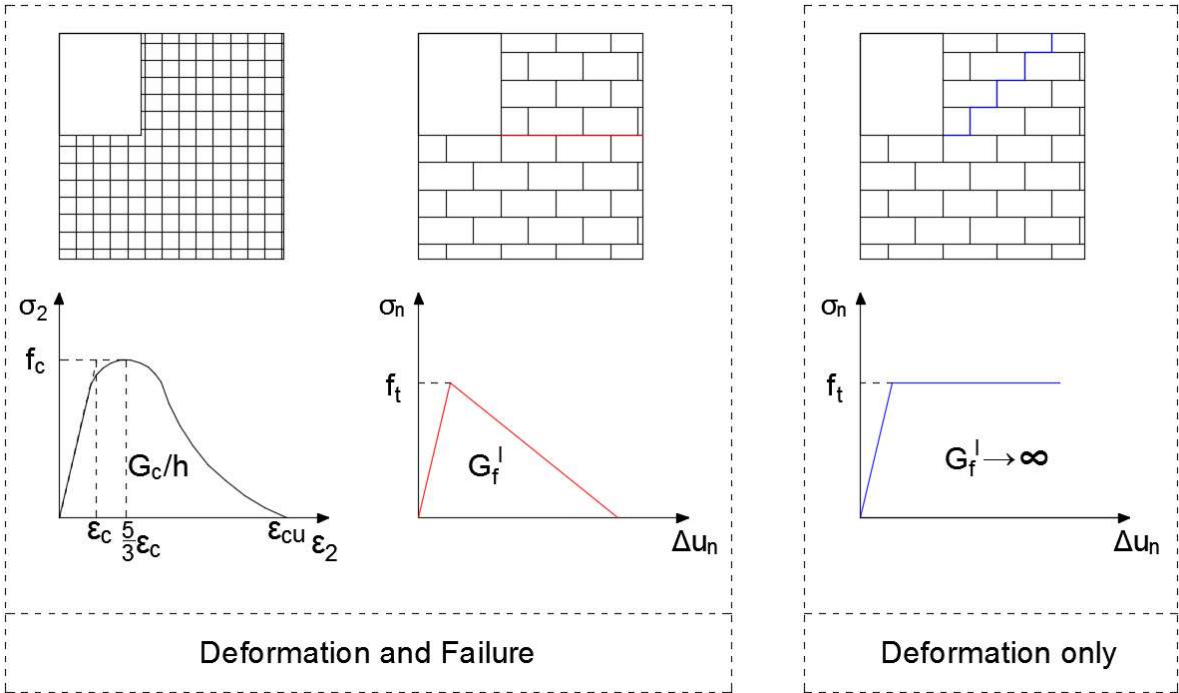


figure 26: SLM elements including the corresponding softening curves

Possible SLM collapse behaviour is either by failure of the horizontal interface elements or by failure of the continuum elements. Collapse by failure of the horizontal interface elements results in form of overturning (figure 27). According to literature this qualifies as loss of stability rather than a collapse mechanism. Therefore only crushing behaviour causes collapse of masonry shear walls within the SLM approach. This crushing behaviour is always a representation of toe crushing.

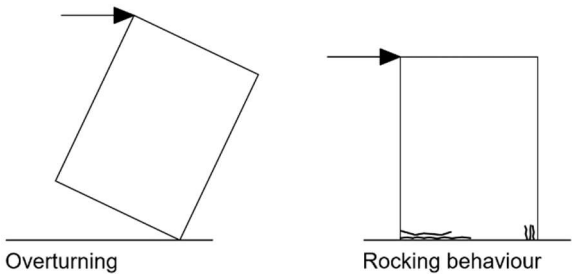


figure 27: Graphic representation of possible SLM collapse mechanisms

3.2 Possible failure behaviour

The analysis concerning the possible failure behaviour of the SLM approach is based on literature regarding the original SLM theory and the clarification of paragraph 3.1. During this analysis the thesis scope will become concrete and specified benchmark qualifications are determined.

The SLM theory states opening of the diagonal interface elements is due to a diagonal compressive strut causing deformation in perpendicular direction (figure 28, hollow arrows). This form of opening is considered a splitting type behaviour. A diagonal compressive strut forms itself after stress redistribution as a result of wall rotation. During this master thesis any form of wall rotation is considered part of rocking behaviour. Next to forming a compressive strut, wall rotation also leads to local compressive zones which eventually cause toe crushing. The influence of these compressive zones are addressed during chapter 5.

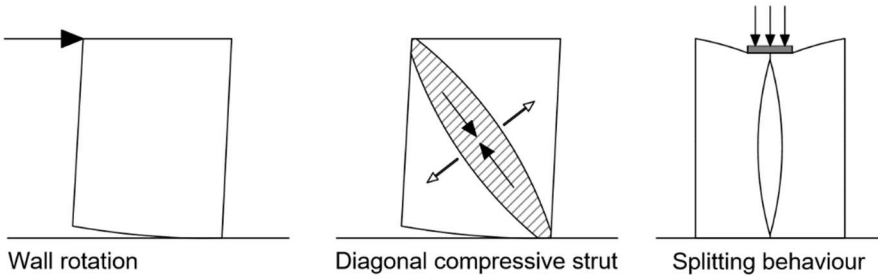
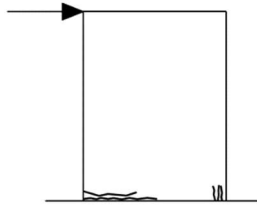


figure 28: Graphical representation of wall rotation (left), the compressive strut principle causing deformation in perpendicular direction (hollow arrows)(middle), splitting phenomenon (right)

As described in literature section 2.1.2, possible shear wall failure mechanisms are rocking, horizontal sliding, stepwise diagonal sliding and diagonal cracking. The next section discusses which of these four failure mechanism can be represented by the SLM approach.

1. Failure mechanisms correctly represented by the SLM approach

At this point, rocking behaviour is the only failure mechanism for which it is guaranteed that the SLM response is correct. Lumping horizontal cracks into interface elements is a valid assumption, also during discrete modelling, and representing crushing by continuum elements is also generally accepted. On top of that, the original SLM report proves by numerous numerical validations rocking behaviour is correctly analysed by the SLM approach.

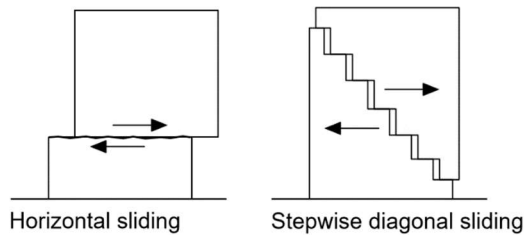


Rocking behaviour

figure 29: Possible SLM failure mode rocking

2. Failure mechanisms the SLM approach cannot represent

Horizontal sliding is a mode II shear failure. The SLM interface elements conform a tension cut-off criteria (section 2.2.2.1) thereby excluding cracking by shear deformation. Therefore the current SLM approach is unable to represent horizontal sliding.

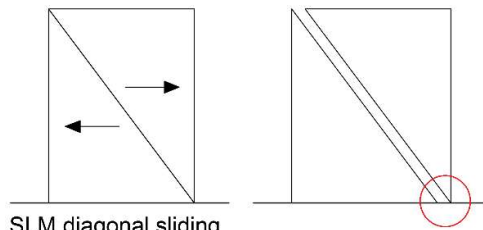


Horizontal sliding

Stepwise diagonal sliding

figure 30: Failure mechanism the SLM approach is not able to represent. The arrows indicate internal forces

Part of the stepwise diagonal sliding is also not representable by the SLM approach. Splitting the wall into two triangular parts is not possible because this would imply that the compressive corner area reduces to a single node and convergence problems would arise (figure 31). Also, as the internal forces show, this sliding behaviour is not conform the compressive strut analogy (figure 30). However, sliding of the bricks is included by the SLM approach via the infinite fracture energy assigned to the diagonal interface elements (section 2.2.1).

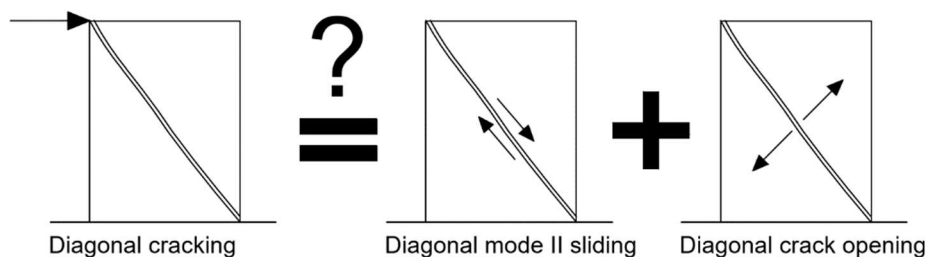


SLM diagonal sliding

figure 31: Impossible failure behaviour of the diagonal interface elements

3. Potential failure mechanisms of the SLM approach

The original SLM report documented promising results of modelling diagonal cracking with the SLM approach. However, it is unclear which requirements the diagonal interface elements need to possess in order to realistically represent this diagonal cracking. It is for that matter not even clear which internal forces cause diagonal cracking. Most likely it is a combination of diagonal sliding and diagonal crack opening (figure 32).



Diagonal cracking

Diagonal mode II sliding

Diagonal crack opening

figure 32: Is diagonal cracking a combination of sliding and crack opening?

Ensuring the SLM approach is capable of representing diagonal cracking in a realistic fashion would greatly enhance the method's value. The main thesis objective is therefore to clarify how the SLM approach analyses diagonal cracking.

To ensure research quality numerous demands will specify a valuable benchmark as is discussed in the upcoming paragraph. The previous section stated that diagonal cracking is always formed after rocking behaviour occurred. Therefore the numerical validations will be performed on a case where this combination is guaranteed.

The main thesis objective is to clarify how the SLM approach analyses diagonal cracking.

3.3 Free-end and fixed-end boundary conditions

The SLM ideology on selecting the correct predefined crack pattern is based on the flexibility of the shear wall's top end. A distinction is made between free-end and clamped-in shear walls (see section 2.2.2.3). This paragraph shows the influence of the different crack patterns on practical applications. This knowledge will determine which boundary condition is most suitable for the numerical SLM-validations along chapters 4 and 5.

Free-end shear wall

The diagonal strut of a free-end shear wall is expected to run from the toe of the wall to the centre top (figure 33). The intersection of diagonal and horizontal interface element is created by an intersection element. The original SLM report states intersection elements may cause locking problems. A second disadvantage of the free-end crack pattern is that interface elements are implemented where no potential crack is observed. This means incorrect failure mechanisms are possible within the SLM approach.

A third questionable aspect of free-end shear walls is which type of diagonal shear failure occurs. The next section 3.3.1 contains an example from the original SLM report where it is attempted to analyse stepwise diagonal sliding with the SLM approach. As stated before this is not possible and an incorrect failure pattern is obtained.

The three described aspects concerning the SLM free-end shear wall failure behaviour indicate further research is recommended. This is not within the research scope of this thesis and therefore free-end shear walls are not qualified for analysing diagonal cracking behaviour.

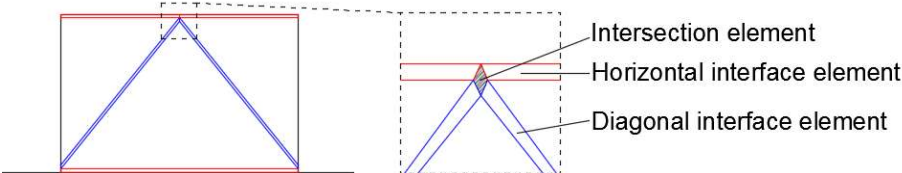


figure 33: free-end SLM shear wall, intersection of interfaces

Clamped-in shear wall

The predefined crack pattern proposed for clamped-in shear walls is presented in figure 34. Modelling two diagonal struts allow for diagonal shear failure in both directions but also creates an intersection element (figure 34a). As mentioned earlier this intersection element may cause locking problems. Within the research scope avoidance of this issues is preferred. For monotonically loaded shear walls the diagonal strut direction is self-evident and therefore a single diagonal strut will suffice (figure 34b). This single strut approach avoids the need for an intersection element. The connection between the diagonal and horizontal interface elements at the toe of the wall is possible without such an intersection element (figure 35).

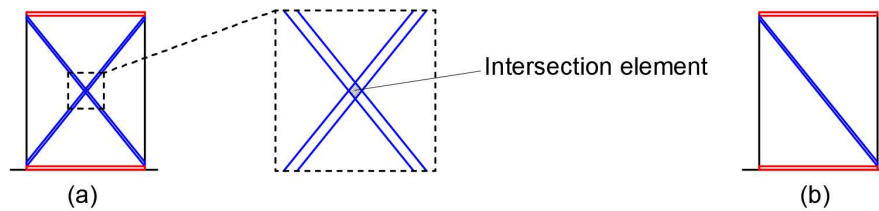


figure 34: Fixed-end shear wall with intersection element (a), solution of single diagonal strut (b)

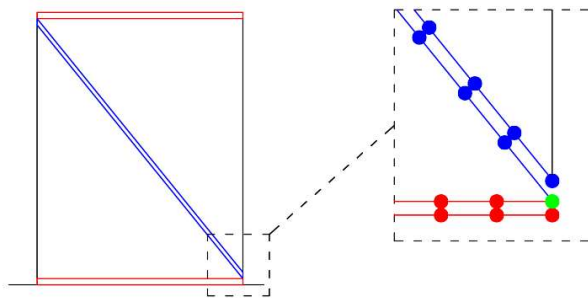


figure 35: The corner connection of interface elements on a FE level

The validation studies performed during chapter 4 and chapter 5 are all on single strut clamped-in benchmarks. By selecting a clamped-in benchmark where the experimental results state failure behaviour as a combination of rocking and diagonal shear failure it will be clear how the SLM approach represent diagonal cracking.

As mentioned earlier, this paragraph contains a numerical validation of the ETH Zurich wall 1 which is presented on the next pages. This validation shows stepwise diagonal sliding cannot be represented by the SLM approach and that diagonal shear failure of a free-end shear wall is not by definition caused by a compressive strut.

3.3.1 ETH Zurich wall 1 – Free-end shear wall validation

Specimen W1 is the first of seven hollow clay shear walls tested by Ganz and Thürlimann. A single panel with flanges at both ends is hold between two concrete slabs. The bottom slab is fixed to the floor where the top slab is free to move. A non-proportional distributed force with a resultant of 415kN in combination with a proportional displacement load (F_d) will cause the wall to collapse. A ductile response is observed with tensile and shear failure along the stepwise diagonal crack (figure 37) resulting in a peak load of 263 kN under a top displacement of 7.6mm. Failure of the flanges is observed as a result of the diagonal shear failure, no horizontal cracks are observed.

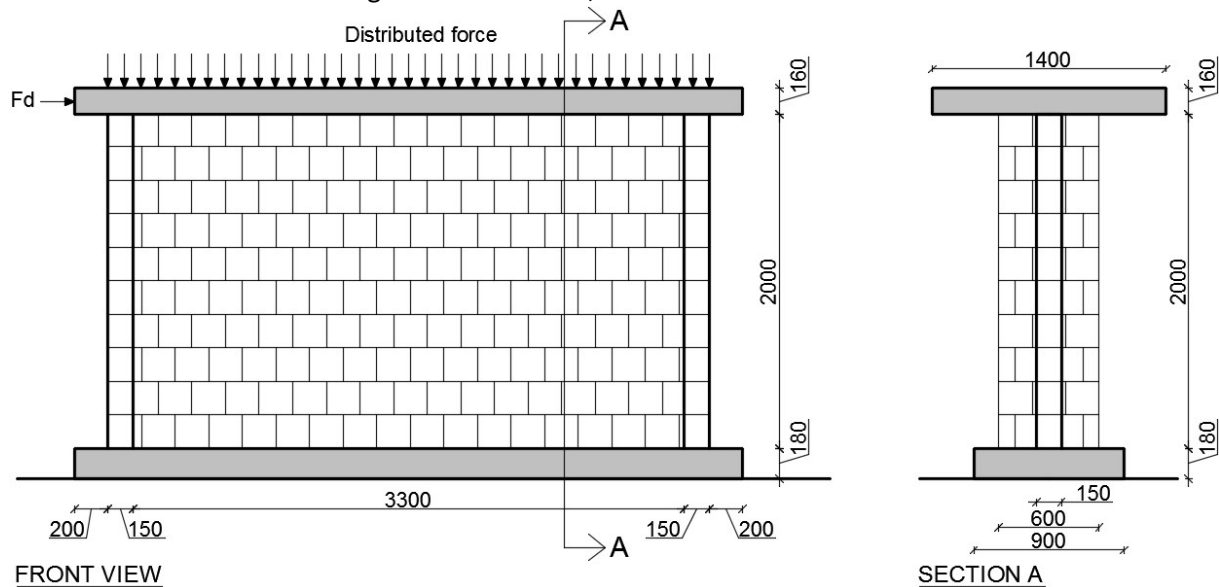


figure 36: Geometry ETH Zurich wall 1

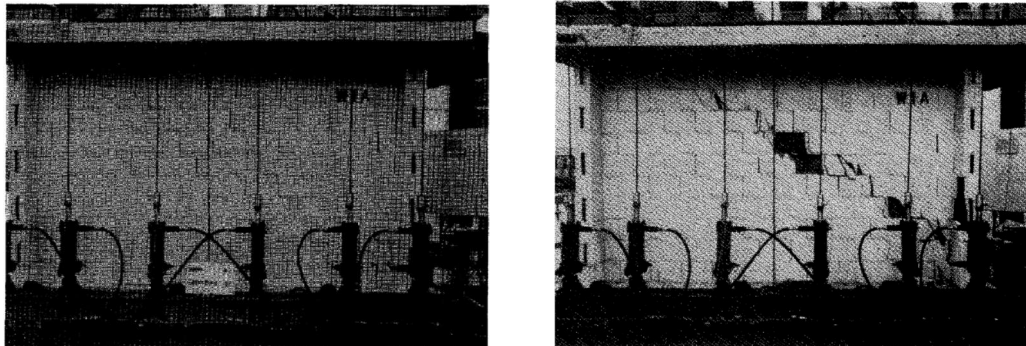


figure 37: failure mechanism ETH Zurich wall 1 [Ganz and Thürlimann]

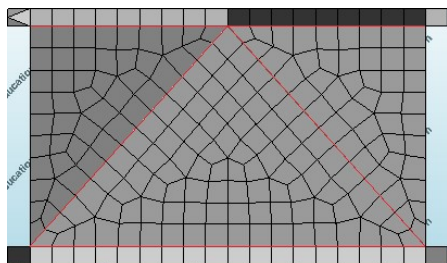


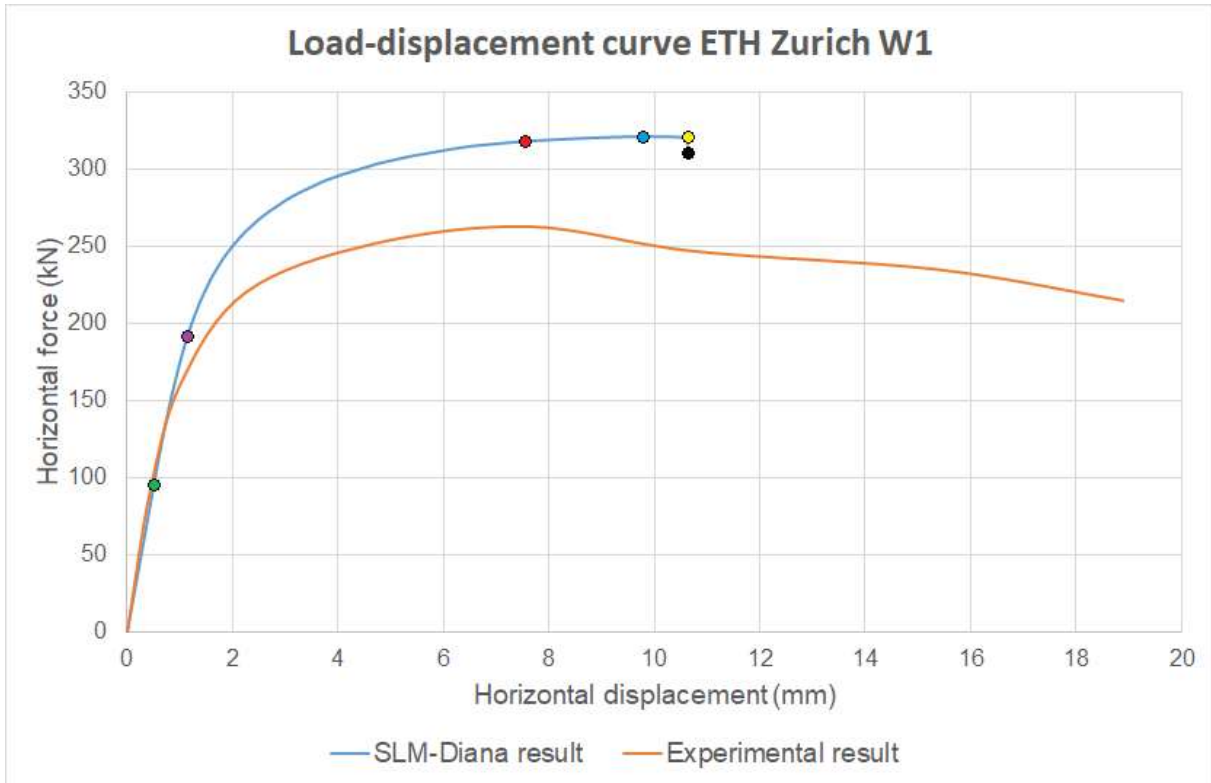
figure 38: Diana mesh (interface elements are indicated in red)

E	3000 N/mm ²
ν	0.2 [-]
f_t	0.03 N/mm ²
G_f	0.02 N/mm
f_c	7.6 N/mm ²
G_c	10 N/mm

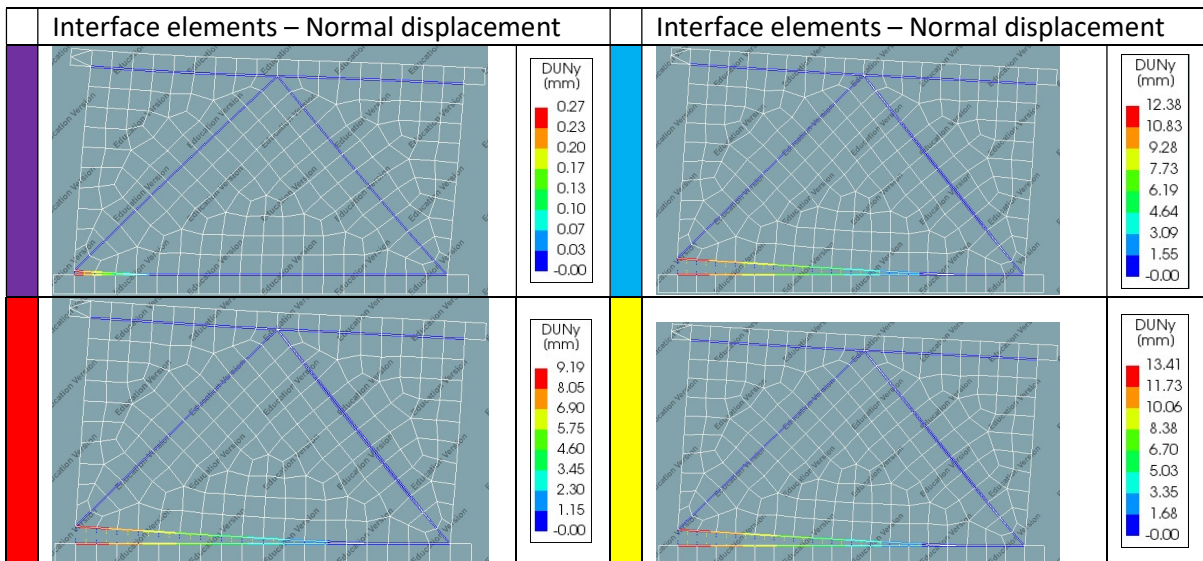
table 1: Material properties

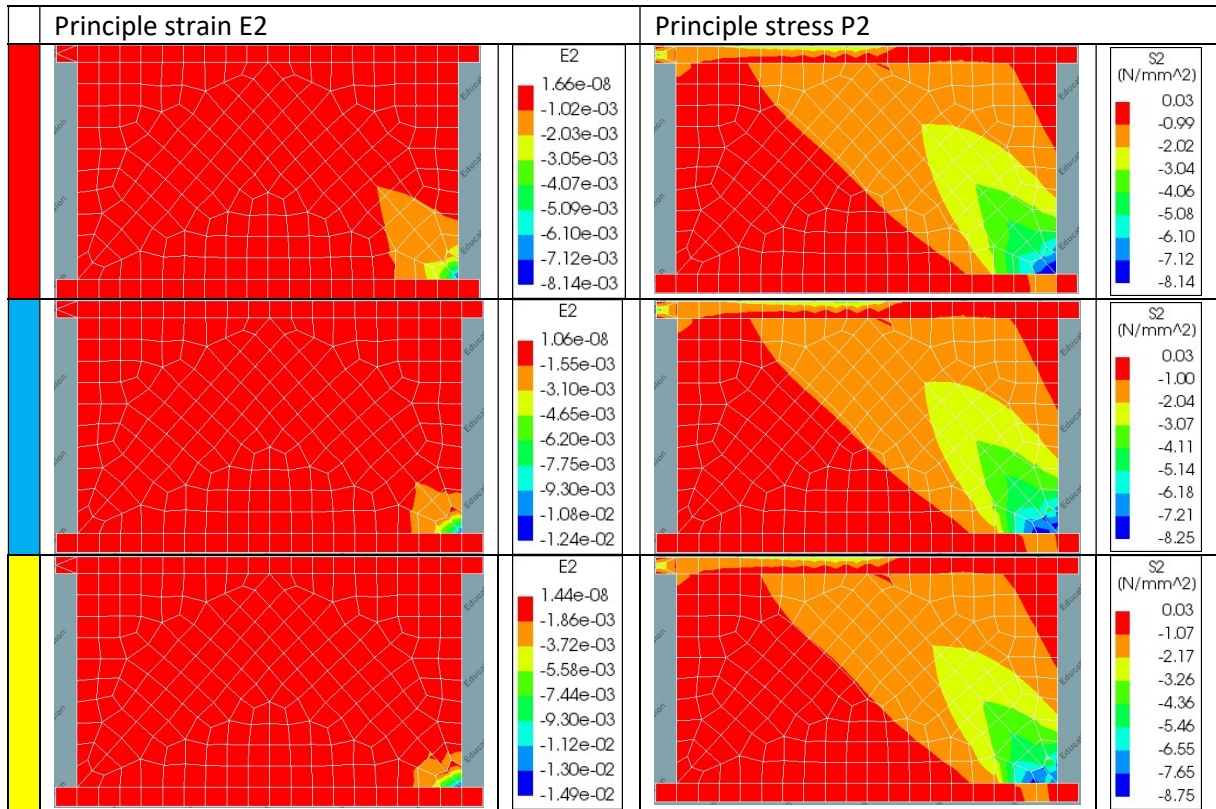
The Diana analysis is performed with the material properties of table 1 and interface elements with a length of 200mm (brick length) forming a mesh containing ± 200 elements. The original SLM rapport [1] states the assumption of removing the flanges in the model as valid since this is in line with SLM philosophy, this assumption is also adopted during this validation study.

Diana results



Point	Description	Displacement	Load
Green	First horizontal interface element opening	0.51 mm	97 kN
Purple	First diagonal interface element opening	1.07 mm	183 kN
Red	Start of compressive toe softening	7.83 mm	318 kN
Blue	Peak resistance	9.93 mm	321 kN
Yellow	Last converged step	10.62 mm	319 kN
Black	No convergence after 50 iterations	-	-





As the Diana result shows, the failure mode starts with opening of the bottom horizontal interface elements followed by limited opening of the diagonal interface elements. By increasing the horizontal displacement of the top concrete slab the horizontal interface elements open even further resulting in an extreme local compression zone at the right toe of the wall. Softening of this local compression zone leads to extreme redistribution and continuation of the analysis is no longer possible.

The experimental behaviour is described as diagonal shear failure (possibly in combination with toe crushing). No horizontal cracking at the base is observed, this is however the leading mechanism of the SLM approach. This incorrect failure mode leads to no convergence at a 10.63 mm forced displacement and a small overshoot of resistance. Coincided, the influence of the diagonal interface elements appears to be limited, no clear opening is observed.

Validation of the SLM theory with the ETH Zurich wall 1 confirms free-end shear walls are to handle with caution. The stepwise diagonal shear described as the experimental failure behaviour cannot be obtained with the SLM approach and is replaced by rocking behaviour. A similar response is described in the original SLM report (figure 39).

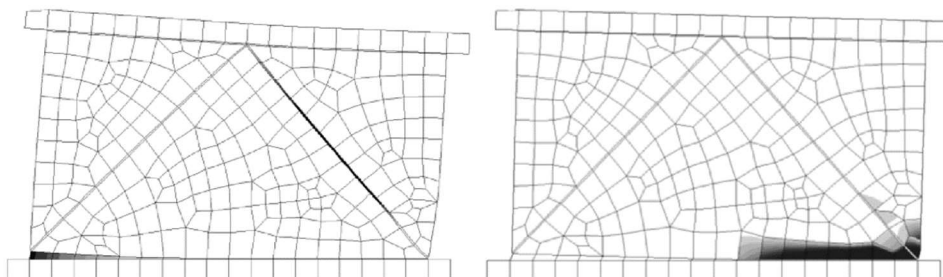


figure 39: Rocking behaviour leading to toe crushing presented in original SLM report [1]

3.4 Conclusion chapter 3

The literary research narrows the thesis scope to an investigation on how the SLM approach represents diagonal cracking. This investigation will be executed by numerical validations during chapter 4. The validation study will be performed on a clamped-in shear wall with a single diagonal strut to ensure the correct failure behaviour is obtained.

Interpretation of the SLM element description provided by the original report led to the conclusion that shear wall collapse is always the result of crushing. By including structural behaviour only toe crushing appears to suffice the crushing criteria. In term of deformation rocking behaviour is the starting failure mechanism of the SLM approach and diagonal shear failure may follow. Therefore diagonal shear failure by itself cannot be represented by the SLM approach. This is confirmed by the interpretation of element types during paragraph 3.1. A second behaviour the SLM approach is unable to represent is horizontal sliding where the shear wall is divided in two parts. However, being able to validate rocking behaviour in combination with diagonal cracking would still classify the SLM approach as a powerful tool regarding in-plane masonry storey mechanisms. The upcoming chapters 4 and 5 will validate whether the SLM approach is indeed able to represent diagonal cracking via tension cut-off interface elements.

Chapter 4. Numerical validation of the SLM approach

The previous chapter states that the main objective for this master thesis is to clarify how the SLM approach analyses diagonal cracking. The present information indicates that via splitting behaviour the diagonal interface elements should open as a result of the compressive diagonal strut. It is not yet established if this splitting behaviour by itself is a correct cracking representation. Furthermore, it is unknown what numerical input should be applied for the interface elements. The original SLM report doesn't present the input settings of any interface element. This chapter will state the settings required to represent diagonal cracking with interface elements. The fixed-end TU Eindhoven wall is used for all validation studies because it perfectly fits the criteria set in chapter 3. The SLM validation during paragraph 4.1 will determine if a correct failure behaviour is obtained when commonly accepted interface input values are applied. By comparing the obtained results with the original SLM report a general expansion of the theory is achieved (paragraph 4.2). Paragraph 4.3 will study the potential diagonal sliding influence by performing a variation study regarding after crack shear deformation. The findings on how the SLM approach represents diagonal cracking are presented in paragraph 4.4.

Input clarification

The material properties of the TU Eindhoven wall are well presented in the original SLM report, but the applied dummy stiffness values are unknown. The theory of the original SLM report states a constant shear retention factor β of 0.01 is applied and this value will be applied during this validation as well. For the dummy stiffnesses κ_n and κ_t it is assumed any realistic value may be applied, leading to the following choices:

$$\kappa_n = 10^6 \text{ N/mm}^3$$

$$\kappa_t = 10^6 \text{ N/mm}^3$$

$$\beta\kappa_t = 10^4 \text{ N/mm}^3$$

To put the dummy stiffness values into perspective the next calculations correspond the stiffness of a dimensionless interface element to the stiffness of a masonry wall with height H . The masonry stiffness applied in the original SLM report is 3000 N/mm^2 .

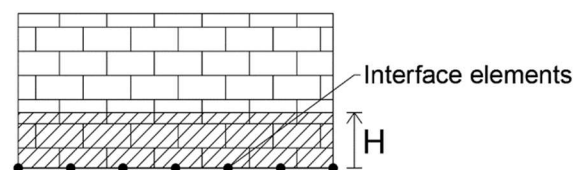


figure 40: Graphic representation of H

The dummy stiffness in normal direction is corresponding to a stiffness of a masonry wall with height $H = E_{\text{masonry}}/\kappa_n = 3000/10^6 = 3 \cdot 10^{-3} \text{ mm}$ and is considered correctly represented by a dimensionless height. The dummy stiffness in shear direction is corresponding to a stiffness of a masonry wall with height $H = G_{\text{masonry}}/\kappa_t = (E_{\text{masonry}} / (2 \cdot (1 + \nu))) / \kappa_t = (3000 / (2 \cdot (1 + 0.2))) / 10^6 = 1.25 \cdot 10^{-3} \text{ mm}$ and is also considered correctly represented by a dimensionless height.

By adding the dummy stiffness values to the material characteristics all required input is available. The next section starts the SLM validation on the TU Eindhoven wall without openings [31].

4.1 TU Eindhoven wall without opening (JDwall)

The TU Eindhoven wall without opening is a shear wall, made from 100mm thick solid clay bricks, clamped-in between two steel profiles. The wall is loaded in two phases, first a vertical, non-proportional, distributed load P of 30 N/mm presses the top steel beam down. The second phase starts with restraining the top profile of vertical movement and loading the profile with a horizontal, proportional, forced displacement F_d . The horizontal forced displacement causes horizontal cracks at the top and bottom corners setting the rocking mechanism in motion, followed by diagonal shear cracking and finally toe compressive failure. A peak resistance of 53 kN under a forced displacement of 2.6 mm is reached.

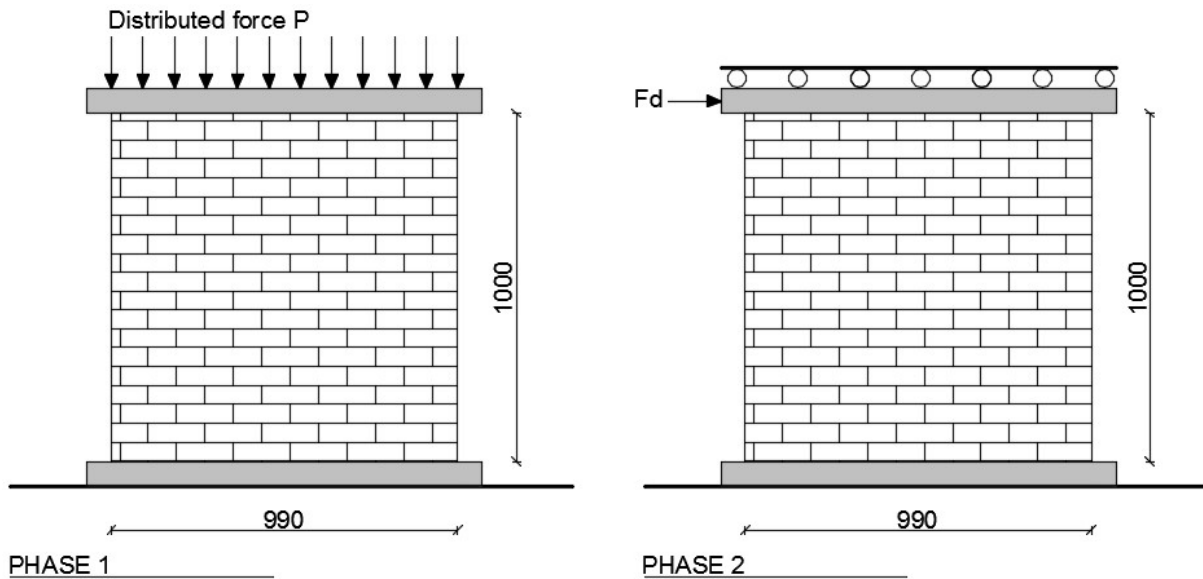


figure 41: Geometry TU Eindhoven wall

The Diana10 model contains the material characteristics presented in table 2 and is meshed with interface elements of length 200mm (brick length) resulting in mesh counting 66 elements. The overlap of the experimental crack pattern and the SLM predefined crack pattern is presented in figure 42.

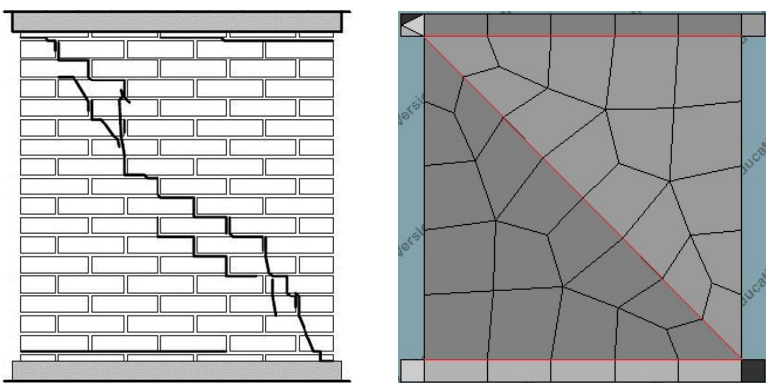
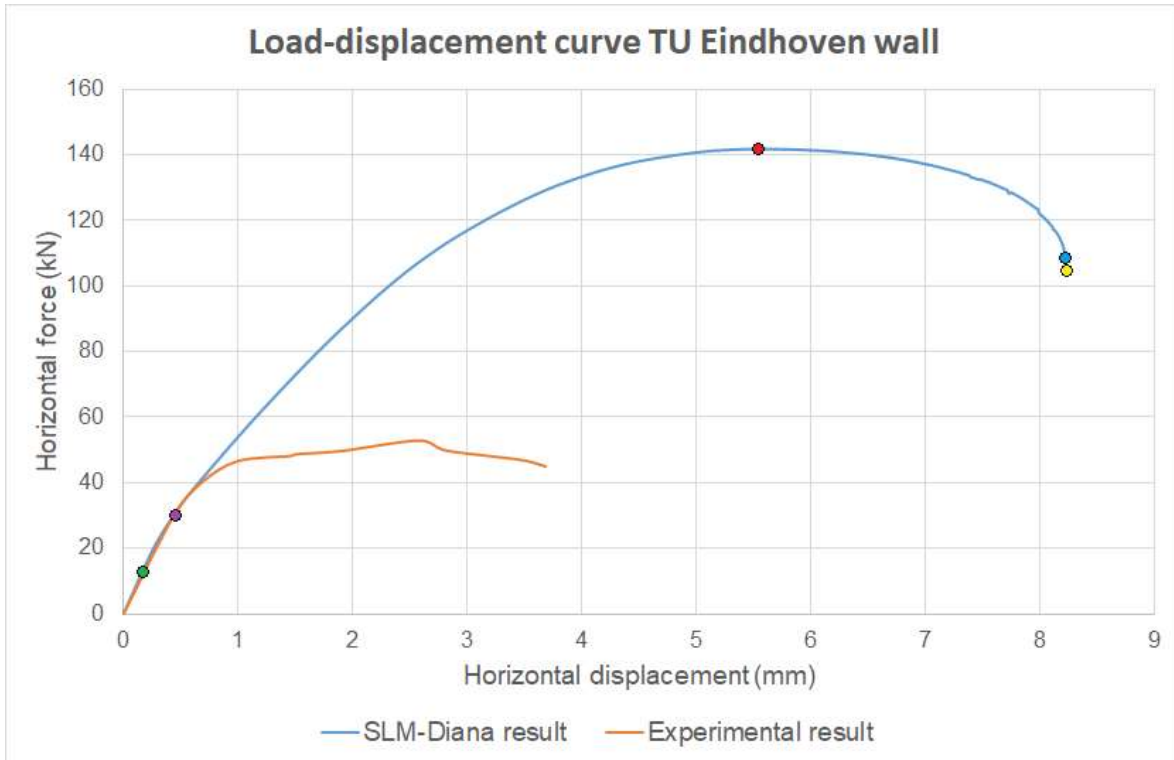


figure 42: Crack pattern JD4 (left)[31], Diana mesh (right)

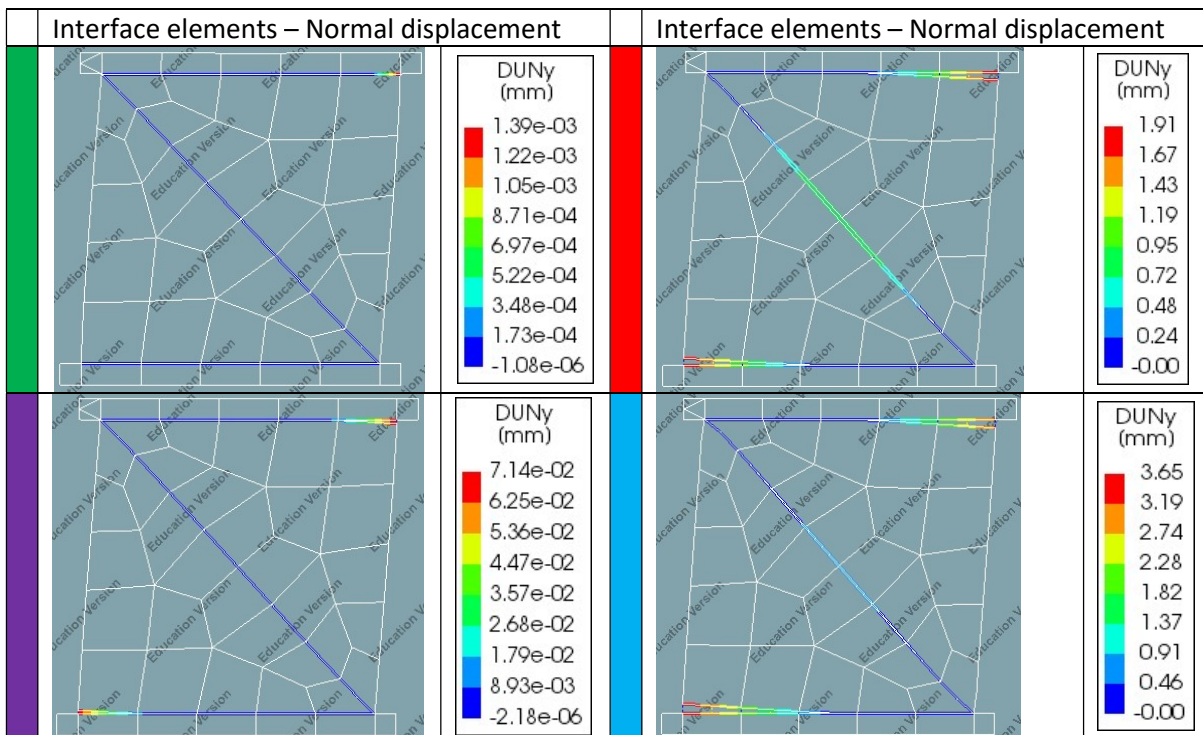
E	3000 N/mm ²
ν	0.2 [-]
f_t	0.25 N/mm ²
G_f	0.05 N/mm
f_c	6.0 N/mm ²
G_c	25 N/mm
K_n	10 ⁶ N/mm ³
K_t	10 ⁶ N/mm ³
β_{K_t}	10 ⁴ N/mm ³

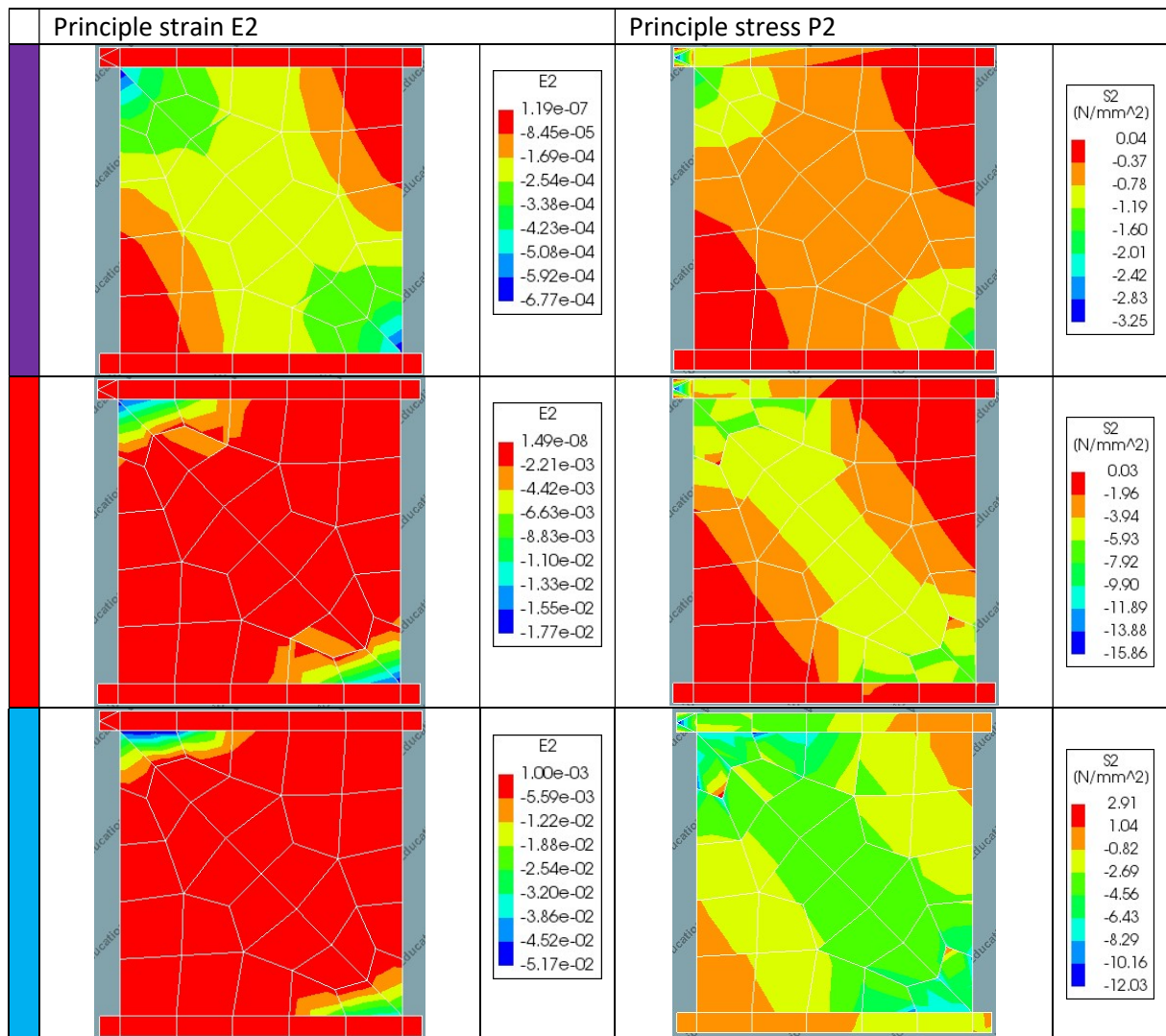
table 2: Material properties

Diana results



Point	Description	Displacement	Load
Green	Top corner horizontal interface element opening	0.16 mm	13 kN
Purple	Centre diagonal interface element opening	0.415 mm	29 kN
Red	Peak resistance	5.585 mm	142 kN
Blue	Last converged step	8.22 mm	108 kN
Yellow	No convergence after 50 iterations	-	-





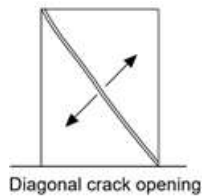
The steel profiles located the top and bottom of the wall are modelled with a Young's modulus of $2.1 \cdot 10^5 \text{ N/mm}^2$ causing the stress legend S2 to show stress levels which are significantly higher than the $f_{c,masonry}$ of 6.0 N/mm^2 .

The SLM approach results in a combination of rocking and diagonal shear failure, which is in accordance with the experimental result. In correspondence with the SLM theory the failure behaviour starts with opening of the horizontal interface elements at a forced displacement of 0.16mm (green) creating a compressive strut leading to the opening of the diagonal interface elements at a forced displacement of 0.415mm (purple). Continuing the forced displacement adds compressive toe softening to the failure pattern and a peak load of 142 kN under a forced horizontal displacement of 5.585mm is reached (red). After the peak load compressive softening becomes more severe and the load bearing resistance reduces until redistribution of forces no longer converges, the analysis stops.

Despite the correct failure mode a 90 kN overshoot of resistance is observed at a displacement twice as large as the experimental result indicate. The following paragraph focusses on the origin of this overshoot and will state how this can be solved.

4.2 Theoretical intermezzo – Shear deformation

The numerical validation in the previous paragraph is performed with a constant shear retention stiffness of 10^4 N/mm^3 . To put this into perspective, a $\beta\kappa_t$ of 10^4 N/mm^3 has a similar shear stiffness as a $H=0.125\text{mm}$ high masonry wall, this is considered stiff. As a results the diagonal interface elements represent only the crack opening part of diagonal cracking (figure 43).



Diagonal crack opening

figure 43: SLM option with a high $\beta\kappa_t$ value

By comparing the results from paragraph 4.1 to the original SLM results it becomes clear the diagonal interface elements must allow a form of shear deformation (figure 44).

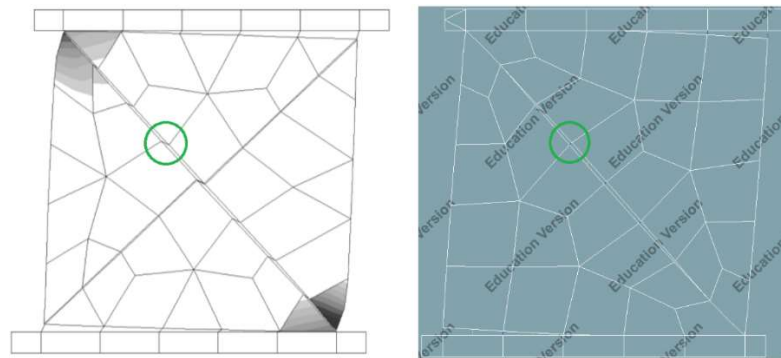


figure 44: Deformation figures of the original SLM report (left) [1] and the paragraph 4.1 result (right)

The tension cut-off interface elements may deform in shear direction but only after cracking has occurred. This deformation can be established by a constant shear setting with a low $\beta\kappa_t$ value or with the zero shear traction setting. Unfortunately the Diana 10.1 version contains a programming error regarding the constant shear retention setting that is of a significant influence on the SLM approach. Appendix A will address this error and its consequences in detail. The upcoming shear deformation study is therefore performed with the zero shear traction setting.

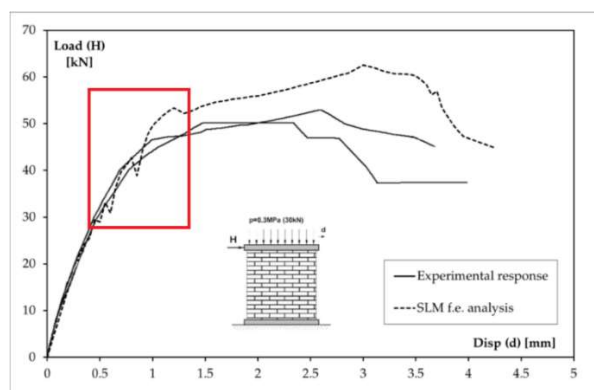


figure 45: Load-displacement curve of the original SLM report [1]

A second phenomenon observed, while comparing the paragraph 4.1 results with SLM report, is the sudden strength drops in the report's load-displacement curve (figure 45, red box). The upcoming paragraph will show the correspondence between the shear deformation and these sudden drops of load-bearing strength via a numerical validation.

4.3 Zero shear traction after cracking

During the previous section it is proposed to allow for shear deformation of the diagonal strut via the zero shear traction setting. Before showing the results of this proposition the zero shear stiffness theory is described including its protentional on the SLM approach.

Theory

Zero shear stiffness after cracking represents brittle shear failure (figure 46). Immediately after cracking in normal direction the shear strength drops to zero. This allows horizontal movement without any stiffness restriction. Opening of a single node already allows this node to move freely in shear direction (figure 47). By separating the top and bottom nodes the shear strength of the entire interface element reduces to zero.

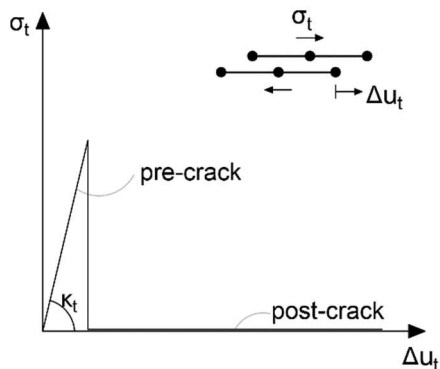


figure 46: Softening curve in shear direction

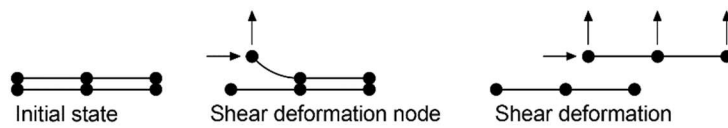


figure 47: Horizontal deformation as a result of zero shear traction

As mentioned in the previous paragraph, a shear stiffness of $\beta_{kt} = 10^4 \text{ N/mm}^3$ is considered stiff and does not allow for any shear deformation of the diagonal strut. In other words, the interface nodes can only move perpendicular to the diagonal strut. Via the zero shear traction setting the interface nodes are no longer restricted to this perpendicular path. As a result the diagonal strut is more flexible after cracking (figure 48).

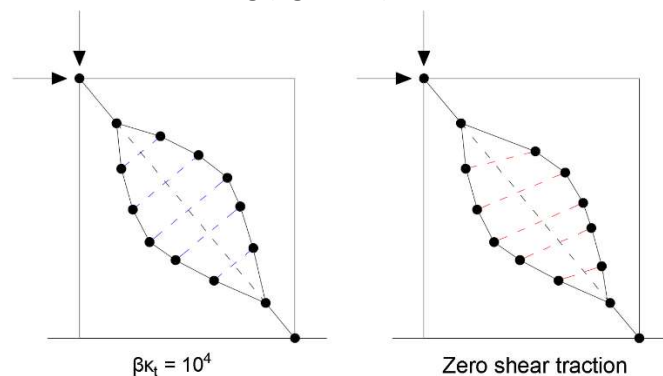
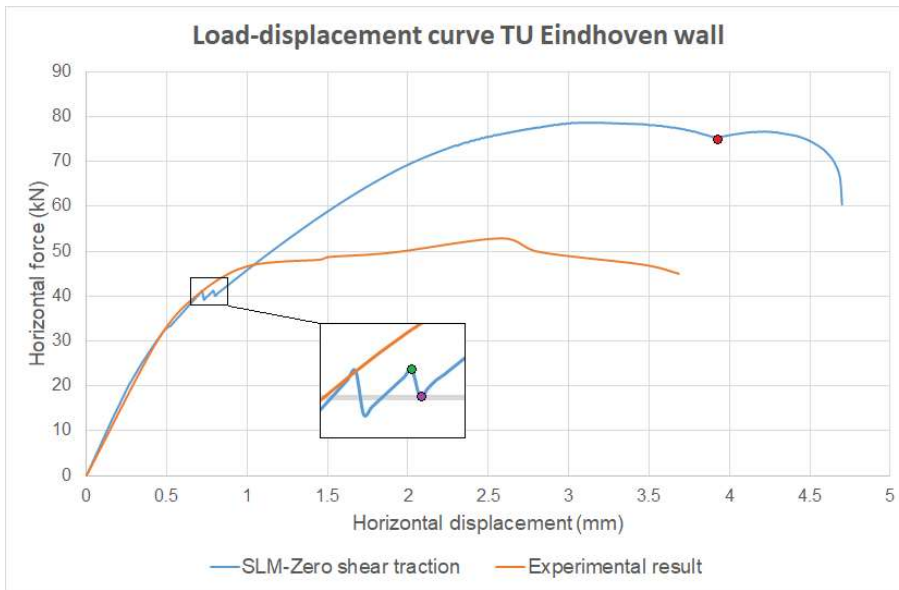


figure 48: The constant shear retention setting of $\beta_{kt}=10^4 \text{ N/mm}^3$ restricts the nodes to move only perpendicular to the diagonal strut. The zero shear traction setting does allow for shear deformation along the diagonal strut.

Results – Zero shear traction

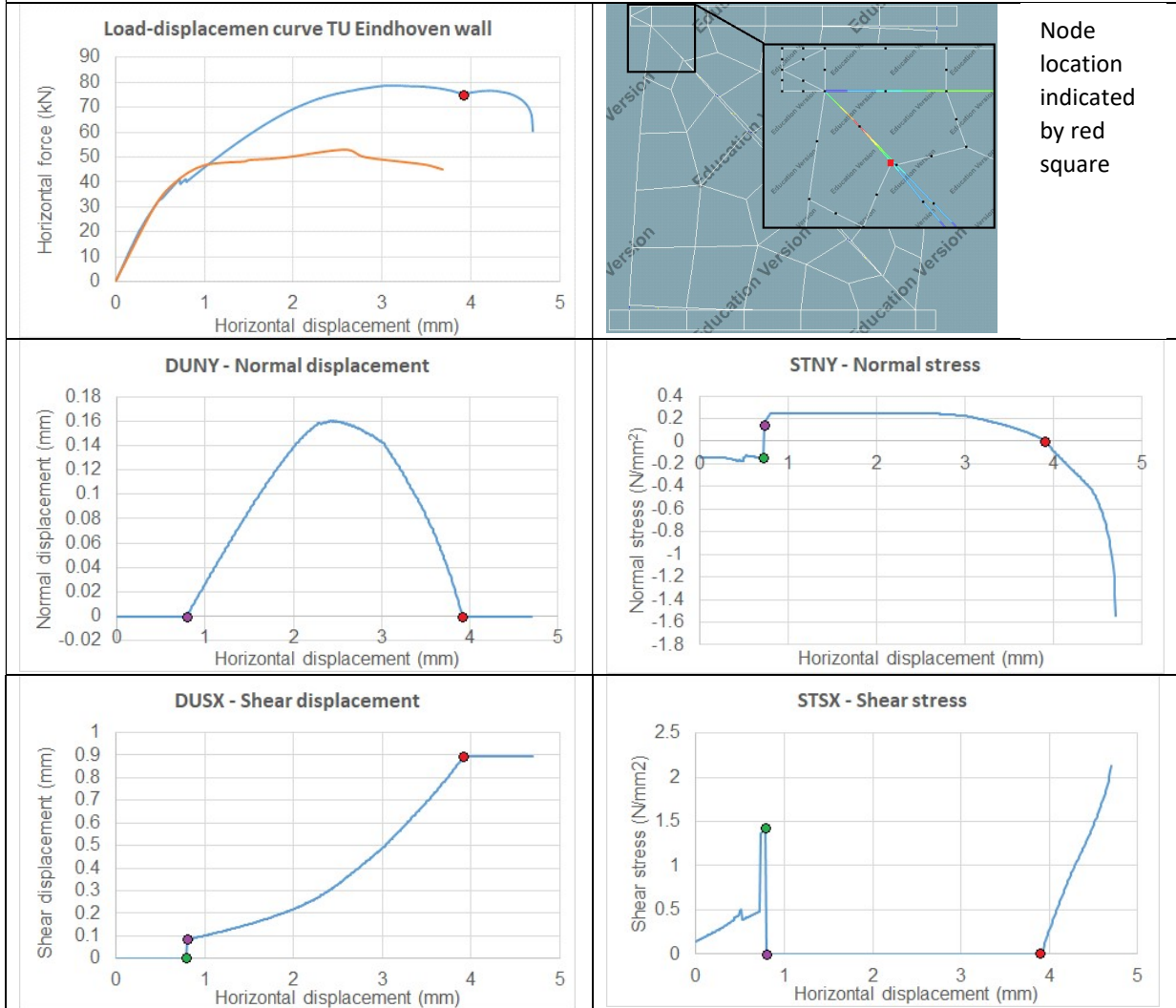
The following two pages present the zero shear traction results. The sudden strength drops in the load-displacement curve are the results of sudden shear deformation. By plotting the behaviour of the top diagonal corner element this phenomenon becomes visible.



Point	Description	Displacement	Load
Green	Last step of closed corner diagonal strut	0.79 mm	41.2 kN
Purple	Shear displacement of corner interface elements	0.80 mm	40.0 kN
Red	Closing of interface element	3.92 mm	75.0 kN



Nodal results in normal and shear direction – Zero shear traction



The influence of the zero shear traction after cracking is represented correct by the DUSX and STSX graphs. Opening of the corner interface element (green dot) causes the shear strength to drop to zero (STSX, purple dot) and shear deformation is possible (DUSX). As indicated in the load-displacement curve, this phenomenon causes the abrupt strength drops of the resistance curve.

As the literature study of chapter 2 describes, closing of the interface element in normal direction reduces the stiffness via secant unloading. When the normal displacement reduces to zero the initial stiffness is regained. During this validation the corner element closes at a horizontal displacement of 3.92mm (red dot) and sets the stiffness in normal and shear direction back to the initial 10^6 N/mm^3 . The only difference with the initial state is a displacement in shear direction (figure 49), which in this case is 0.9 mm (DUSX-graph).

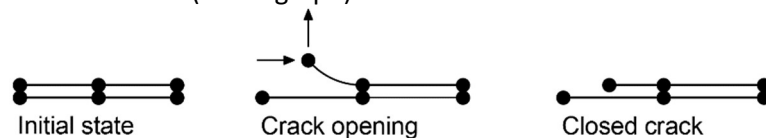


figure 49: Shear deformation after crack closure

In conclusion, setting the shear deformation after cracking to zero shear traction leads to promising results and proves that the SLM approach is in need of shear deformation along the diagonal strut to avoid extreme overshoots of load-bearing resistance.

4.4 Conclusion chapter 4

Shear deformation along the diagonal strut has proven to be of great importance for the SLM analogy. Zero shear traction is a possible setting to allow shear displacement along the diagonal strut. This setting reduced the overshoot of resistance during the TU Eindhoven wall validation significantly, but still an overshoot is obtained. The upcoming chapter will address how to reduce this overshoot.

By allowing shear deformation along the diagonal strut the structural response is changed. Opening of the diagonal strut now has two stages. The first stage is crack opening as a result of splitting behaviour. After several interface elements are open the second stage becomes active where sliding along the strut is also achieved (figure 50). The performed validation study indicates the SLM approach represent diagonal cracking as a splitting-sliding combination leading to realistic failure behaviour and promising results.

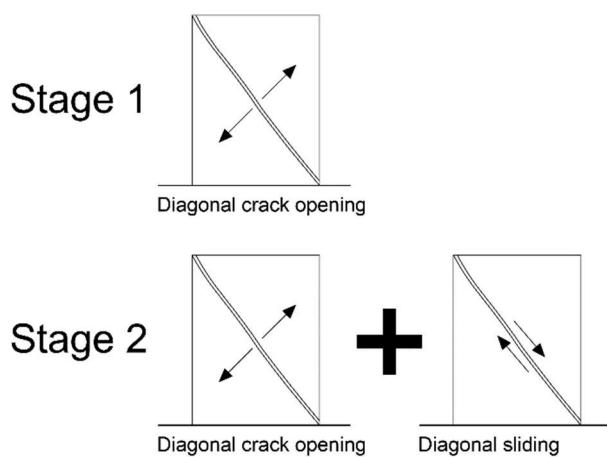


figure 50: SLM approach; Stage 1: opening of diagonal strut by splitting behaviour, Stage 2: after sufficient opening diagonal sliding behaviour is represented as well.

This chapter showed that the splitting-sliding combination is a crucial part of the SLM approach. The next step for the SLM validation study is to discover the influence of modelling diagonal crack opening as a splitting type behaviour. This will be done during the upcoming chapter.

Chapter 5. Splitting behaviour

As presented in the previous chapter, the SLM approach represents diagonal cracking by interface elements in a form of splitting and sliding behaviour. Splitting behaviour is the result of a diagonal compressive strut pushing the interface elements open. To form the compressive strut rocking behaviour must have taken place. The combination of rocking and splitting behaviour results in a very local compressive zone at the wall's toe. This chapter will show the influence of these local compressive zones on the splitting behaviour by introducing a new theoretical part followed by numerical validations.

5.1 Theory of splitting behaviour by interface elements

As mentioned during the introduction, the compressive diagonal strut is a result of rocking behaviour forming localized compressive zones by the toes of the wall. These localized compressive zones ensure the corner diagonal interface elements remain closed for at least half their length (figure 51). Full opening of this element by a splitting type behaviour would result in a dimensionless compressive area and convergence issues occur.

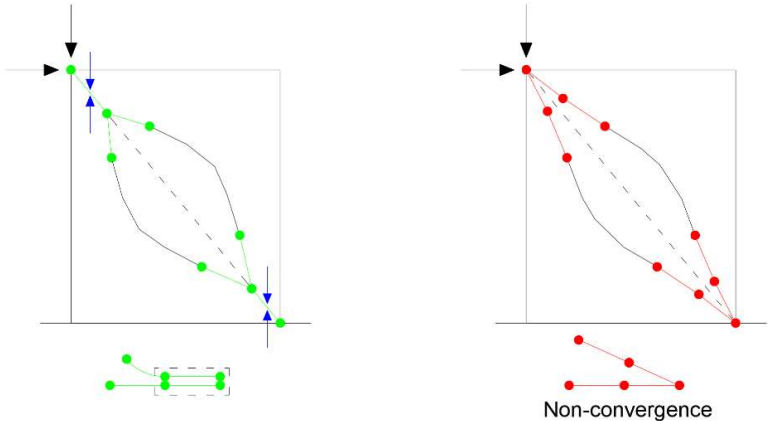


figure 51: Internal forces (blue) keeping half the corner interface element closed, thereby avoiding convergence issues

By keeping half the interface element closed the length of the interface element could be decisive on the flexibility of opening. In other words, small interface elements may allow the diagonal opening to be wider, where larger interface elements may restrict this opening (figure 52). Secondly, the sliding capacity may depend on the opening length of the diagonal strut. Smaller elements therefore not only allow for a wider opening but might also form a larger sliding length to increase flexibility.

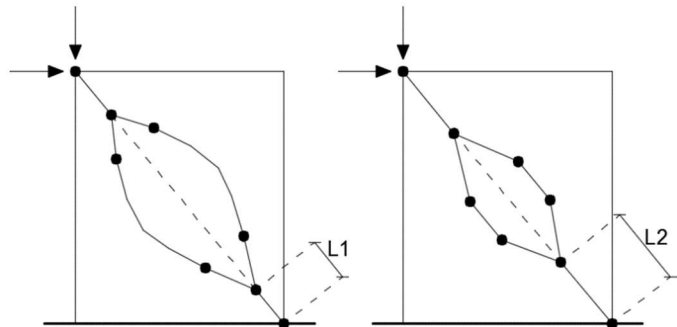


figure 52: Possible influence of the corner diagonal interface element length resulting in a flexible opening of the diagonal strut (left) or a restricted opening (right) when $L2 \gg L1$

To validate if the diagonal interface element length influences the SLM procedure a variation study is performed during chapter 5.2.

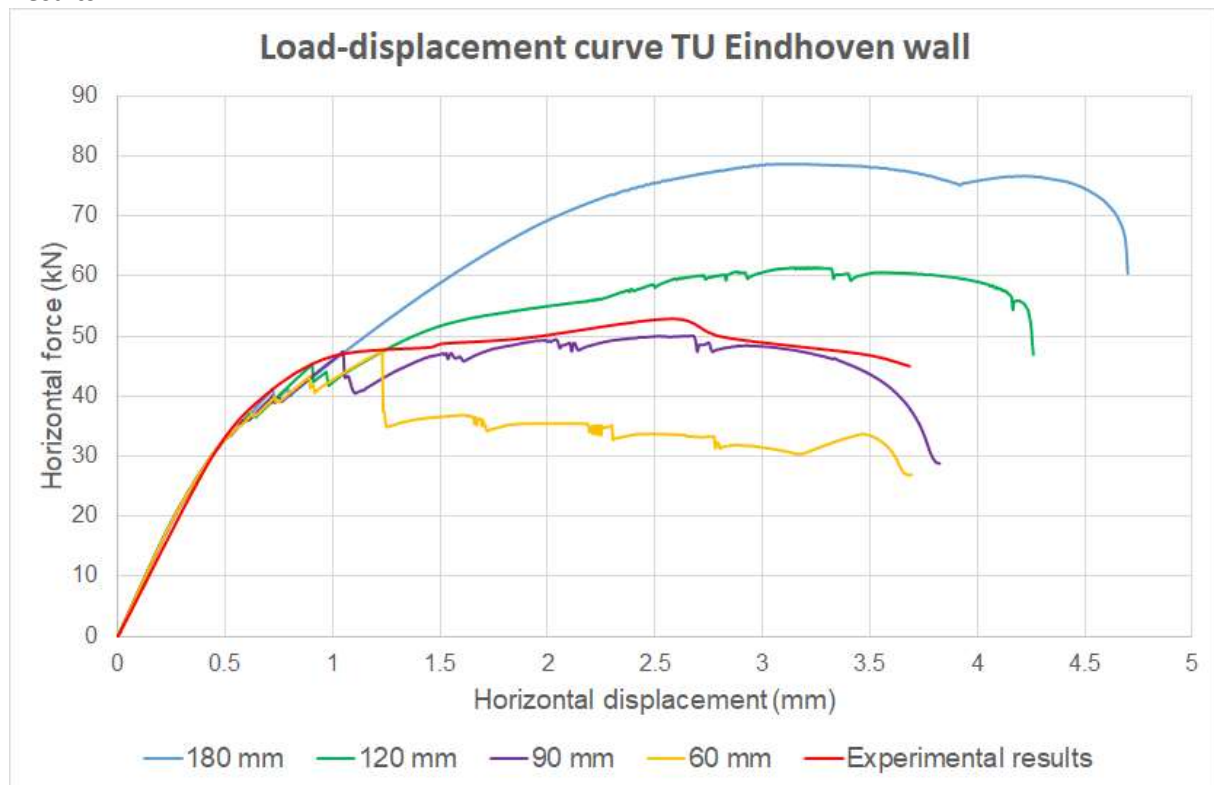
5.2 Mesh dependence study

The theory of paragraph 5.1 proposes a study with respect to mesh dependence because the diagonal interface elements length may influence the opening potential of the diagonal strut. The results obtained during chapter 4 are an overestimation of resistance and therefore this mesh dependence study will validate the TU Eindhoven wall with refined meshes. As displayed in table 3 the original length of 180mm will be reduced to 120mm, 90mm and 60mm, thereby reducing the closed percentage of the diagonal strut.

Length diagonal interface elements	Percentage closed
180 mm	12.8%
120 mm	8.5%
90 mm	6.4%
60 mm	4.3%

table 3: Mesh variants based on the length of diagonal interface elements

Results



The load-displacement curve shows that four different mesh variations result in four different responses. Hence, no convergence to the experimental response is obtained. This is identified as a form of mesh dependence.

A reduction of the interface element length influences the failure behaviour of the structure. Section 5.2.1 will address this in finer detail by comparing the splitting and sliding behaviour of all mesh variations.

Furthermore, mesh refinement may lead to convergence issues. The 90mm and 60mm responses contain a number of steps where no convergence is obtained. The option 'continue without convergence' had to be applied. A possible cause of this non-convergence will be addressed during the final part of section 5.2.1.

5.2.1 Mesh dependence study – Structural behaviour

The previous sections showed mesh refinement leads to a reduction of load-bearing resistance. This coincides with a change in failure behaviour of the diagonal strut. By plotting the normal and shear displacement of the centre diagonal element it becomes clear mesh refinement reduces the splitting influence (figure 53) and at the same time increases the shear deformation.

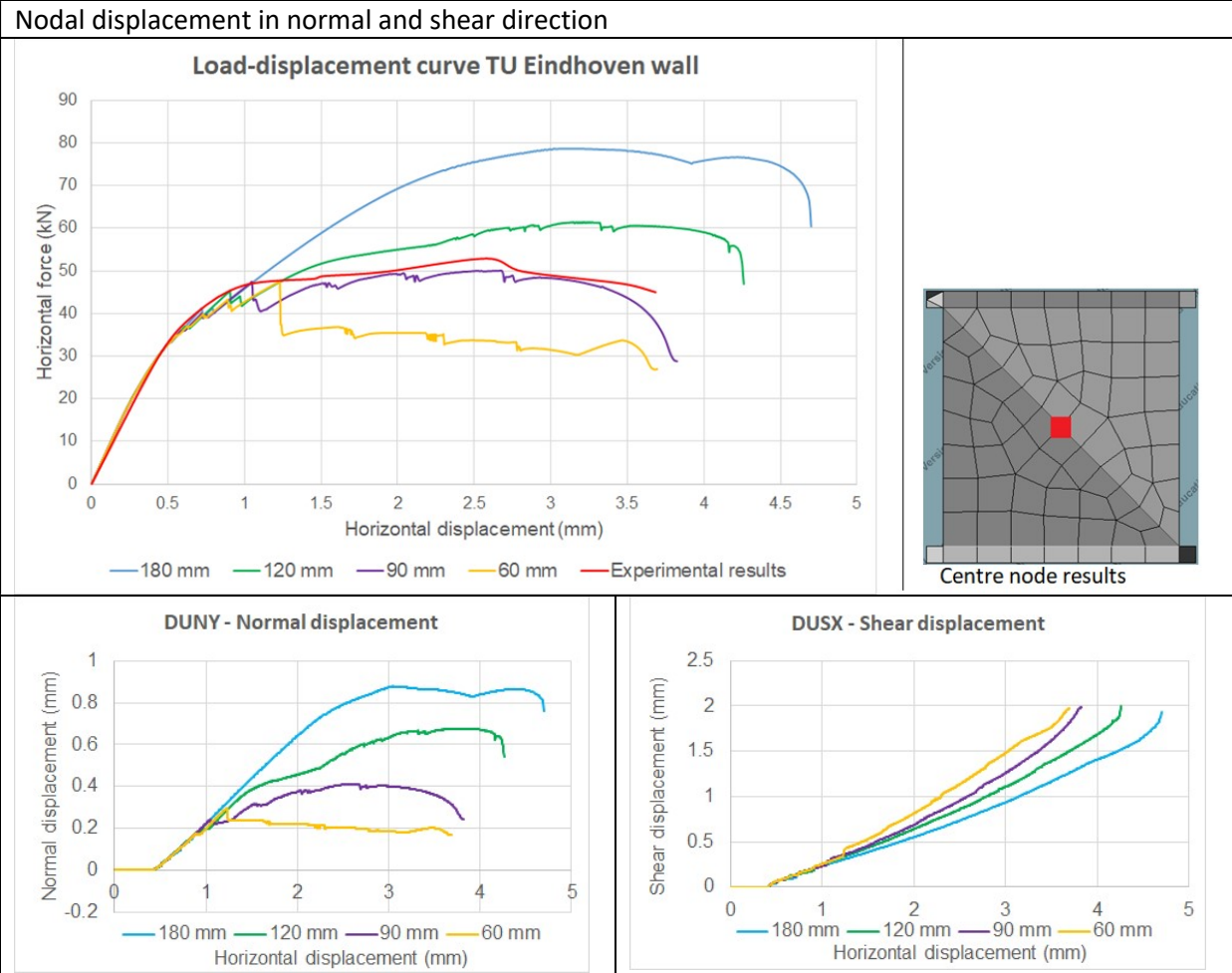


figure 53: Normal and shear deformation of diagonal centre node

The observed results from figure 53 indicate that the splitting-sliding relation of the diagonal strut is influenced by mesh choice. Further studies towards this relation are recommended.

Analysing the mesh refinement on an element level leads to the following observation. The 180mm mesh shows that a larger corner element opens for a longer period of time, thereby activating the plastic softening behaviour (figure 54). This increase in opening is caused by the splitting behaviour that remains valid for almost the entire analysis (figure 54, DUNY blue). A different behaviour is observed for smaller corner elements (60mm mesh). Here the element instantly closes after opening and no form of plastic behaviour is observed (figure 54). Via secant unloading the relation between the reduction in normal deformation and the tensile strength is established (figure 56). The consequence of the first opening is a change in stiffness when the element is re-opened (figure 57). The smallest re-opening activates the zero shear traction setting and thereby influencing the shear behaviour significantly. The abrupt change in normal and shear stiffness results in numerical problems when re-opening and closing of the corner interface elements.

Normal and shear displacement of corner interface element for meshes 180mm and 60mm

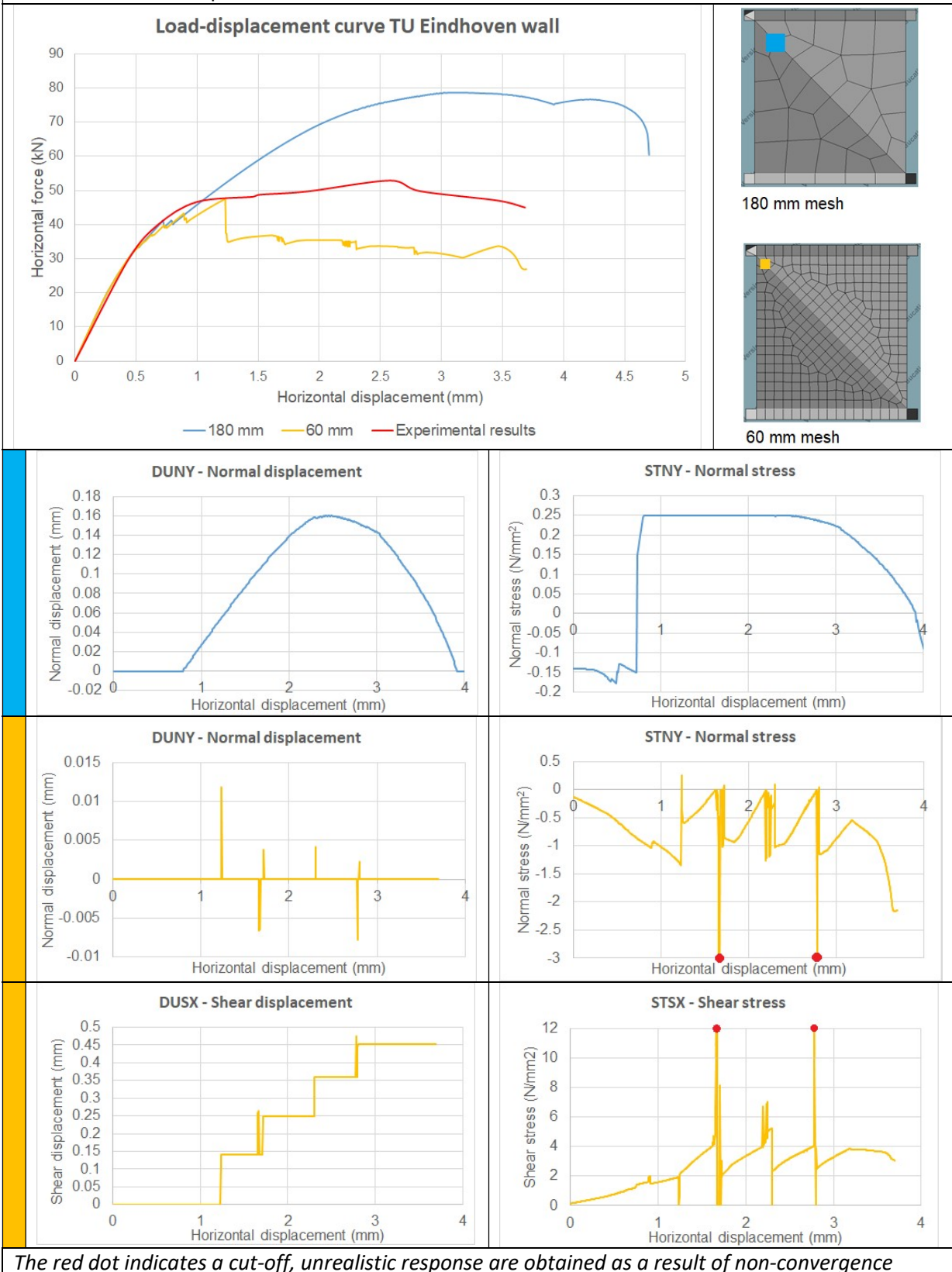


figure 54: Normal and shear displacement of the diagonal corner element

The previous finding is clarified through a simplified model showing the observed difference between a fine and a coarse mesh with respect to the corner interface element.

Coarse mesh

For a large corner element it is observed that after the first opening splitting behaviour increases and the plastic softening analogy becomes valid (figure 55).

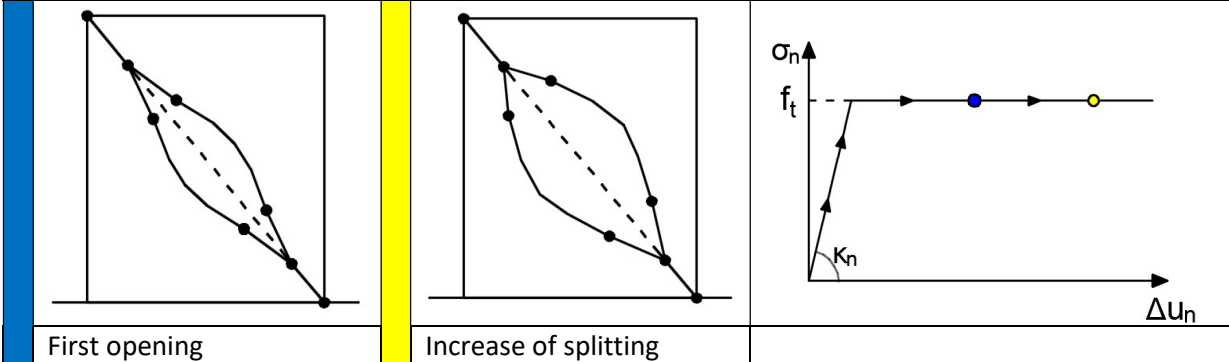


figure 55: A coarse mesh leads to plastic deformation of the corner element

Fine mesh

For a smaller corner element it is observed that the first opening is conform the plastic softening analogy but the next load-step leads to immediate closure. When, as a results of splitting behaviour, the corner element re-opens the zero shear traction setting becomes active. Every time the corner element tries to re-open abrupt shear deformation is observed and the splitting behaviour significantly reduces. During the previous analysis it is observed that the $\kappa_{n,1}$ obtained due to secant unloading remains valid for the rest of the analysis. As a result the softening curve became as shown in figure 57.

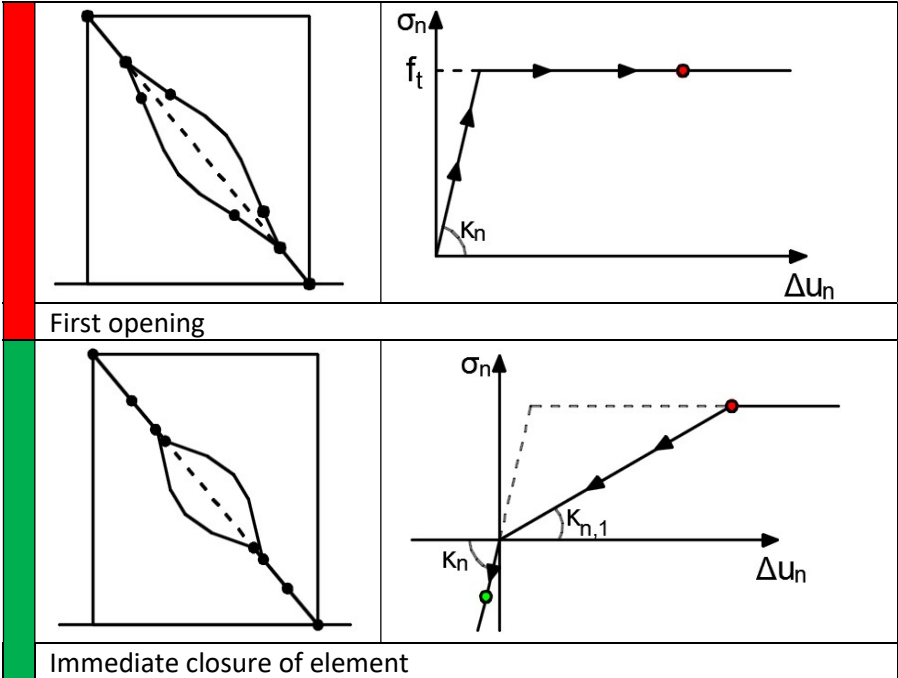


figure 56: Softening behaviour valid for smaller corner elements

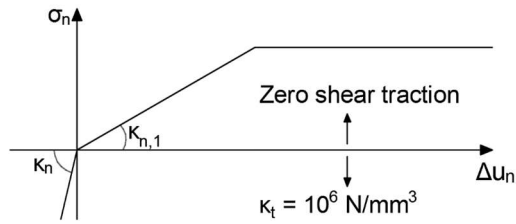


figure 57: Softening curves valid after opening. Re-opening instantly suggests zero shear traction

In conclusion, the obtained results are in line with the presented theory of section 5.2. Depending on the length of the corner interface element a larger part of the diagonal is able to open. The splitting influence thereby reduces and only the sliding deformation increases.

5.3 Conclusion of chapter 5

This chapter showed that the diagonal interface element length influences the diagonal opening. The theory states at least half the corner interface element must remain closed to preserve a compressive zone. The length of the corner element now determines the allowed opening percentage of the diagonal strut. By performing a mesh dependence study it became clear that the element length influences the opening percentage and therewith the splitting-sliding relation. For longer elements hold that splitting behaviour is of significant influence during the analysis, where for shorter elements sliding becomes crucial. In other words, the splitting-sliding relation seems to be mesh dependent.

A second influence of mesh refinement is the behaviour of the corner interface elements. For a coarse mesh holds that half the element opens and during the analysis this opening increases, thereby activating the plastic softening analogy. When a finer mesh is applied the corner elements close immediately after opening, thereby not activating the plastic behaviour. The re-opening and closing of this element leads to convergence issues.

In conclusion, mesh refinement influences the diagonal splitting-sliding relation and thereby reducing the load-bearing resistance. This phenomenon is considered a form of mesh dependence and further studies towards this splitting-sliding relation are strongly recommended.

Chapter 6. Combining the SLM approach with the SLA procedure

The previous chapters clarified the influences of the SLM assumptions. As described in the previous chapter, representing the diagonal strut by splitting behaviour leads to mesh dependence. The quality of the approach becomes thereby debatable. However, it is now known how the approach operates and what to expect when validating the TU Eindhoven wall. Therefore starting a SLM-SLA pilot is still an appropriate manner of validating if the SLA procedure can be combined with a lumping technique.

The SLA theory, presented in chapter 2, states that SLA is a damage based procedure characterised by representing the stress-strain relation via a saw-tooth analogy. Publications regarding SLA discrete modelling, or interface elements in general, are not available. Therefore appendix B contains a validation study regarding interface elements on a four point bending test. This study concludes that the ripple curve is a valid saw-tooth type, although using a coarse mesh does influence the stiffness behaviour.

During chapter 4 it is proven that the SLM diagonal strut must be able to deform in normal and shear direction. Via a zero shear traction setting this shear deformation after cracking is accomplished. The SLA procedure currently only functions in an older Diana version (9.3) which contains an error in the zero shear traction setting (appendix C). Therefore the upcoming analyses will be performed with the constant shear retentions setting and a $\beta\kappa_t$ -value of 10^{-6} N/mm^3 .

The upcoming SLM-SLA validation is performed on the TU Eindhoven wall. A benchmark description, including the wall geometry and material characteristics, is presented in chapter 4.1. The SLA ripple curves are present in the upcoming section. Because of the SLM's mesh dependency, discovered in chapter 5, a mesh is created out of 180 mm long diagonal interface elements (similar to the mesh of chapter 4). A mesh variation is performed during paragraph 6.2. This chapter's findings are summarised in paragraph 6.3.

6.1 SLM-SLA procedure – TU Eindhoven shear wall

Performing a SLA analysis demands a manually implemented softening curve. In this case tension softening curves for the horizontal and diagonal interface elements, and compressive softening for the continuum elements. All curves are formed according to the ripple curve analogy.

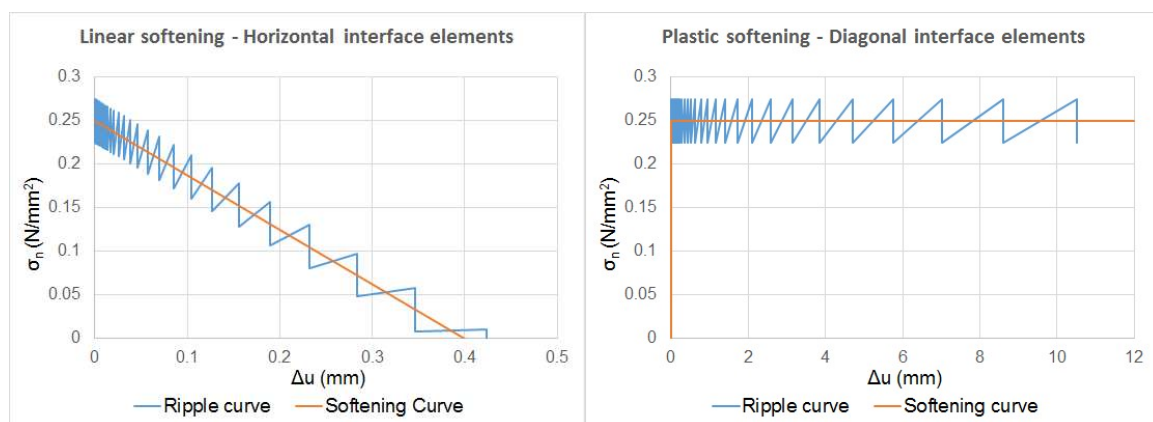


figure 58: Tensile softening curves for horizontal and diagonal interface elements

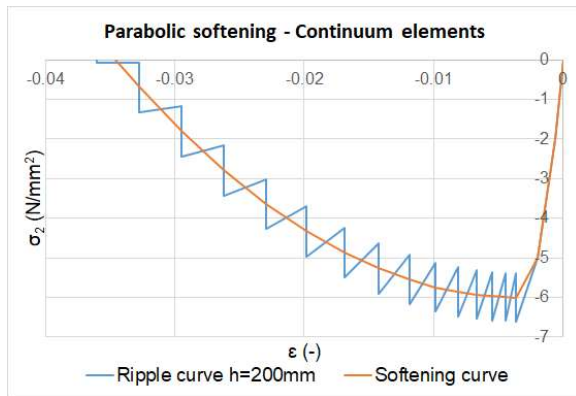
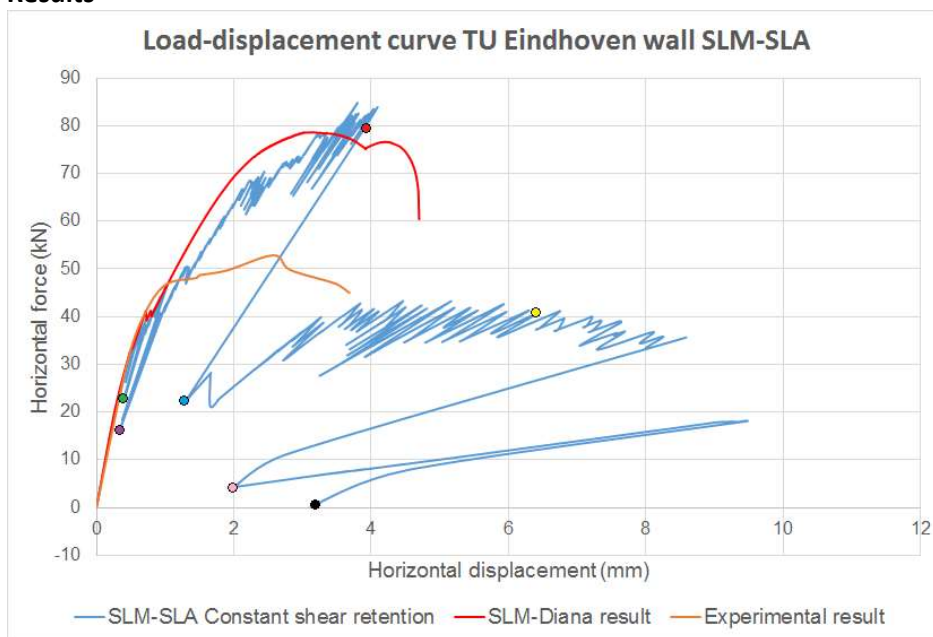


figure 59: Compressive softening curve for the continuum elements

Results



Point	Step	Description	Displacement	Force
Green	2673	Opening of the corner diagonal interface element	0.5165 mm	24 kN
Purple	2874	Shear deformation of the corner diagonal interface	0.3465 mm	16.5 kN
Red	4131	Last step before snap-back	3.858 mm	78.5 kN
Blue	4132	Snap-back	1.312 mm	22.6 kN
Yellow	4800	Influence failure mode change	6.217 mm	38 kN
Pink	4838	Top left corner snaps through	2.007 mm	4.3 kN
Black	4982	Bottom right corner snap through + closure of the corner diagonal interface element	3.199 mm	0.144 kN

The SLM-SLA procedure starts according to the traditional SLM behaviour. First the horizontal interface elements open, representing rocking, followed by opening of the diagonal strut. With opening of half the corner interface elements the diagonal strut has its full potential regarding normal and shear deformation (green dot). In contrast to the traditional SLM behaviour opening of the diagonal interface elements does not immediately results in shear deformation. Shear deformation of the corner diagonal is indicated by the purple dot 200 steps after it opened. The results from the corner diagonal interface element are presented by graphs on page 57.

After opening of all the allowed interface elements the SLM-SLA result is very similar to the traditional SLM result. The obtained shift (figure 60) between the two lines is observed during the validation studies in appendix B as well. There the influence of the ripple curve changed the overall stiffness. A mesh refinement improved those results. Chapter 6.2 will describe if a mesh refinement also increase the accuracy for the SLM-SLA procedure.

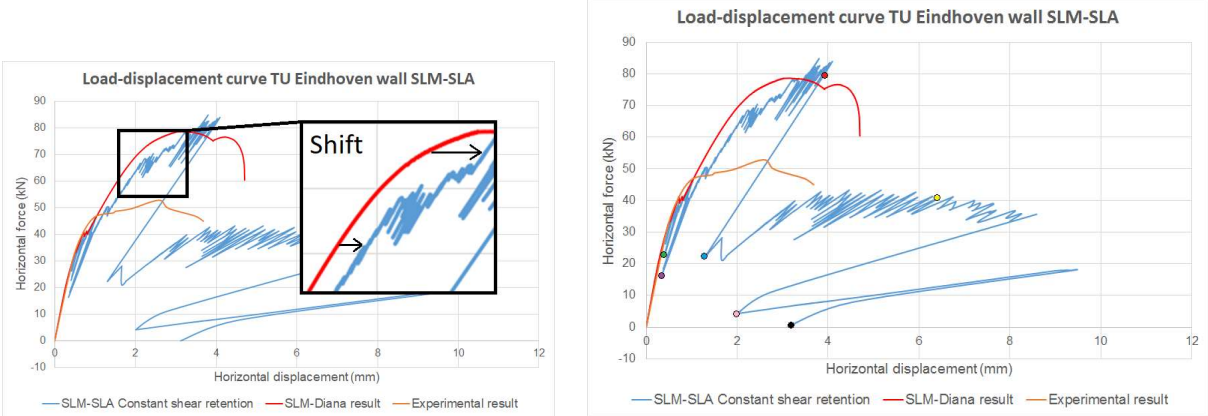


figure 60: Shift as a result of the applied ripple curve(left), load-displacement curve including the coloured dots (right)

A significant difference between the traditional SLM and the SLM-SLA procedure is the abrupt resistance drop from the red dot to the blue dot. This abrupt reduction of load-bearing resistance is caused by a change in failure behaviour as the splitting-sliding combination turns into merely sliding. The Newton-Raphson method was able to skip this behaviour change by the ‘continue after no convergence’ setting (chapter 5), but the SLA procedure is capable of modelling extreme snap-backs and behaviour transitions. Results obtained from the yellow dot show sliding has become the new and only failure behaviour until eventually toe crushing occurs. Now that sliding behaviour is decisive, compression zones along the diagonal are no longer shown only at the toe but are divided over the diagonal strut. Therefore full opening of the corner diagonal interface elements is allowed, leading to possible shear deformation along the entire diagonal strut (pink and black dots). As a result the load-bearing resistance drops significantly.

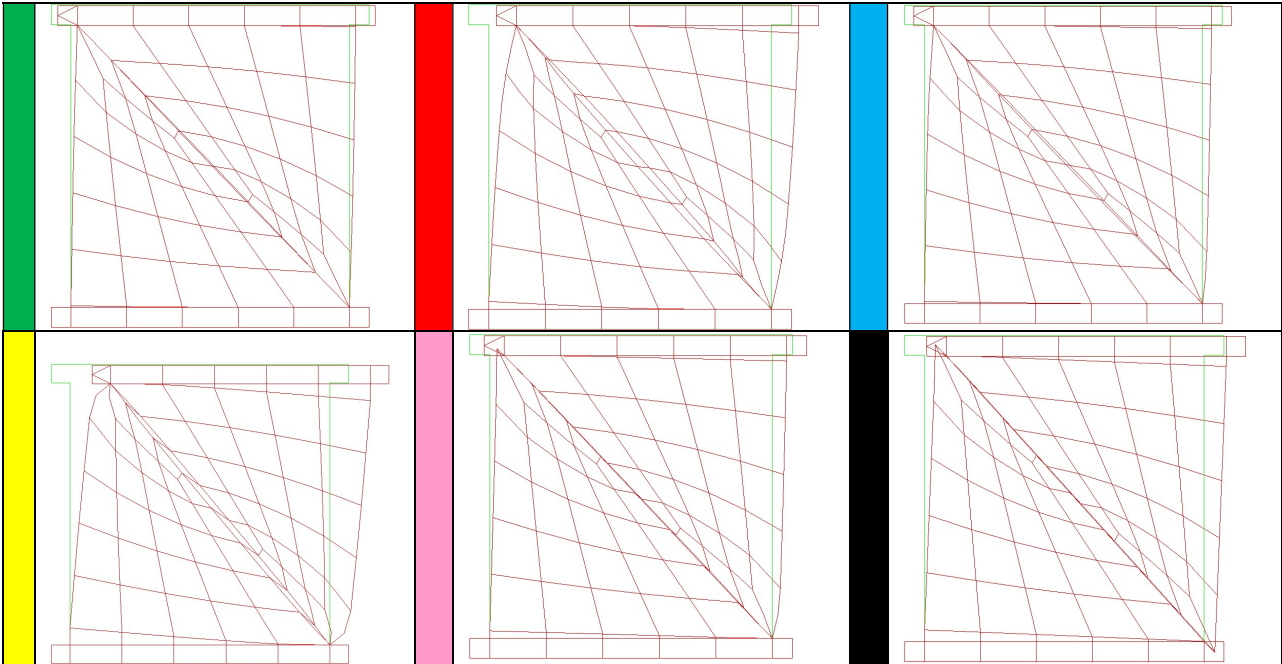


figure 61: Deformation plots (factor 25) of the TU Eindhoven wall

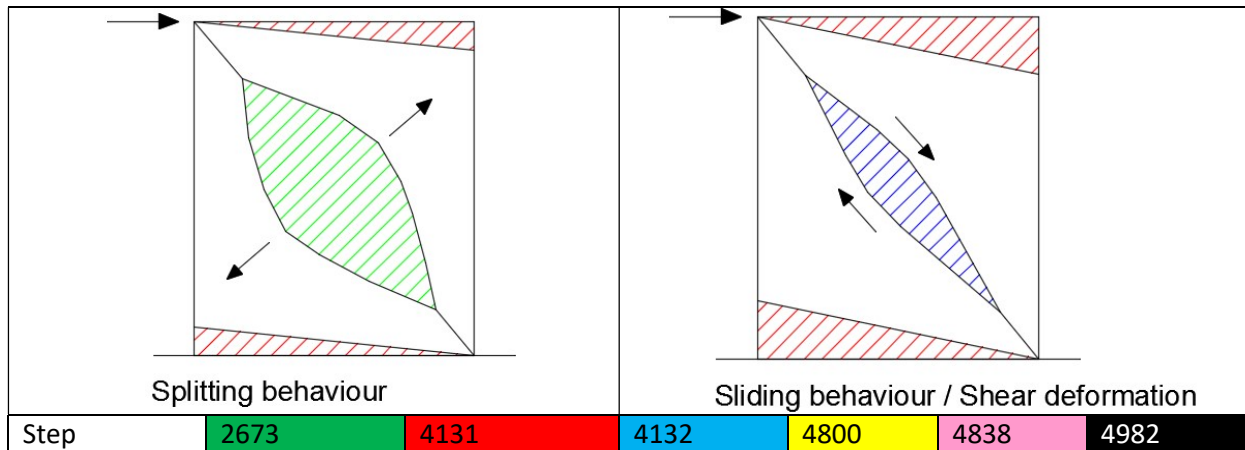


figure 62: Change in failure behaviour from splitting to sliding

The responses obtained from an integration point level are presented on the next page. The results from the centre diagonal element confirm that the splitting-sliding behaviour changes to merely sliding after the red dot. During the correct splitting-sliding relation the stress in normal direction reaches 0.275 N/mm^2 , but when sliding becomes decisive this will drop and remain at 0.15 N/mm^2 . Because the sliding deformation (PTY) continues to increase this proves the splitting-sliding behaviour turns into sliding behaviour. The colour plots in figure 63 confirm that compressive softening plays no part during the redistribution.

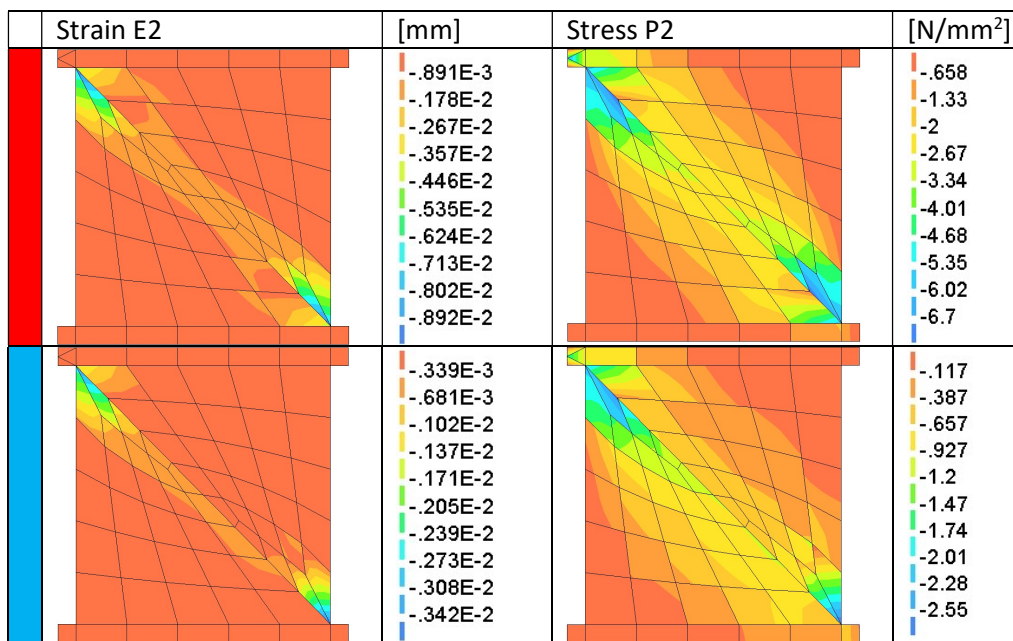


figure 63: Compressive stresses and strains at the resistance drop

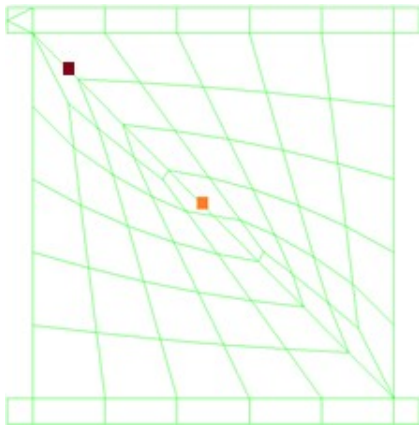


figure 64: Gauss point indication

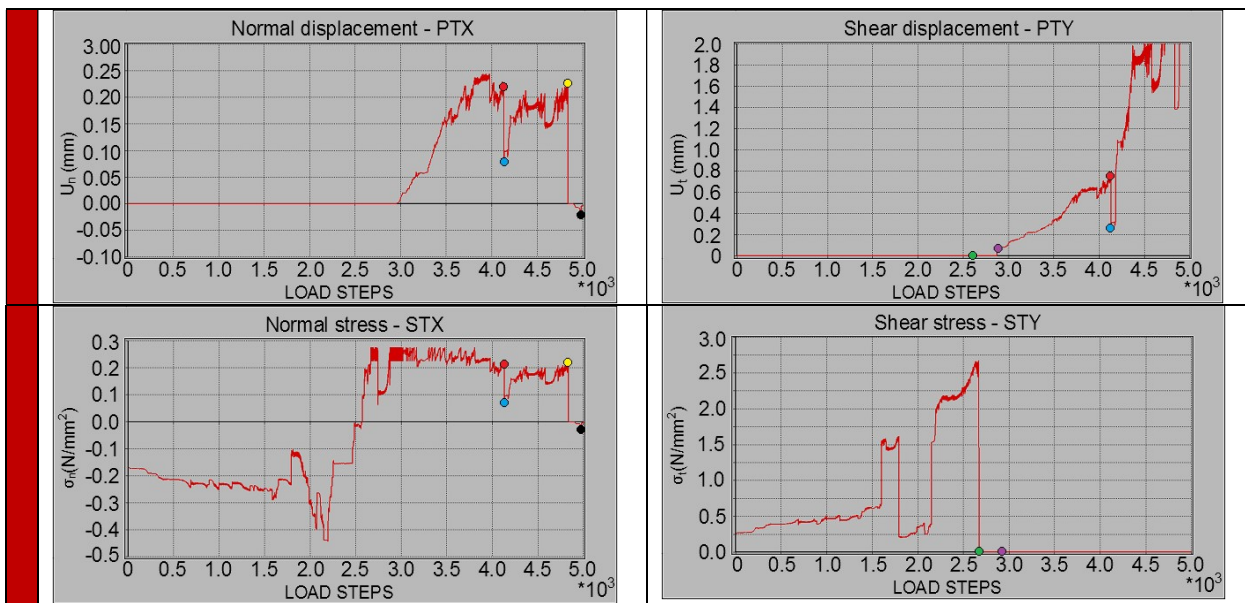
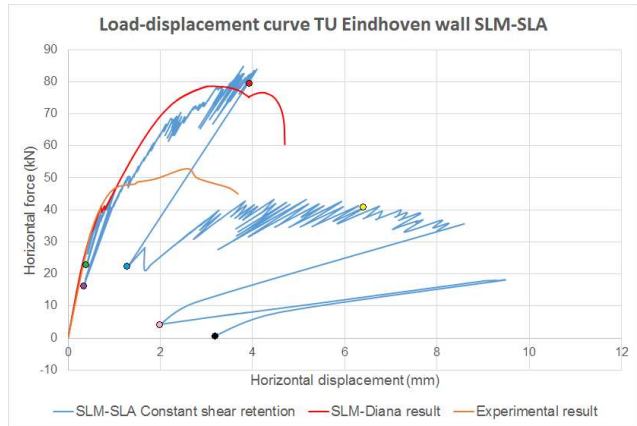


figure 65: Stresses and strains in normal and shear direction of the corner diagonal interface element

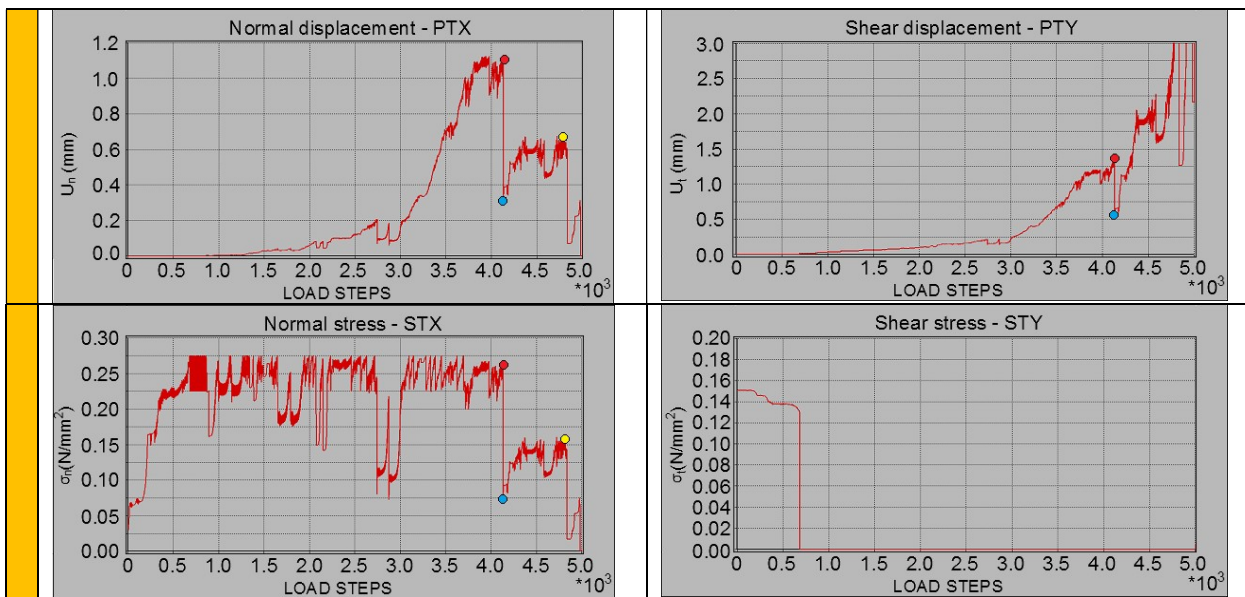


figure 66: Stresses and strains in normal and shear direction of the centre diagonal interface element

6.2 Mesh refinement to 120 mm

As indicated by appendix B and suggested in the previous section, the SLA interface elements benefit from mesh refinement. This paragraph reduces the interface element length from 180mm to 120mm. The load-displacement curve is presented in figure 67. As predicted during the last paragraph, refining the mesh will exclude any shift between the SLA and Newton-Raphson curves. Besides the improved accuracy and the more realistic peak load, mesh refinement does not lead to a different failure behaviour then observed during paragraph 6.1.

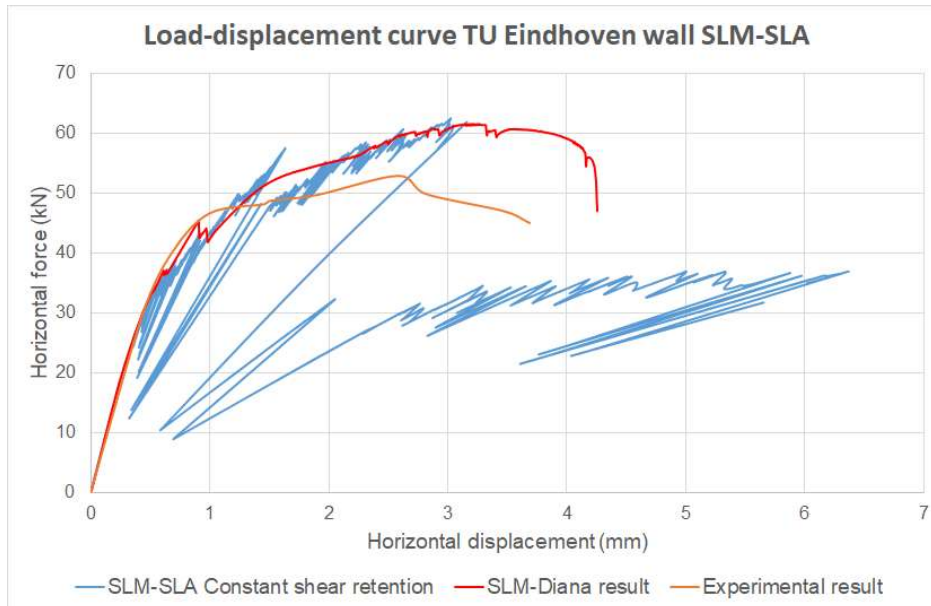


figure 67: Load-displacement curve of the SLM-SLA procedure, Newton-Raphson approach and the experimental result

6.3 Conclusion of chapter 6

This SLM-SLA pilot concludes that combining the SLA with a lumping technique is possible. The results show similarities with the SLM-Newton-Raphson approach, although a snap-back in the load-displacement curve is the influence of the SLA procedure. It is demonstrated that this snap-back represents the transition from splitting-sliding behaviour to merely sliding along the diagonal strut. Furthermore it became clear again that the SLA interface elements in combination with the ripple-curve benefits from mesh refinement. To continue the development regarding the SLA procedure in combination with a lumping technique it is recommended to first develop and describe the SLA discrete modelling in more detail so the mesh choice has less influence on the response.

Chapter 7. Conclusion master thesis

The SLM research has clarified the potential of the approach via literature and numerical validations by showing how the approach operates and which failure behaviour can be correctly analysed. Unfortunately, a form of mesh dependence influences the behaviour of the diagonal strut. Therefore the SLM approach at its current state does not meet the requirements to be an universal modelling tool. At the end of this chapter numerous recommendations are addressed, followed by a proposed solution to the observed mesh dependence. But first the thesis findings are summarized on the basis of the three objectives presented in chapter 1.

Objective 1 – Determine the consequences of the SLM assumptions

The SLM approach is based on several assumptions at element and structural level. With respect to the SLM elements only the continuum elements cause structural collapse as a result of crushing. The SLM interface elements do influence the structural deformation. On a structural level the SLM assumptions influence the failure mechanism by a predefined crack pattern formed out of interface elements. The use of tension cut-off interface elements does exclude horizontal sliding behaviour but, in combination with the continuum elements, represents rocking behaviour correctly. At this point the question remains whether diagonal cracking can be represented by tension cut-off interface elements. The following objective will answer this question.

Objective 2 – Form a description on how the SLM approach functions

As mentioned during the previous description the main focus of the SLM validation will be on how the diagonal interface elements represent diagonal cracking. It is determined that the diagonal elements will open by a splitting type behaviour due to a diagonal compressive strut. Via numerical validation it is shown an extreme overshoot of resistance is overcome by allowing shear deformation along the diagonal strut. The zero shear traction setting fulfils this demand and as showed during chapter 4 will reduce the overshoot. To clarify, the diagonal cracking contains two stages. First the elements will open as a result of the compressive strut representing a splitting type behaviour. Secondly, after opening shear deformation is possible and the diagonal strut represents both sliding and splitting behaviour. By allowing deformation in both directions diagonal cracking seems to be analysed correctly.

Objective 3 – Determine the influence of mesh choice

The previous objectives show the SLM approach has the potential to represent rocking behaviour in combination with diagonal cracking. Unfortunately splitting behaviour along the diagonal strut is influenced by mesh choice. The structural deformation as a result of the SLM approach forms very local compressive zones. The compressive forces make sure at least half the corner interface elements remain closed.

The possible opening of the diagonal strut is therefore depending on element size. Longer corner elements will keep a larger part of the diagonal strut closed, leading to splitting behaviour during a significant part of the analysis. The splitting behaviour keeps the corner element constantly open and plastic deformation is observed.

For smaller elements also hold that splitting behaviour opens all diagonal element except for half the corner elements. In comparison with a coarser mesh, a larger part of the diagonal strut is therefore influenced by the zero shear traction setting when not in compression. A difference with the coarser mesh is that for a finer mesh the corner elements do not remain open longer than a single load-step and therefore no plastic deformation is observed. The elements are closed for most of the analysis. When splitting behaviour tries to open the corner elements the zero shear tractions setting becomes active and significant shear deformation seems to avert the splitting procedure. A change in failure behaviour is thereby observed where mainly sliding deformation is present. It is recommended to

study the splitting-sliding relation along the diagonal strut in more detail in order to overcome this form of mesh dependence.

As all objectives are accomplished the SLM research is completed within the scope of this thesis. Next to the objective a pilot has been launched during chapter 6 where the SLM-SLA combination is validated. The combination shows potential but also insinuates that the SLA discrete modelling procedure should be developed further before combining the procedure with lumping methods. Appendix B contains a validation study where it is proven that the ripple curve can be used for discrete modelling but mesh dependence is obtained for coarse meshing.

7.1 Recommendations

To enhance future development of the SLM approach the following statements are recommended:

-Find a solution to the mesh dependence reported in chapter 5. (see section 7.2 for proposed alternative) Mesh refinement influences the diagonal splitting-sliding relation and thereby reducing the load-bearing resistance. Further studies towards the splitting-sliding relation are strongly recommended.

-An important aspect is the geometrical limit in which the SLM assumptions are valid. During this master thesis a clamped in benchmark with a 1:1 length-width ratio formed a 45° angle for the diagonal strut. For this angle the splitting-sliding relation shows promising results, but within what range will this relation stay correct? A geometric validation study with respect to clamped-in benchmarks is therefore recommended.

-During this thesis the zero shear traction setting leads to a realistic response. It would be a huge advantage if this setting works for all SLM validations since no additional input is required. It is recommended to validate different benchmarks with this setting to ensure its quality.

-The splitting-sliding relation of the diagonal strut should be investigated for different levels of pre-compression.

-Next to the clamped in boundary condition it is recommended to study the splitting-sliding relation for free-end walls in more detail. Part of the original SLM-report can be used as a foundation for this enhanced study.

As addressed earlier, before combining the SLA procedure with a lumping technique the research towards SLA discrete modelling is recommended.

It is recommended that the programming error concerning the constant shear retention setting in Diana10.1 is corrected (see appendix A).

Appendix B states negative displacement of the SLA interface elements is possible. This is not conform the Diana theory and should therefore be corrected.

7.2 Proposed alternative of the SLM approach

An important discovery of the SLM research is the observed mesh dependence regarding the diagonal strut. Splitting behaviour is influenced by shear deformation when a larger part of the diagonal strut is able to open. In order to reduce this mesh dependency it is proposed to investigate a model where the corner parts of the diagonal strut are always closed and shear deformation is prevented. By taking a step back from the material model to the physical model the following alternative is proposed.

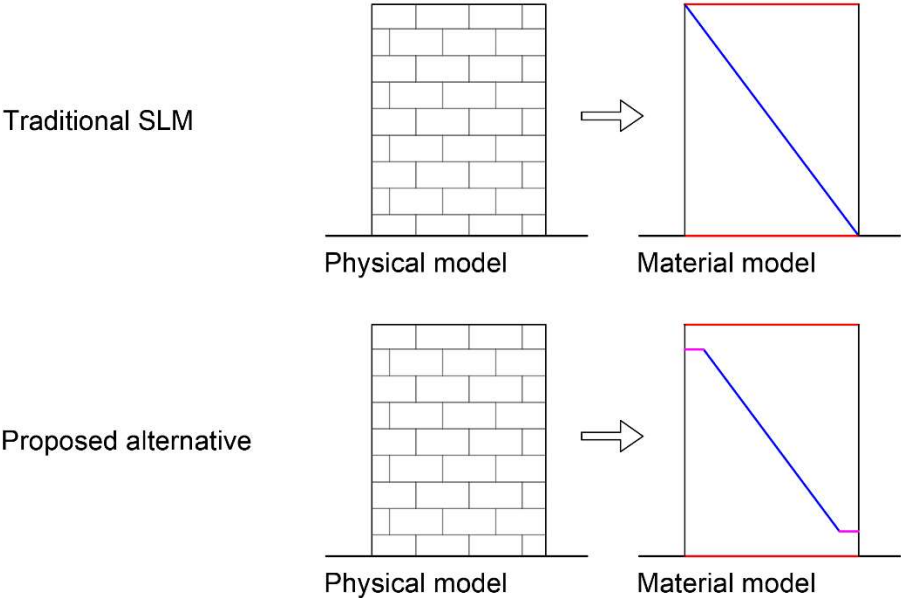


figure 68: Proposed alternative

By enclosing the diagonal strut between horizontal interface elements a separation between the compressive zones and the diagonal shear failure is achieved. It is now possible for the entire diagonal strut to open and still preserve a compressive corner area (figure 69). If the diagonal fully opens in all cases the influence of mesh choice on the splitting behaviour reduces significantly.

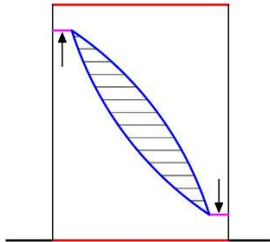


figure 69: Indication of the compressive zones

The proposed alternative is also in need of an improved study regarding the splitting-sliding relation of the diagonal strut.

Literature

- [1] Messali F. Hollow brick masonry wall: in-plane seismic response and strengthening techniques with reinforced high-performance mortar coatings. PhD thesis, 2015.
- [2] Cattari S, Lagomarsino S. A strength criterion for the flexural behaviour of spandrels in unreinforced masonry walls. Proceedings of 14th WCEE, 2008.
- [3] Lagomarsino S, Penna A, Galasco A, Cattari S. An equivalent frame model for the nonlinear seismic analysis of masonry buildings. *Engineering Structures* 56, 2013.
- [4] Marques R, Lourenco PB. Possibilities and comparison of structural component models for the seismic assessment of models unreinforced masonry buildings. *Computers and structures* 89, 2011: 2079-2091.
- [5] Lourenco PB, Rots JG, Blaauwendraad J. Two approaches for the analysis of masonry structures: micro and macro-modeling. *HERON* vol 40. No 4, 1995.
- [6] Balkema AA. *Structural masonry*, 1997.
- [7] Lourenco PB, Rots JG. Possibilities of modeling masonry as a composite softening material: Interface modeling and anisotropic continuum modeling.
- [8] Lourenco PB. Two aspects related to the analysis of masonry structures: size effect and parameter sensitivity. TU-DELFT report no. 03.21.1.31.25; Nov 1997.
- [9] Lourenco PB. An anisotropic macro-model for masonry plates and shells: implementation and validation. TU-DELFT report no. 03.21.1.31.07; Feb 1997.
- [10] Lourenco PB, Rots JG. Understanding the behaviour of shear walls: a numerical review. 10th IB2MaC; July 5-7 1994.
- [11] Lourenco PB. Computational strategies for masonry structures. PhD thesis, 1996.
- [12] Durgesh CR, Subhash CG. Seismic strengthening of rocking-critical masonry piers. *Journal of structural engineering*; Oct 2007: 1445-1452.
- [13] Pari M. Modelling of out of plane biaxial flexure of unreinforced masonry walls. Master thesis, 2015.
- [14] Bahman G, Masoud S, Abbas AT. Seismic evaluation of masonry structures strengthened with reinforced concrete layers. *Journal of structural engineering*; June 2012.
- [15] Rots JG. Sequentially linear continuum model for concrete fracture. In: de Borst R, Mazars J, Pijaudier-Cabot G, van Mier JGM, Balkema AA, editors. *Fracture mechanics of concrete structures*. The Netherlands: Lisse, 2001: 831-839.
- [16] Rots JG, Invernizzi S. Regularized sequentially linear saw-tooth softening model. *International journal for numerical and analytical methods in geomechanics*. No 28, 2004: 821-856.
- [17] Rots JG, Belletti B, Invernizzi S. Robust modeling of RC structures with an “event-by-event” strategy. *Engineering fracture mechanics*. No 75, 2008: 590-614.
- [18] DeJong MJ, Hendriks MAN, Rots JG. Sequentially linear analysis of fracture under non-proportional loading. *Engineering fracture mechanics*. No 75, 2008: 5042-5056.
- [19] DeJong MJ, Belletti B, Hendriks MAN, Rots JG. Shell elements for sequentially linear analysis: lateral failure of masonry structures, 2009.
- [20] VanDeGraaf AV, Hendriks MAN, Rots JG. Sequentially linear analysis of masonry structures under non-proportional loading. *Computational modelling workshop on concrete, masonry and on fiber-reinforced composites*; June 17-18, 2009.
- [21] Mariani V, Hendriks MAN, Slobbe AT. Application of sequentially linear analysis to the seismic assessment of slender masonry towers. Conference paper; Sept 2013.
- [22] Kraus J. Sequentially linear modelling of combined tension/compression failure in masonry structures. Master thesis, 2014.
- [23] Hendriks MAN, Rots JG. Sequentially linear versus nonlinear analysis of RC structures. *Engineering computations*. No 30 Iss 6, 2013: 792-801.
- [24] DeJong MJ, Harrison SAM. A biaxial failure criterion for sequentially linear analysis. 8th International masonry conference, 2010.

- [25] Harrison S. A biaxial failure criterion for masonry. Fourth-year undergraduate project, University of Cambridge; 26th May 2010.
- [26] Giardina G, VanDeGraaf AV, Hendriks MAN, Rots JG, Marini A. Numerical analysis of a masonry facade subject to tunnelling-induced settlement. *Engineering structures*. No 54, 2013: 234-247.
- [27] Slobbe AT, Hendriks MAN, Rots JG. Sequentially linear analysis of shear critical reinforced concrete beams without shear reinforcement. *Finite elements in analysis and design*. No 50, 2012: 108-124.
- [28] Slobbe AT. Propagation and band width of smeared cracks. Thesis 2015.
- [29] Voormeeren LO. Extension and verification of sequentially linear analysis to solid elements. Master thesis, 2011.
- [30] Diana 10.1 User's manual. <https://dianafea.com/manuals/d101/Diana.html>
- [31] Vermeltfoort AT, Raijmakers TMJ. Deformation controlled test in masonry shear walls, Part 2, Report TUE/BKO/93.08, Eindhoven University of Technology, 1993.
- [32] Fracture mechanics, Wikipedia. https://en.wikipedia.org/wiki/Fracture_mechanics

Appendices

Table of content

Appendix A – Diana10.1 error regarding constant shear retention

Appendix B – SLA interface elements validated on a four-point bending test

Appendix C – Error observation in the SLA zero shear traction setting

Appendix A – Diana10.1 error regarding constant shear retention

The numerical SLM-validation performed during chapter 4 established shear deformation along the diagonal strut as essential when representing diagonal cracking via mode I interface elements. The shear deformation is obtained with the zero shear traction setting. The intended research towards shear deformation was a variant study with different β_{k_t} -values for the constant shear retention setting. Unfortunately the Diana10.1 contains a modelling error which causes this setting to be unreliable. Appendix A will describe this error and its consequences.

Variation study

The variation study regarding shear deformation concerns four different β_{k_t} -values for the diagonal interface elements of the TU Eindhoven shear wall. As indicated by table 4 one of these variations is the zero shear traction variant. This variant 4 is described in detail during chapter 4 and will not be repeated here. The same holds for the section on how to obtain H and the variation 1 response.

	Variation 1	Variation 2	Variation 3	Variation 4
β_{k_t}	10^4 N/mm^3	6.25 N/mm^3	0.01 N/mm^3	Zero shear traction
H	0.125 mm	200 mm	125 m	-

table 4: Overview variations

It is expected that the setting from variation 3, containing extremely low shear stiffness, will result in a similar load-displacement curve as the variation 4 curve. However, as indicated by figure 70, this is not the case. The load-bearing resistance of variation 3 (yellow line) is significantly larger than the resistance of variation 4 (green line).

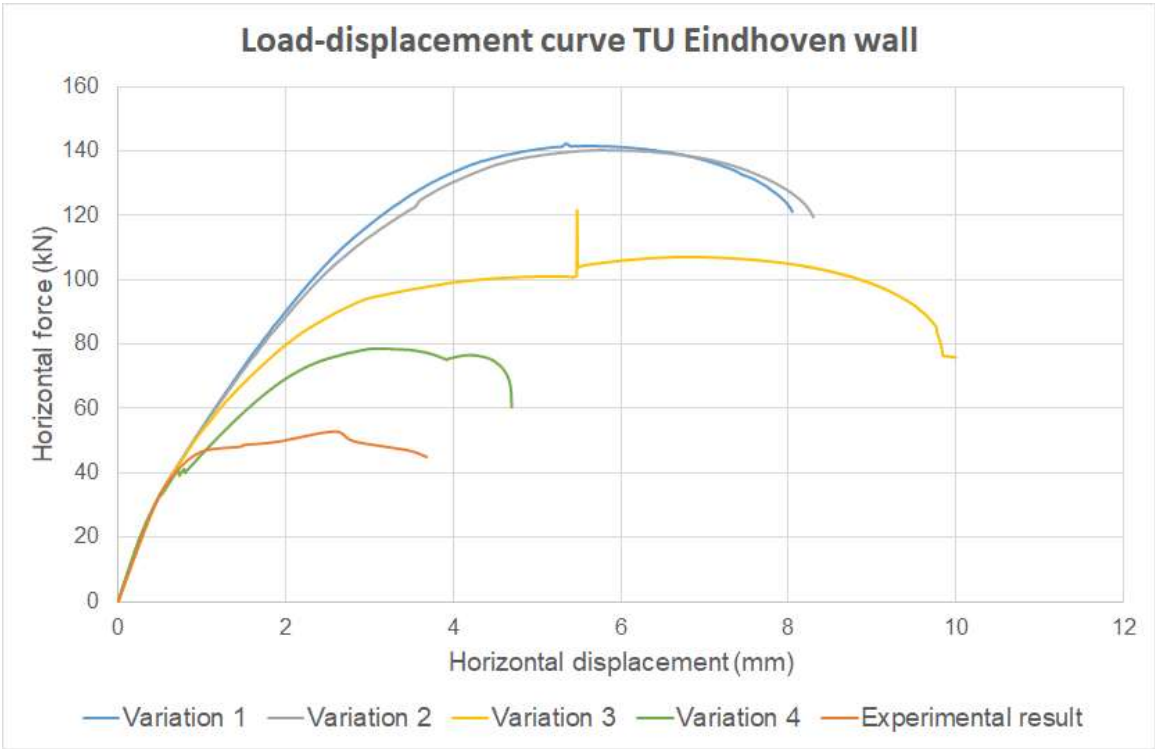


figure 70: Load-displacement curve variation study

The difference between variation 3 and 4 is the result of a modelling error in the Diana10.1 version concerning the constant shear retention setting. According to the Diana theory opening of the interface element will cause the shear stiffness to abruptly drop and continue linearly by a β_{k_t} slope instead of the initial k_t slope (figure 71). However, in practice opening of the interface elements leads

only to a change in stiffness and no drop of shear strength is detected. This means that when low βk_t -values are applied an almost plastic behaviour forms itself where the maximum shear strength is depending on the opening moment of the interface element. For the TU Eindhoven shear wall this results in different shear strength for all diagonal interface elements. The corner elements open at a later stage and therefore contain a higher shear resistance than the centre elements (figure 72). The sliding behaviour of the diagonal strut can therefore not be executed in a controlled environment.

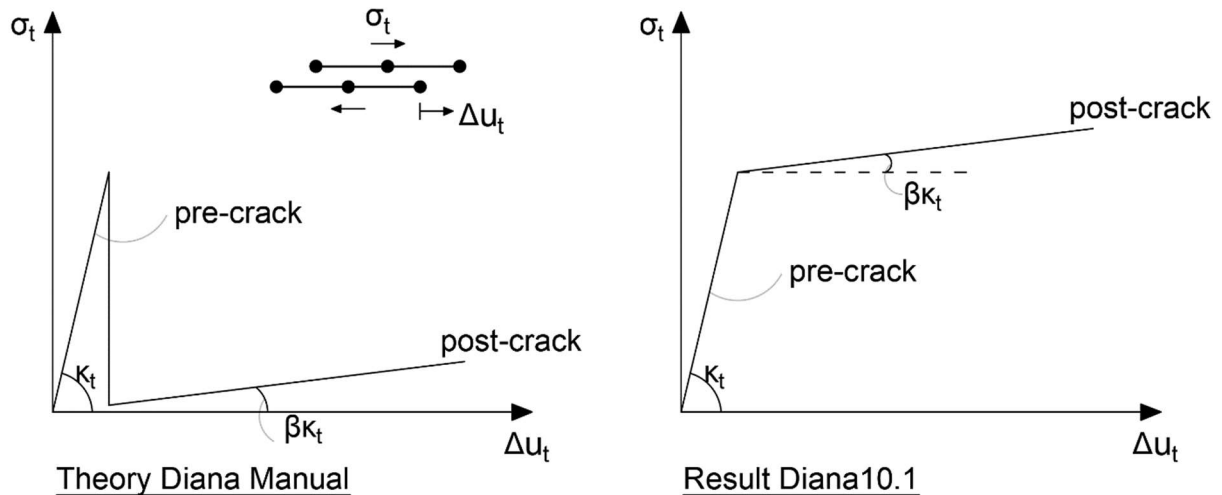


figure 71: Diana theory vs modelling practice

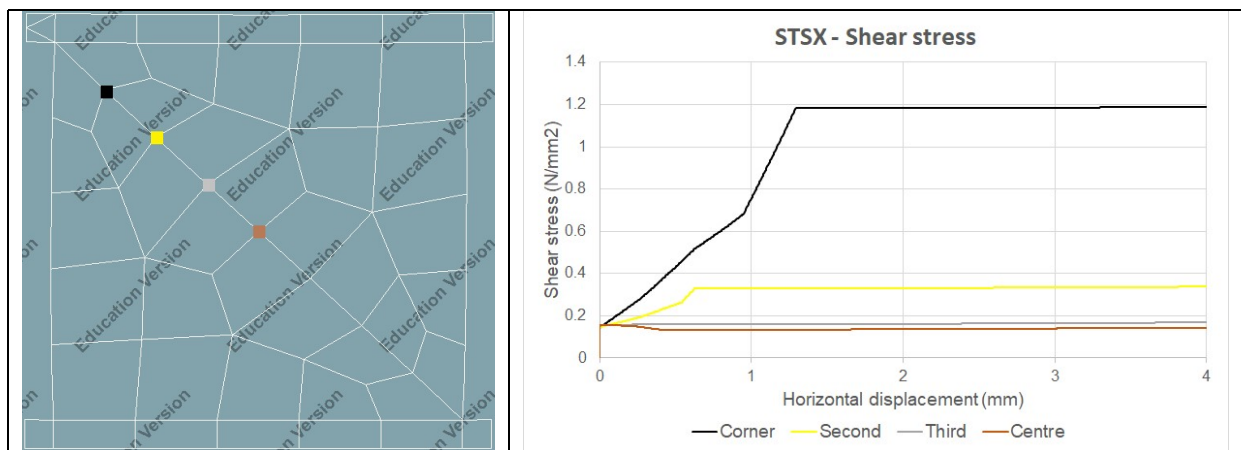


figure 72: Influence of the modelling error on the TU Eindhoven wall benchmark.

A second difference between the zero shear traction setting and the constant shear retention setting is the response on closure of the element. When applying the zero shear traction setting re-closure of an interface element does not influence the achieved shear deformation. However, when using the constant shear retention setting the shear deformation will instantly snap to zero as the interface element closes (figure 74).

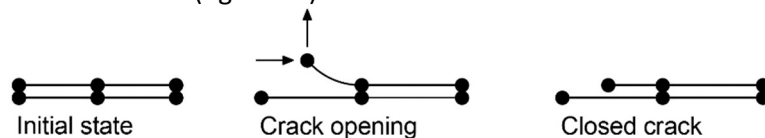


figure 73: Interface closure with the zero shear traction setting

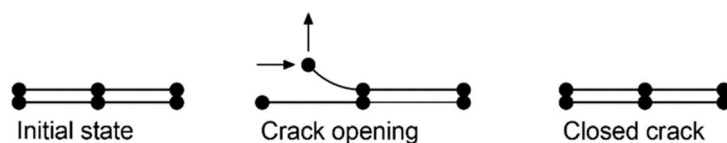


figure 74: Interface closure with the constant shear retention setting

With respect to the TU Eindhoven wall the abrupt snap-back of shear deformation results in a resistance jump. Indicated by the purple node is the moment where the interface element is still open. Complete reduction of normal deformation leading to abrupt shear deformation is indicated by the red node. Immediately after closing, the element opens again (blue dot) but shear deformation is no longer possible.

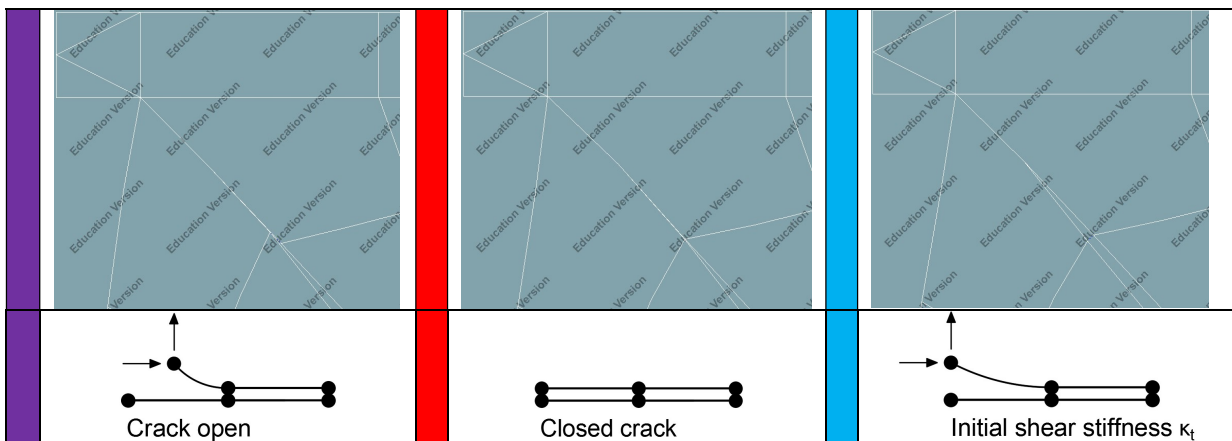
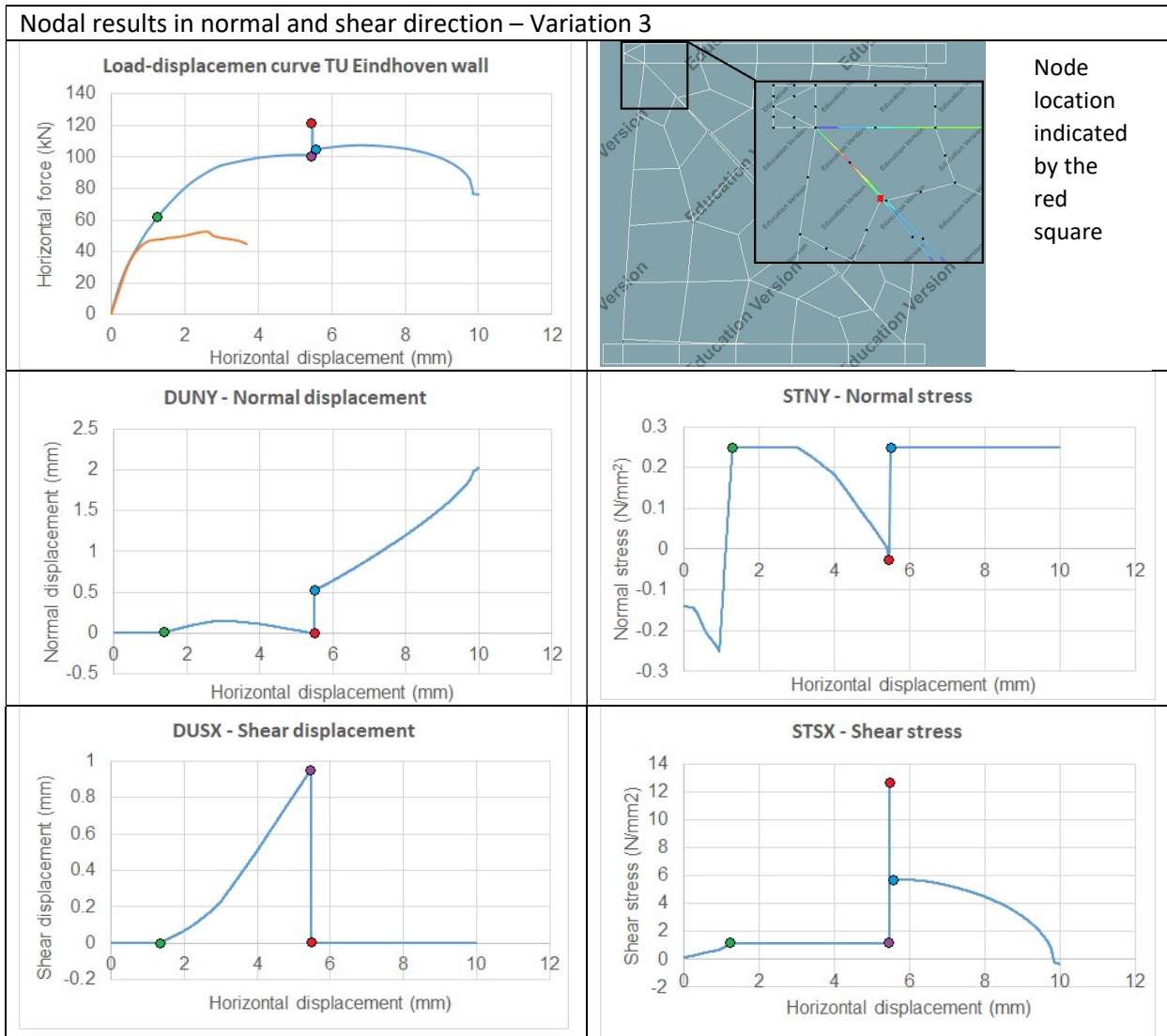
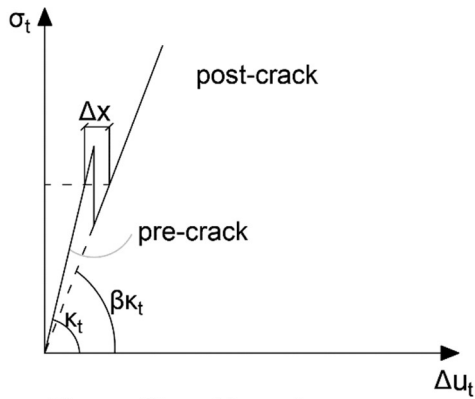


figure 75: Closing crack behaviour of the constant shear retention setting. Green dot: opening of the interface element, purple node: last opening stage, red node: closed interface element, blue node: reopening of the interface element.

Conclusion appendix A

This appendix proves the error regarding the constant shear retention setting has a significant influence on the SLM response. For small $\beta\kappa_t$ -values the Diana10.1 version is unreliable and not suitable for the SLM approach. However, during this thesis it is assumed interface elements with the constant shear retention setting can still be applied as long as the $\beta\kappa_t$ -value is high, representing extreme stiffness. With the help of the figure below this statement will be argued.



Theory Diana Manual

figure 76: Representation of Δx

When using high κ_t and high $\beta\kappa_t$ -values the Δx length will reduce to almost zero. This means a potential reduction of shear strength after cracking is no longer observed. Therefore the observed modelling Diana10.1 error does no longer influence the results. It is assumed the horizontal SLM interface elements are correctly represented by the constant shear retention setting as long as the following values are applied, $\kappa_t = 10^6$ and $\beta\kappa_t = 10^4$.

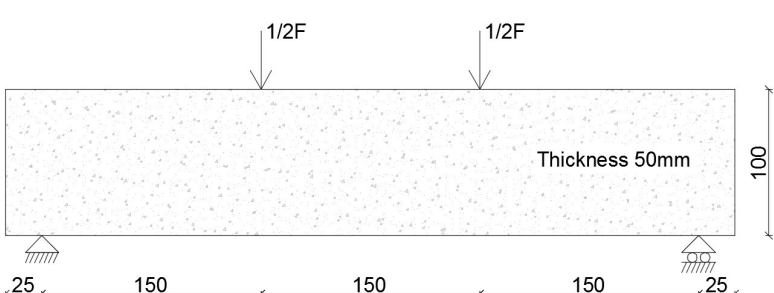
Appendix B – SLA interface element validation

The SLA method is in development and part of this development is validating if the procedure can be used for discrete modelling. During discrete modelling potential cracks are represented by interface elements with matching dummy stiffness values. There are no publications available describing SLA interface elements, but the elements are used in other theses and implemented in the Diana 9.3 version. Before starting the SLM-SLA combination in chapter 6, this appendix will validate the quality SLA interface elements.

This validation is performed with a four-point bending test. The goal of the validation is to check if the ripple-curve is a correct saw-tooth type for the SLA interface elements. The four-point bending test characteristics are obtained from course CIE5148 “Computational modelling of structures” and refer to the laboratory experiment performed by Hordijk (1991).

The benchmark concerns a concrete beam with the sizes 500x100x50 mm³ that is supported on both ends. A deformation load F, divided over two points, will break the beam. The material characteristics are presented in the table below.

Material parameters	
Young’s modulus	40000 N/mm ²
Poisson ratio	0,2 (-)
Tensile strength f_t	3,0 N/mm ²
Softening curve	Linear
Fracture energy G_{fl}	0,125 N/mm
K_n	10^6 N/mm ²
K_t	10^6 N/mm ²



To model the beam interface elements are implemented in the centre. These CL12I interface elements have non-linear tensile characteristics, but react linear elastic when under compression. The rest of the beam is modelled via CQ16M quadratic continuum elements.

This validation study is based on a comparison between the Newton-Raphson approach and the SLA procedure. This means the obtained responses will not be compared to any experimental results but only with each other.

Newton-Raphson method

As mentioned earlier this validation study is based on a comparison between the Newton-Raphson approach and the SLA procedure. This section will present the Newton-Raphson response. The described benchmark will be analysed with different mesh sizes. These meshes contain 3,4,5 or 8 interface elements. As an example the mesh of 4 interface elements (red) is presented below.

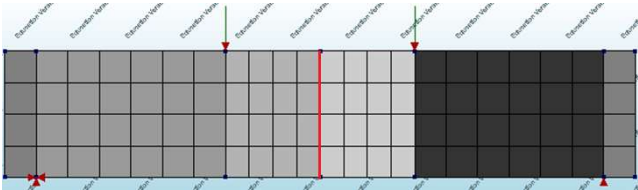


figure 77: Example with 4 interface elements of length 25mm

The results of the mesh variation are visualised by a load-displacement curve (figure 78). The responses are in line with each other and thereby mesh dependence is excluded. But as expected a coarser mesh leads to a coarser response.

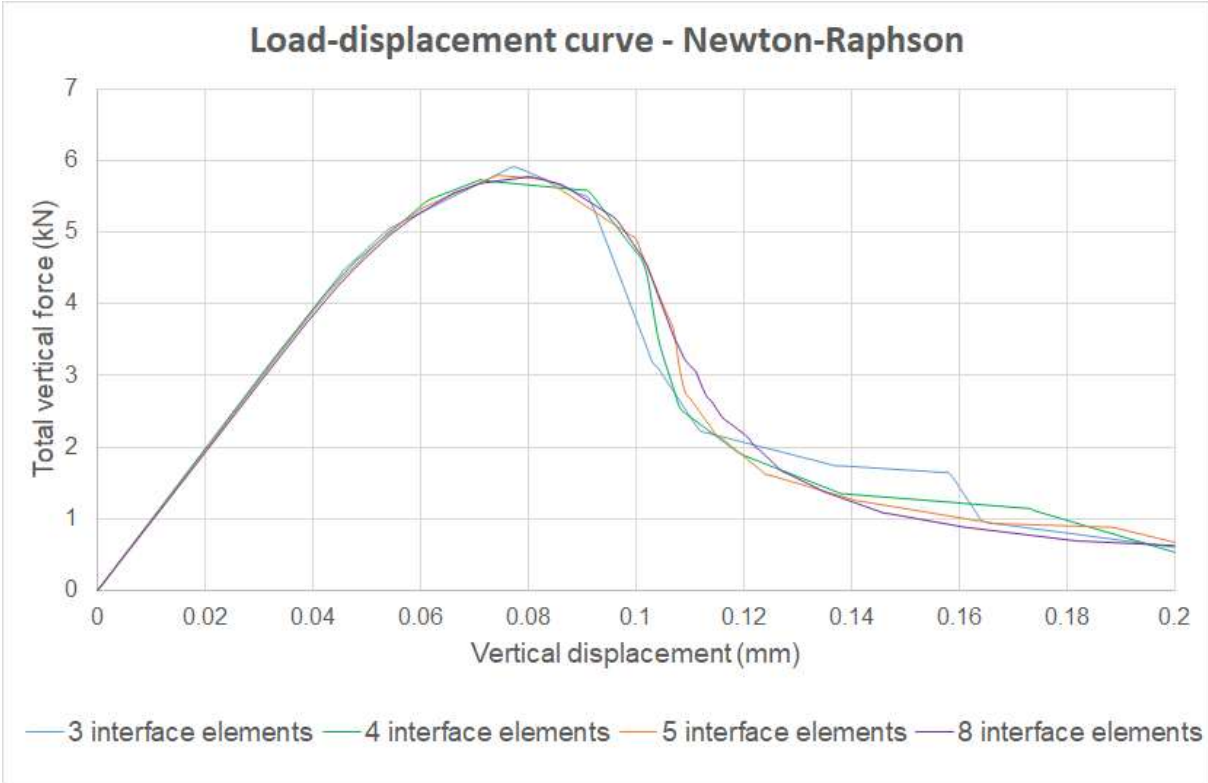


figure 78: Load-displacement curve Newton-Raphson mesh variation study

The 4 interface element variant will be used to validate the SLA study in the next section.

The SLA method

To validate the SLA method by the concrete beam, manual implementation of the saw-tooth curve is required. There is no recommended saw-tooth type for the interface elements and therefore the ripple-curve is applied. A dummy stiffness of $\kappa_n = 10^5$ and $p = 0.1$ results in a 40 tooth ripple-curve. The validation starts with the 4 interface element mesh.

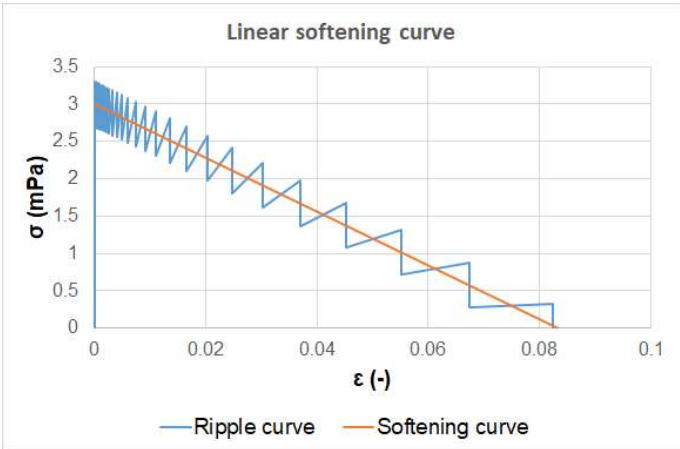


figure 79: Applied ripple curve

The SLA results are plotted against the Newton-Raphson results in a load-displacement curve (figure 80). The general shape of the SLA curve is conform the Newton-Raphson curve. An agreement is found regarding the peak load but at different vertical displacements. After the maximum resistance the tail of the SLA curve has shifted to right compared to the Newton-Raphson curve. This shift is the result of the ripple-curve. The stress graphs in figure 81 show that after the peak load the stress-strain relation of the bottom two interface elements is represented by coarser teeth. This means a lower stiffness is obtained and accuracy of the analysis drops.

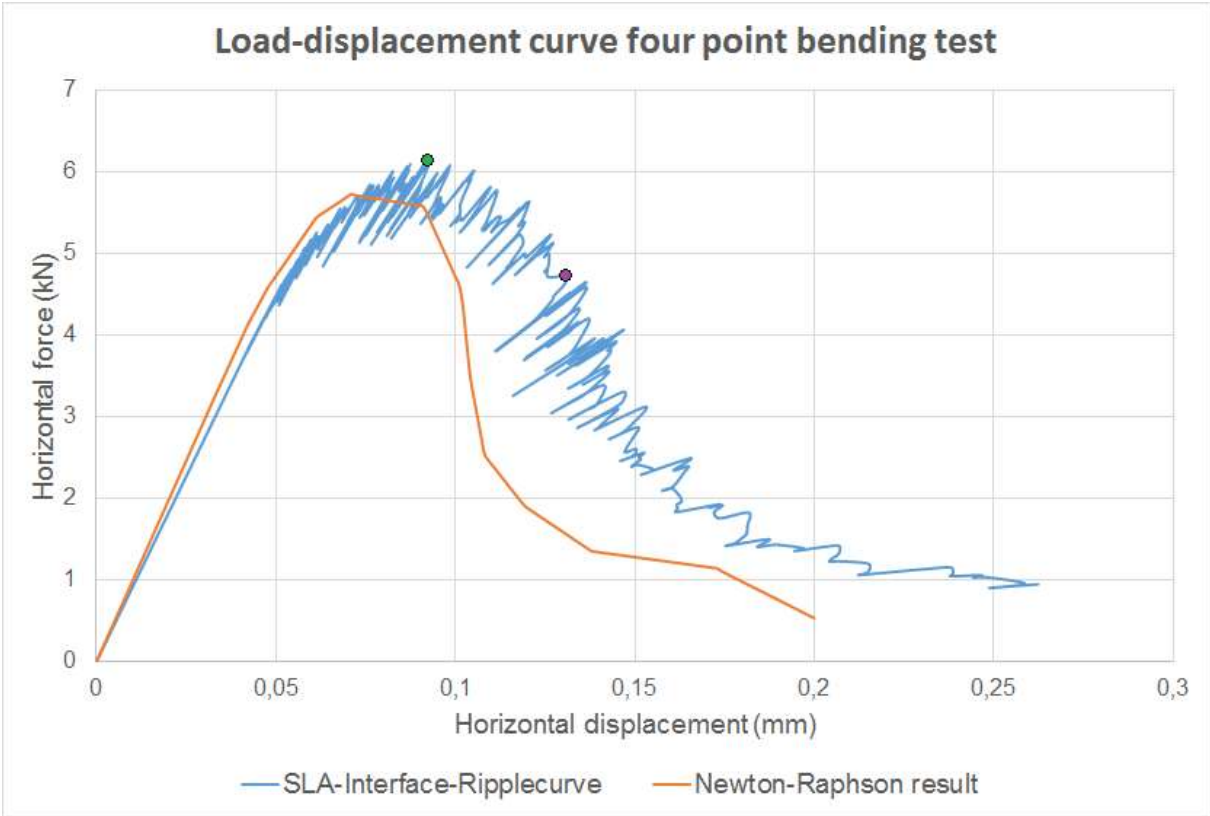


figure 80: Load-displacement curve, ripple curve approach vs Newton Raphson result

Point	Description	Displacement	Force	Step
Green	Peak load	0.09189 mm	6.128 kN	233
Purple	After peak load	0.1361 mm	4.64 kN	387

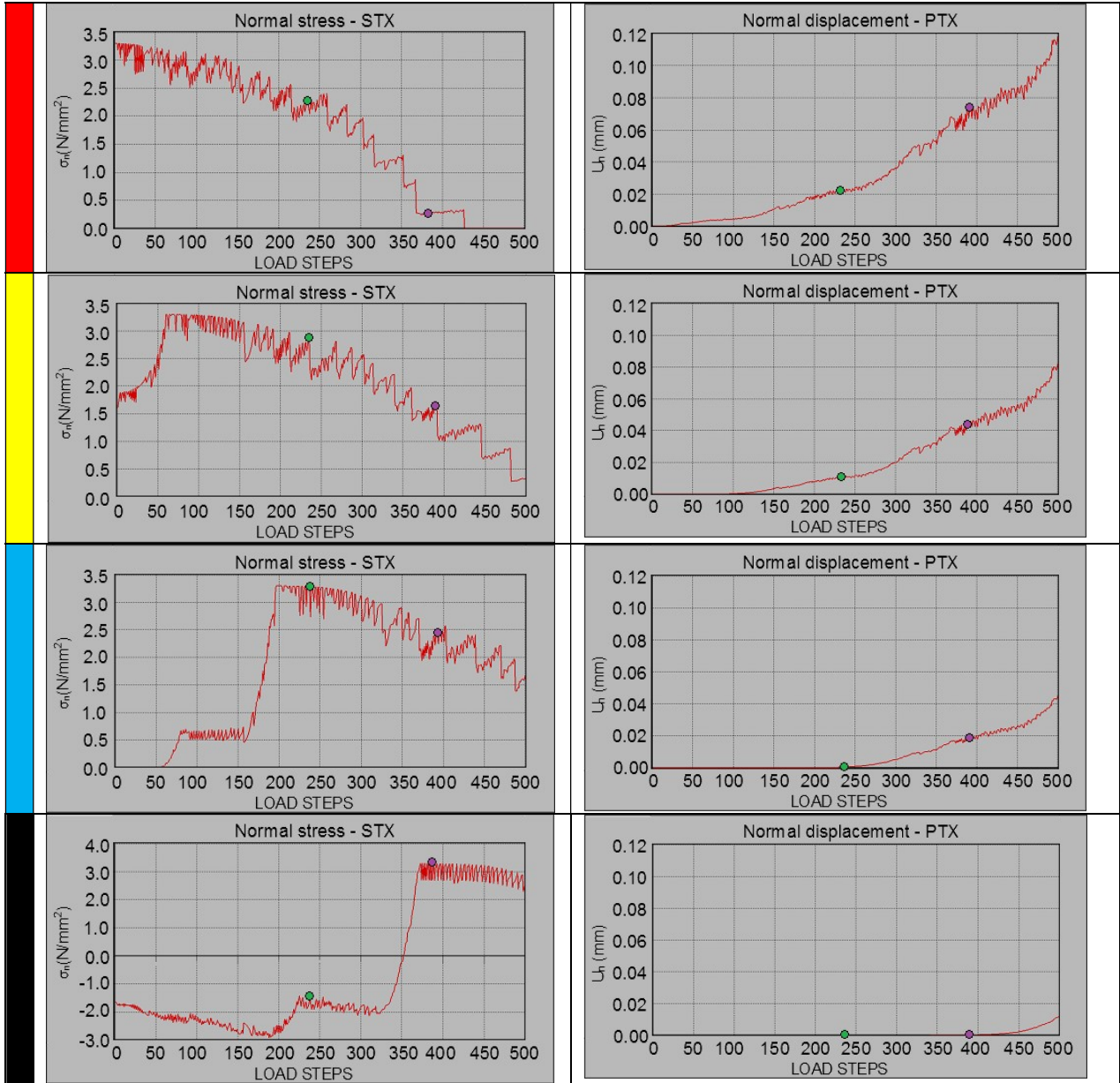
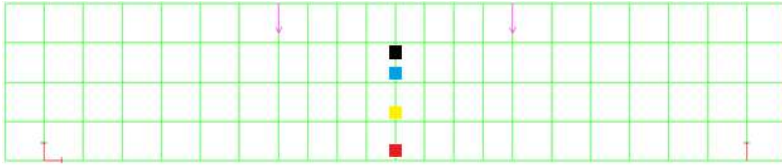


figure 81: Stress and strain graphs of the SLA interface elements

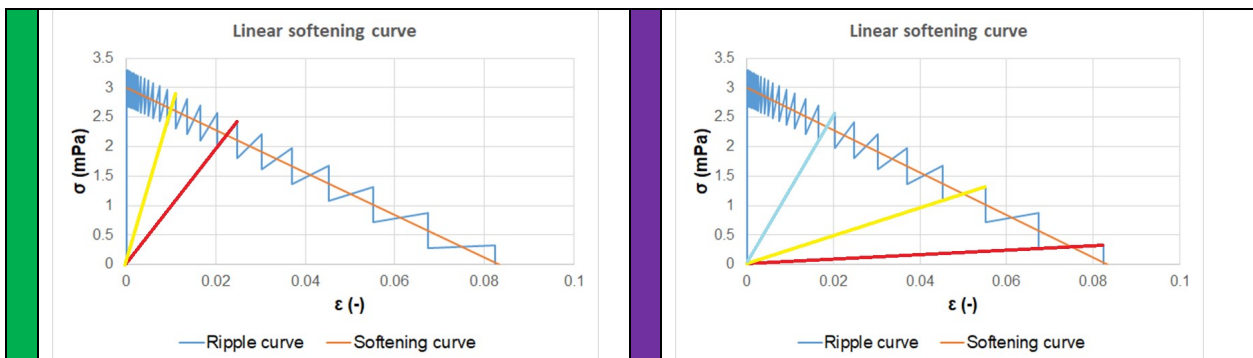


figure 82: The coloured lines show which element is represented by which tooth

The coarser part of the ripple curve reduces the accuracy regarding the stress-strain relation and thereby causes a difference between the SLA and Newton-Raphson curves. By increases the number of interface elements this influence might reduce. Via a mesh variation study this is validated. Similar to the Newton-Raphson section the different meshes are defined by the number of interface elements, in this case 4,5 or 8 elements.

Results

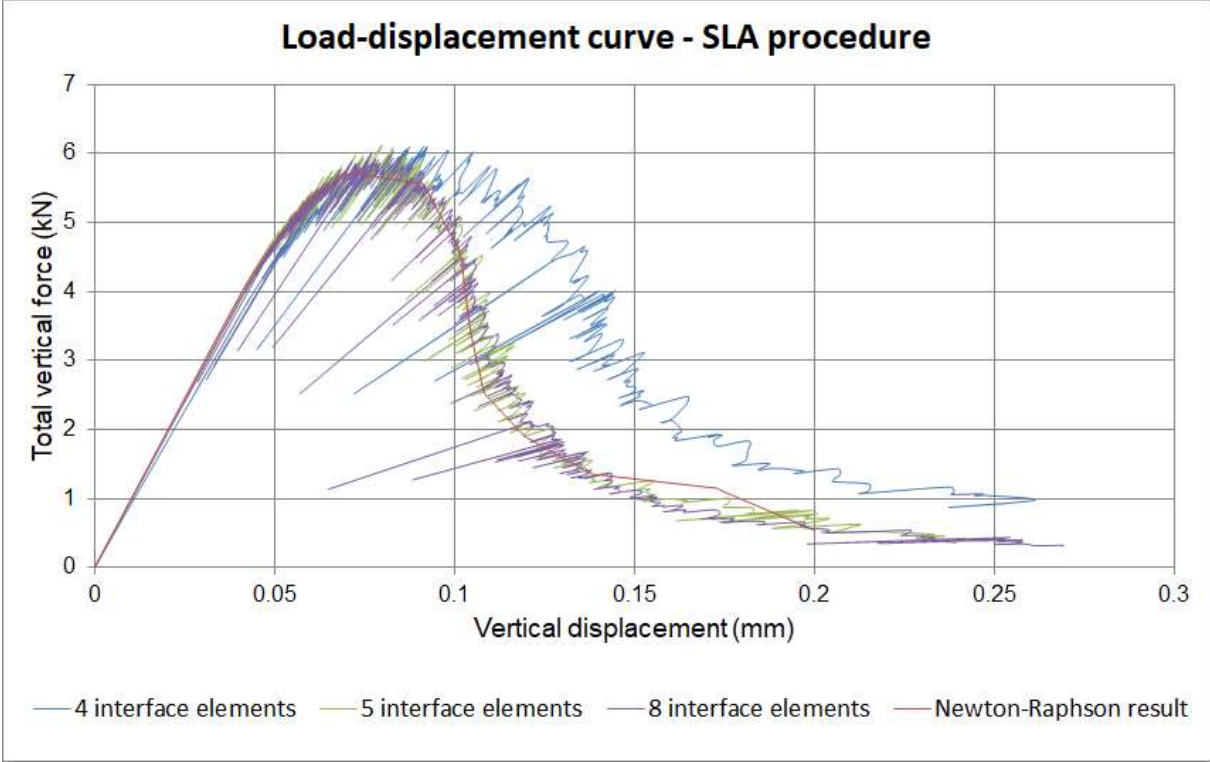


figure 83: Load-displacement curve SLA mesh variation

Mesh refinement has a positive influence on the results. Both the 5 and 8 element meshes converge to the Newton-Raphson curve.

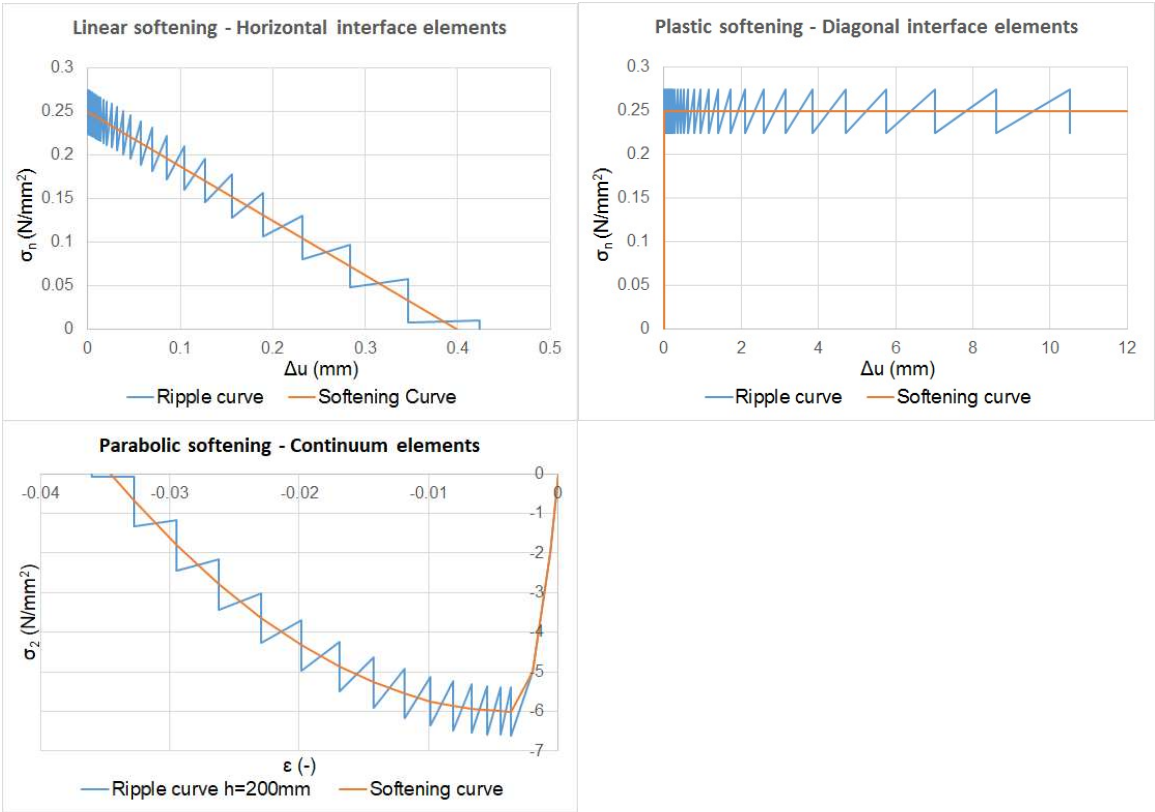
Conclusion appendix B

The SLA interface elements can be used in combination with the ripple curve, but applying a coarser mesh might influence the result. More validation regarding SLA discrete modelling is recommended, but not within the scope of this master thesis.

Appendix C – Error observation in the SLA zero shear traction setting

Currently the SLA procedure is only available in an older Diana version (9.3). Interface elements are implemented in this version but unfortunately an error is observed in the zero shear traction setting. This appendix C describes the error and its influence. The TU Eindhoven wall will be used for validation (see chapter 4 for the benchmark description).

As mentioned in appendix B, the SLA softening curve has to be manually implemented. The applied curves are presented below, all curves are based on the ripple-curve analogy (similar to chapter 6).



Chapter 5 showed the choice in mesh influences the SLM results. For this validation is chosen for 180mm long interface elements have been chosen, similar to the meshes used during chapters 4 and 6. It is expected that this mesh choice results in a small overshoot of resistance.

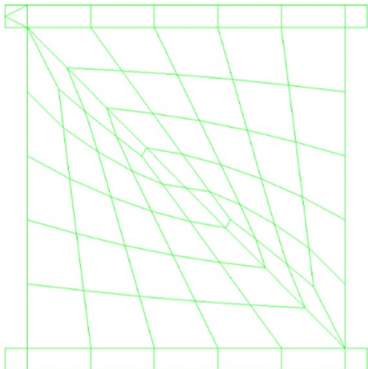
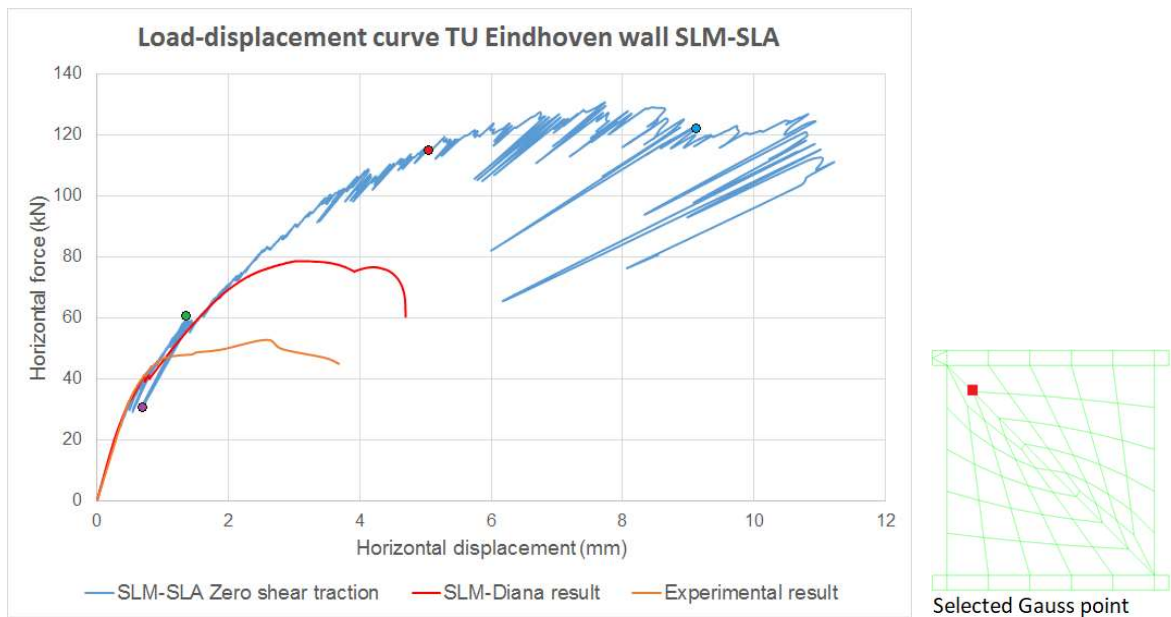


figure 84: Applied mesh (180mm interface elements)

Results



Point	Step	Description	Displacement	Force
Green	2717	Opening corner diagonal interface	1.113 mm	50.56 kN
Purple	2981	Shear deformation diagonal interface	1.273 mm	54.15 kN
Red	3776	Closing diagonal interface	5.05 mm	115.4 kN
Blue	4200	Influence closing diagonal interface	8.983 mm	92.95 kN

The load-displacement curve presented above contains the experimental result (orange), the SLM result of chapter 4 (red) and the SLM-SLA result (blue). As mentioned during the introduction of this chapter an overshoot due to the coarse mesh is expected but the SLM-SLA procedure shows an overshoot of 140%. The reason for this overshoot has a modelling background. Setting the after crack behaviour to zero shear traction does not set the β_{κ} value to zero but to one (representing a $H=1.25\text{m}$ masonry wall height stiffness). Comparing the PTY-graph with the STY-graph clearly shows a factor 1 relation between the shear deformation and shear stress after opening (purple dot). Therefore a higher shear stiffness is obtained resulting in an overshoot of resistance.

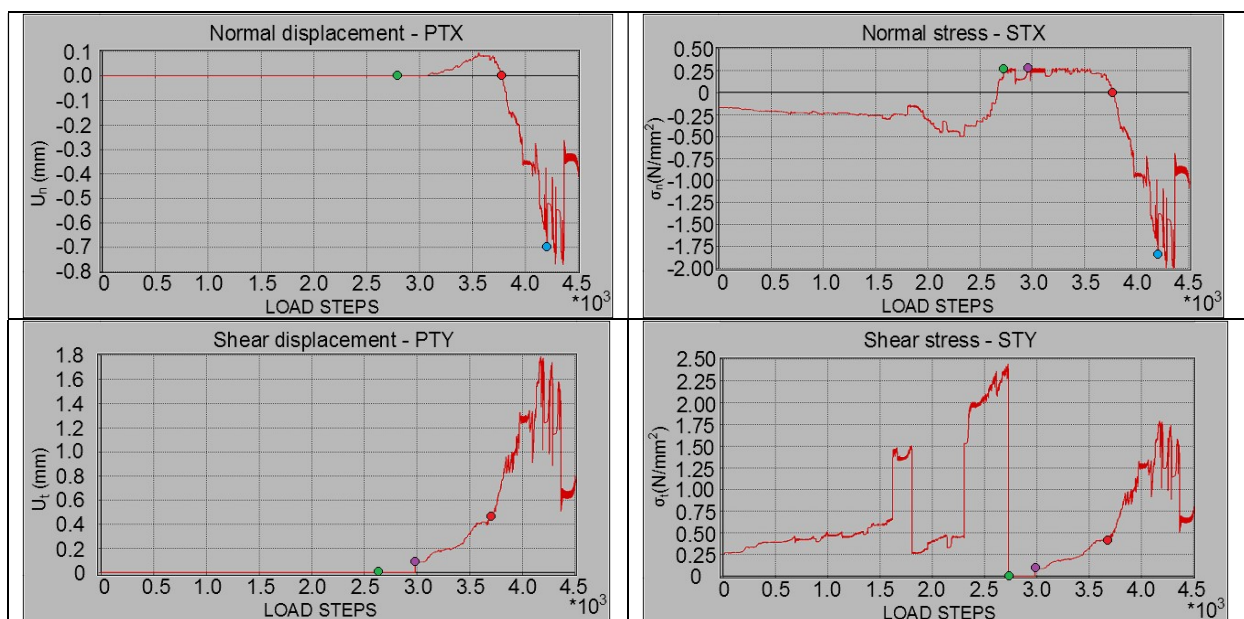


figure 85: Stress and strain results of the top corner diagonal interface element (see selected Gauss point above)

A general observation holding for all SLA interface elements is the occurrence of negative displacement. As indicated in former chapters the initial stiffness should regain after closure of an interface element. This does not hold for the SLA interface elements. Here the reduced stiffness as a result of tensile damage remains valid even once the elements are exposed to compression. A graphical representation of this phenomenon is given by figure 86. For the TU Eindhoven wall this means after reclosing of the corner interface elements (red dot), compressive forces push these elements to deform in negative direction. This negative displacement remains valid for the rest of the analysis. This means the SLM ideology is no longer valid when the corner element recloses.

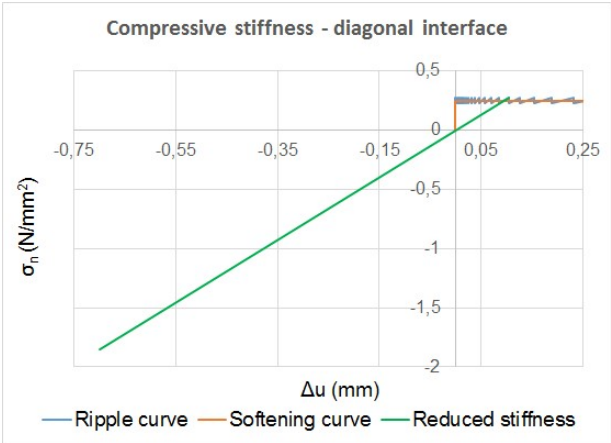


figure 86: The stress-strain relation for negative displacement of corner interface elements at the blue point location

Conclusion appendix C

The zero shear traction setting for Diana9.3 results in a stress-strain relation of one instead of zero. This has a significant influence on the SLM approach and is therefore an unsuitable setting. As shown by chapter 6 this can be solved with the constant shear retention setting in combination with an extremely low $\beta\kappa_t$ -value.

The performed validation study also showed negative displacements possible for the SLA interface elements. This can lead to unrealistic results and should not be allowed.